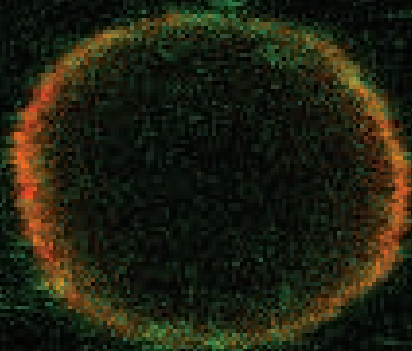


# Insights into alpha-synuclein oligomer interactions with model membranes



Anja Stefanović

**INSIGHTS INTO ALPHA-SYNUCLEIN  
OLIGOMER INTERACTIONS WITH  
MODEL MEMBRANES**

---

**Anja Stefanović**

## **Members of the thesis committee**

Prof. dr. V. Subramaniam	University of Twente (Promotor)
Prof. dr. ir. M.M.A.E. Claessens	University of Twente (co-Promotor)
Prof. dr. ir. P. Jonkheijm	University of Twente
Prof. dr. J.A. Killian	Utrecht University
Prof. dr. S.M. van der Vies	VU University Medical Center
Prof. dr. R.J.A. van Wezel	University of Twente
Prof. dr. C. Wyman	Erasmus University Medical Center

The work described in this thesis was financially supported by the "Nederlandse Organisatie voor Wetenschappelijk Onderzoek" (NWO) through the NWO-CW TOP program number 700.58.302.

Additional funding was provided by the Stichting Internationaal Parkinson Fonds.

The work described in this thesis was carried out at the:

Nanobiophysics group

MESA+ Institute for Nanotechnology

Faculty of Science and Technology

University of Twente

P.O. Box 217

7500 AE Enschede

The Netherlands.

Copyright © A. Stefanović, All rights reserved

ISBN: 978-90-365-3771-1

DOI: 10.3990/1.9789036537711

**INSIGHTS INTO ALPHA-SYNUCLEIN  
OLIGOMER INTERACTIONS WITH  
MODEL MEMBRANES**

DISSERTATION

to obtain

the degree of doctor at the University of Twente,

on the authority of the rector magnificus,

prof. dr. H. Brinksma

on account of the decision of the graduation committee,

to be publicly defended

on Wednesday 5<sup>th</sup> of November 2014 at 14:45 h

by

Anja Stefanović

born on 14<sup>th</sup> of August 1984

in Belgrade, Serbia

Dit proefschrift is goedgekeurd door:

Prof. dr. V. Subramaniam en Prof. dr. ir. M.M.A.E. Claessens

*To my family*



## Table of Contents

<b>Chapter 1:</b>	<b>Introduction</b>	1
	1.1 Alpha synuclein and Parkinson's disease	1
	1.2 Properties of alpha-synuclein	2
	1.3 Oligomeric alpha-synuclein	3
	1.4 Formation and characterization of oligomeric alpha-synuclein	3
	1.4.1 High concentration-induced oligomers	4
	1.4.2 Metal ion-induced oligomers	4
	1.4.2 Metal ion-induced oligomers	4
	1.4.4 HNE/ONE-induced oligomers	5
	1.5 Alpha-synuclein membrane interactions	6
	1.6 Scope of this thesis	7
	1.7 References	8
<b>Chapter 2:</b>	<b>Oligomer binding to bilayers with increasingly complex lipid compositions</b>	15
	2.1 Abstract	15
	2.2 Introduction	15
	2.3 Materials and Methods	17
	2.3.1 Expression and purification of $\alpha$ -synuclein	17
	2.3.2 Labeling of alpha-synuclein	17
	2.3.3 Preparation of labeled $\alpha$ S oligomers	18
	2.3.4 Qualitative oligomer binding assay	18
	2.4 Results	19
	2.4.1 The effect of cholesterol and sphingomyelin on $\alpha$ S oligomer binding in the presence of negatively charged lipids	19
	2.4.2 The effect of lipid headgroup on oligomer binding	22
	2.4.3 The effect of Cardiolipin on $\alpha$ S oligomer binding	23
	2.4.4 The effect of brain lipids on oligomers binding	25
	2.5 Discussion	27
	2.6 References	30



<b>Chapter 3:</b>	<b>Alpha-synuclein oligomers distinctively permeabilize complex model membranes</b>	33
	3.1. Abstract	33
	3.2 Introduction	34
	3.3 Materials and methods	36
	3.3.1 Expression and purification of $\alpha$ S	36
	3.3.2 Labeling of $\alpha$ S	36
	3.3.3 Preparation of unlabeled and labeled $\alpha$ S oligomers	36
	3.3.4 LUVs preparation and calcein release assay	37
	3.3.5 Semi-quantitative $\alpha$ S monomer and oligomer binding assay	38
	3.3.6 SUVs preparation and binding of $\alpha$ S oligomers to SUVs	38
	3.4 Results	40
	3.4.1 Binding of $\alpha$ S monomers to bilayers that mimic lipid composition of natural membranes	40
	3.4.2 Do $\alpha$ S oligomers bind to bilayers mimicking the lipid composition of natural membranes and does this binding result in conformational changes?	42
	3.4.3 Kinetics of membrane permeabilization (Dye release assay)	44
	3.5 Discussion	47
	3.6 Acknowledgments	51
	3.7 References	52
<b>Chapter 4:</b>	<b>Characterization of oligomers formed from disease-related alpha-synuclein amino acid mutations</b>	57
	4.1 Abstract	57
	4.2 Introduction	58
	4.3 Material and methods	59
	4.3.1 Preparation of oligomeric alpha-synuclein	59
	4.3.2 SUVs preparation and binding of $\alpha$ S monomers to SUVs	60
	4.3.4 LUV preparation and calcein release assay	60
	4.3.5 Small-Angle X-ray Scattering	60

4.3.6 Kinetics of aggregation	62
4.3.7 Atomic force microscopy (AFM)	62
4.4 Results	63
4.4.1 Binding of $\alpha$ S monomers to SUVs	63
4.4.2 Aggregation studies	65
4.4.3 Calcein release assay	65
4.4.4 Aggregation number	67
4.5 Discussion	72
4.6 Acknowledgments	74
4.7 References	74
<b>Chapter 5: Are alpha-synuclein oligomers toxic species?</b>	79
5.1 Introduction	79
5.2 Materials and Methods	80
5.2.1 Expression of $\alpha$ S and preparation of oligomers	80
5.2.2 Assay conditions	80
5.2.3 Labeling of SH-SY5Y cells	81
5.2.4 Cell viability in SH-SY5Y cells	81
5.3 Results and discussion	82
5.4 Acknowledgments	87
5.5 References	88
<b>Chapter 6: Alpha-synuclein amyloid multimers act as multivalent nanoparticles to cause hemifusion in negatively charged bilayers</b>	91
6.1 Abstract	91
6.2 Introduction	92
6.3 Material and Methods	93
6.3.1 Expression and purification of $\alpha$ S	93
6.3.2 Labeling of $\alpha$ S-A140C	93
6.3.3 Preparation of unlabeled and labeled $\alpha$ S oligomers	94
6.3.4 LUVs preparation	94
6.3.5 GUVs preparation for clustering experiment and imaging of clustered vesicles	95
6.3.6 Content mixing	95

6.3.7 Lipid mixing	96
6.3.8 Fluorescence Correlation Spectroscopy	96
6.3.9 Estimation of $\alpha$ S oligomers-membrane binding equilibrium	97
6.4 Results	98
6.4.1 $\alpha$ S oligomers induce vesicle clustering	98
6.4.2 Oligomer-induced vesicle fusion	99
6.4.3 Oligomer-induced hemifusion	101
6.5 Discussion	104
6.6 Acknowledgments	106
6.7 References	107
<b>Chapter 7: Conclusion and future recommendations</b>	<b>111</b>
<b>Summary</b>	<b>115</b>
Samenvatting	117
List of abbreviations	119
Acknowledgments/Dankwoord/Zahvalnica	121
List of publications	125
Curriculum vitae	129





# Chapter 1

## Introduction

### 1.1 Alpha synuclein and Parkinson's disease

Alpha-synuclein ( $\alpha$ S) is a 140-amino acid, intrinsically disordered protein encoded by a single gene located on chromosome 4 [1, 2]. It was first described as a neuron-specific protein whose gene is expressed only in neuronal tissue [3]. Almost 10 years later,  $\alpha$ S got attention as a protein linked to familial cases of Parkinson's disease [4]. Together with Alzheimer's disease, Parkinson's disease (PD) is one of the most common neurodegenerative disorders; it affects more than 1% of the population older than 65 [5]. Neurodegenerative disorders are usually characterized by the loss of structure and functionality of neurons [6]. The prevalence of neurodegenerative diseases is growing with a rapidly aging population. PD manifests with movement disorders such as resting tremor, muscular rigidity, bradykinesia, and postural instability. For these symptoms usually the term Parkinsonism is used. Besides motor symptoms, patients may suffer from cognitive impairment, depression, olfactory deficits, psychosis, and sleeping problems [7-10].

The main problem of finding cures for PD is that the symptoms only manifest when already 80% of dopaminergic neurons in the *substantia nigra pars compacta* are lost in the midbrain [11, 12]. Besides the substantia nigra other regions of the brain such as the basal ganglia, brainstem, autonomic nervous system and cerebral cortex are affected. Between 10-20% of all PD patients have a hereditary form of the disease with a reported family disease history [13]. In the last 20 years 5 different missense mutations in addition to gene multiplication of  $\alpha$ S have been linked to PD: A53T [14], A30P [15], E46K [16], H50Q [17, 18] and G51D [19, 20]. On the cellular and tissue levels PD is characterized by the presence of Lewy bodies (LB) and neurites (LN). These inclusion bodies contain proteins aggregated into amyloid fibrils. In LB and LN the protein alpha-synuclein ( $\alpha$ S) is the main fibrillar component.

## 1.2 Properties of alpha-synuclein

From the soluble cytosolic brain fraction, it was estimated that  $\alpha$ S comprises 1% of the total cellular protein content [21]. Although there are several physiological roles proposed for  $\alpha$ S, including a function in the release and trafficking of synaptic vesicles, lipid binding, regulation of certain proteins and survival of neurons, the exact role of  $\alpha$ S is still not known. The protein consists of a positively charged N-terminal region (residues 1-60) containing KTKEGV repeats, a hydrophobic NAC region (residues 61-95) and a negatively charged C-terminal region (residues 96-140) (See **Figure 1.1**). The N-terminal region has an apolipoprotein lipid-binding motif and this motif can result in the formation of amphiphilic  $\alpha$ -helices that play a role in membrane binding [22, 23]. The NAC region has been identified to have a role in aggregation and formation of amyloid fibrils [21]. The occurrence of a 12 amino acid sequence in the NAC region (between positions 71-82) has been reported to play a role in oligomerization and formation of amyloid fibrils [24].

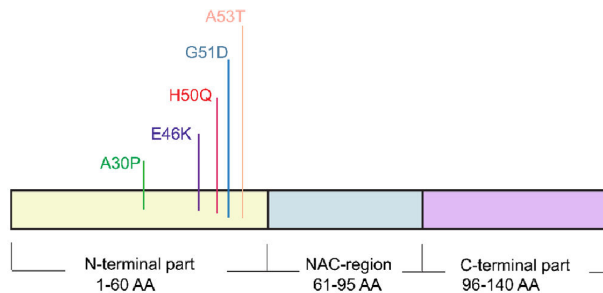


**Figure 1.1: Schematic representation of alpha-synuclein amino acid sequence together with familiar point mutations of PD**

Aggregation is the key process where the  $\alpha$ S protein loses its putative function and gains toxicity [21-24]. The aggregation of  $\alpha$ S starts from intrinsically disordered monomers, which self-assemble and form dimers and then possibly with the help of additional factors convert to (on- and off-pathway) oligomers [25-27], which may assemble into fibrils (**Figure 1.2**) [28]. The aggregated proteins in the fibrils have a characteristic  $\beta$ -sheet conformation and are packed perpendicular to the fiber axis [29]. Although earlier studies assumed fibrils to be toxic, currently it is suggested that oligomers are the main toxic species involved in the cell death of

dopaminergic neurons [30-36]. In the research presented in this thesis I will focus on  $\alpha$ S oligomers. Using different methods and analytical techniques I have studied their interactions with membrane systems and have tried to answer the main research question: *how do the various oligomers bind and permeabilize membranes*. The mechanism of these interactions is still an open question and in this thesis I will focus on model membranes in order to get mechanistic understanding of binding and permeabilization.

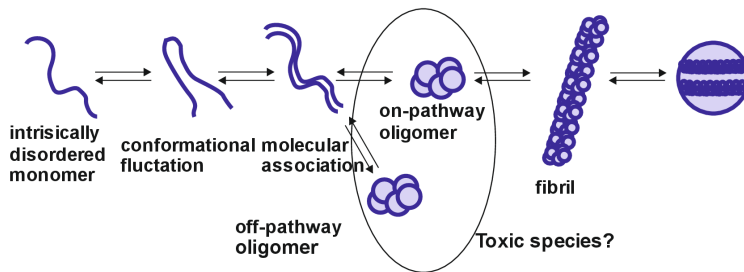


Figure 1.2: Schematic representation of aggregation process of  $\alpha$ S

### 1.3 Oligomeric alpha-synuclein

The current literature proposes oligomers to be the toxic species involved in the neuronal cell death in PD [30-33, 35, 36]. *In vitro* studies showed that it is possible to make stable and/or toxic oligomers under different conditions incubating  $\alpha$ S in: a) high concentrations (mM range) [37, 38] or with: b) metal ions ( $\text{Cu}^{2+}$ ,  $\text{Fe}^{3+}$ ,  $\text{Fe}^{2+}$ ,  $\text{Ni}^{2+}$ ,  $\text{Mg}^{2+}$ ,  $\text{Cd}^{2+}$ ,  $\text{Zn}^{2+}$ ,  $\text{Co}^{2+}$ ,  $\text{Ca}^{2+}$ ) [39-46], c) dopamine [32, 47, 48], and d) lipid peroxidation products (acrolein, 4-oxo-2-nonenal (ONE) and hydroxynonenal (HNE)) [34, 49, 50]. Together these studies underline the significance of soluble  $\alpha$ S oligomers as the toxic species in PD.

### 1.4 Formation and characterization of oligomeric alpha-synuclein

In my thesis I have explored different ways to form and characterize oligomers, based on approaches already described in the literature.



### 1.4.1 High concentration-induced oligomers

Duplications and triplications of SNCA can lead to more severe form of PD [51, 52]. Literature data also suggested that overexpressed wt  $\alpha$ S can be toxic [53-55], in addition to the disease mutants. It was shown *in vitro* that monomeric  $\alpha$ S in higher concentration (in mM range) could form oligomers [37, 38]. Some of these oligomeric species are defined to have ~30 monomers, which was characterized by single molecule photobleaching [56], while some other authors found that oligomers consist of 20-26 monomers [57], and SAXS data analysis suggested that oligomers consist of 30 monomers [58].

### 1.4.2 Metal ion-induced oligomers

Iron deposits have been found in *substantia nigra* of postmortem PD patients [59], and increased levels of copper ions have been found in cerebrospinal fluid of PD patients [60]. *In vivo* studies on neuroblastoma cell lines showed that oligomers in the presence of 100  $\mu$ M  $\text{Cu}^{2+}$  decreased cell viability to  $\leq 50\%$  [61], while  $\text{Fe}^{2+}$  ions increased vulnerability of BE-M17 cells [43]. Metal ions can cause oxidative stress and enhance the fibrillation rate of  $\alpha$ S *in vitro*. It was shown that iron can simulate aggregation of WT, A30P and A53T  $\alpha$ S mutants [43]. The size of spherical and annular metal-induced oligomers has been characterized and varies between 0.8 and 4 nm for  $\text{Cu}^{2+}$ ,  $\text{Fe}^{3+}$  and  $\text{Ni}^{2+}$  up to 70 and 90 nm for  $\text{Ca}^{2+}$  induced oligomers [46]. During fibril formations, 70-90% of  $\text{Cu}^{2+}$  is incorporated into fibrils via a defined primary binding site at His-50 on N-terminus [62]. Recently, two more binding domains for Cu(I)/Ag(I) ions on  $\alpha$ S on positions 1-5 and 116-127 associated with methionine were confirmed by CD and NMR spectroscopy [42].

### 1.4.3 Dopamine-induced oligomers

In PD, oxidation of dopamine is one of the possible causes of cell death. Oxidation of dopamine gives an excessive production of semiquinones,  $\text{H}_2\text{O}_2$  and  $\cdot\text{HO}$  radicals. *In vivo* studies have shown that  $\alpha$ S is the negative regulator of dopamine neurotransmission [63, 64]. Mosharev *et al.* [65] confirmed that increased levels of dopamine (and its metabolic products) and  $\text{Ca}^{2+}$  ions in dopaminergic neurons that are overexpressing  $\alpha$ S are selectively neurotoxic for these neurons. Furthermore,

dopamine can accelerate oligomerization of  $\alpha$ S in intracellular vesicles, but not in the cytosol, and cause the secretion of oligomers in the extracellular matrix [66]. On the molecular level, dopamine covalently modifies  $\alpha$ S in 1:1 ratio through lysines present in the  $\alpha$ S sequence [67, 68]. In the presence of dopamine,  $\alpha$ S forms stable oligomers, which do not fall apart in the presence of SDS and do not convert into fibrils after 6 days [32]. Electron microscopy studies showed that dopamine-induced oligomers vary in size and shapes [32]. Other studies on dopamine-induced oligomers have shown that the oxidation of all four  $\alpha$ S methionine residues is the essential step in the formation of soluble  $\alpha$ S SDS resistant soluble oligomers [47]. Mutation of methionines to alanines resulted in the formation of non-SDS resistant oligomers [47]. Recently two oligomerization mechanisms which may occur in dopamine/Cu induced oligomers were proposed: 1) by noncovalent/reversibly covalent cross-linking or 2) via formation of free radicals [69].

#### **1.4.4 HNE/ONE-induced oligomers**

An increased presence of reactive oxygen species (ROS) in neurons can initiate the peroxidation of polyunsaturated fatty acids (PUFA). The main degradation products of lipid peroxidation in the cell are aldehydes (4-hydroxy-2-nonenal (HNE), 4-oxo-2-nonenal (ONE), acrolein). At physiological conditions, HNE is present in concentrations of approximately 0.1  $\mu$ M [70-72]. However, this concentration can increase during oxidative stress. A 10-200 fold increase of HNE concentration has been reported to cause inhibition of DNA and protein synthesis [73]. Close to peroxidated membranes the concentration of lipid peroxidation products can be enhanced more than 1000 fold. This increase leads to unspecific cell death and inhibition of catabolic (e.g. mitochondrial respiratory chain reactions) and anabolic (e.g. DNA or protein synthesis) metabolic reactions in the cells [74]. It has been shown that the concentration of HNE in isolated microsomal lipid bilayers can be up to ~5 mM and at such high concentrations HNE targets membrane proteins [75, 76]. Lipid peroxidation products are known to be efficient protein modifiers [50, 73, 77]. They can cause oxidative modification of proteins by reacting with histidine and lysine, which than can further accelerate crosslinking of  $\alpha$ S with other proteins [50, 73]. A recent study [78] on HNE-induced oligomers has shown that they are toxic to dopaminergic neuronal cells.

Oligomers produced in the presence of the lipid peroxidation product ONE are approximately 2000 kDa, 40-80 nm wide and 6-8 nm high and rich in  $\beta$ -sheet structure [49]. ONE-induced oligomers have been reported to be a highly soluble and stable species that do not convert into fibrils [34, 49]. HNE-induced oligomers are reported to be 100–200 nm in width and 2–4 nm high [49]. Beside inducing oligomerization of  $\alpha$ S [79], HNE can lead to oligomerization of other proteins such as light chains of immunoglobulin (Ig) [80] and A $\beta$  [81]. HNE- and ONE-induced  $\alpha$ S oligomers showed toxicity on SH-SY5Y cells [49]. Liquid chromatography-tandem MS analysis showed that the primary binding site for these molecules is position His50 [82].

Over the last 10-15 years, oligomeric species described above have been produced and characterized *in vitro*. Their toxicity has been tested on different cell model systems to shed light on molecular species causing cell death in PD. In these studies, cellular membranes have been indicated as major sites for oligomer-induced damage. Our goal here is to better understand which membranes are targeted by  $\alpha$ S oligomers and how these oligomers cause membrane damage.

### 1.5 Alpha-synuclein membrane interactions

To gain a clearer picture on the interaction between membranes and  $\alpha$ S monomers or oligomers, many studies have made use of *in vitro* model membrane systems. Model membranes, such as lipid vesicles, mimic lipid membranes of cells and organelles. Early studies on the colocalization of  $\alpha$ S with synaptic vesicles led to the suggestion that  $\alpha$ S can interact with lipids [21]. Others [83] showed that  $\alpha$ S also binds to model membranes and suggested that  $\alpha$ S-membrane interactions have an important physiological and pathological role.

As mentioned before, the N-terminal part of  $\alpha$ S plays a crucial role in membrane binding [22, 23]. In solution the monomeric intrinsically disordered protein  $\alpha$ S has no secondary structure [84], but upon binding to phospholipid membranes and detergent micelles the protein adopts an  $\alpha$ -helical conformation [22, 37, 85-88]. Circular dichroism (CD) experiments show that the  $\alpha$ -helical content upon binding to membranes increases from 3 to 80% [85]. According to the literature 41% of the  $\alpha$ S protein becomes  $\alpha$ -helical when bound to sodium dodecyl sulfate (SDS) micelles [89], while upon the binding to 1,2-dioleoylphosphatidylglycerol (DOPG): 1,2-dipalmitoylphosphatidylglycerol (DPPG) (DOPG:DPPG) vesicles, 61% of the protein adopts  $\alpha$ -helical structure [90]. Additionally, binding of monomers to

membranes has been characterized using various other biophysical techniques such as fluorescence correlation spectroscopy (FCS) [91-93], fluorescence anisotropy [88], fluorescence recovery after photobleaching (FRAP) [94] and electron paramagnetic resonance spectroscopy (EPR) [86]. These and many other studies showed that the binding of  $\alpha$ S to membranes strongly depends on the presence of negatively charged lipids [84, 85, 91-93, 95, 96]. The amount of protein bound to lipid membranes depends on the available binding sites and the fraction of negatively charged lipids in the lipid mixture [91, 95]. There is still a dispute on the binding of  $\alpha$ S to neutral membranes and although some authors claim that there is no binding [85, 97], other reports do not support these results [91, 98]. It has been suggested that zwitterionic PE together with negatively charged PS enhances  $\alpha$ S membrane interactions in brain lipid extracts [83]. In model membranes  $\alpha$ S shows a higher affinity for PA and PI than for PS membranes [83, 91, 93, 98].

***Oligomer-induced membrane permeabilization.*** Monomers and oligomers both show a high affinity for negatively charged membranes. However, monomers and oligomers differ structurally and only a small fraction of the monomers in the oligomers adopt an  $\alpha$ -helical conformation upon binding to membranes [37]. Moreover while oligomers permeabilize negatively charged membranes at relatively low concentrations (equivalent monomer concentration) [37, 99-101], monomer binding leaves the bilayers intact at these concentrations. Although much is known about the binding of oligomers to negatively charged model membranes [37, 38, 99, 101-103], still little is known on how oligomers interact with membranes containing physiologically relevant fractions of negatively charged lipids.

## 1.6 Scope of this thesis

There are two hypotheses on how oligomers induce membrane permeabilization: the amyloid pore and the carpet hypothesis. The first proposes that  $\alpha$ S oligomers can permeabilize membranes and form trans-membrane pores that disturb the  $\text{Ca}^{2+}$  signaling pathways in the cells [104-106]. Although some groups confirmed the existence of pore-like structures by AFM [107, 108], it is still not clear if oligomers form true annular pores in membranes or that the interaction causes defects at the protein lipid interface or alternatively leads to membrane thinning. The carpet hypothesis suggests that oligomer-induced membrane damage occurs due to strong interactions between the oligomer/monomer amyloid protein and the membrane.

## Chapter 1

These interactions lead to accelerated fibrillization and the growth of lipid-protein aggregates on the membrane [109]. Uptake of the lipids from the membrane by the lipid-protein aggregates causes membrane damage [109, 110].

Our goal here is to gain insights into the details of the mechanism of  $\alpha$ S oligomer-membrane interactions and to answer the following questions:

1. How do different oligomers bind and permeabilize physiologically relevant lipid membranes?
2. Based on model membrane systems, which cellular membranes are most likely involved in oligomer-induced leakage?
3. How do oligomers of the different disease-related mutants (E46K, A53T, A30P, H50Q, G51D) affect membrane integrity in comparison to WT oligomers?
4. How can we characterize different oligomers?
5. Upon the addition of oligomers, what is happening with the membrane: (1) membrane permeabilization or (2) lipid rearrangement? Do  $\alpha$ S oligomers induce fusion/clustering of the vesicles? Is this physiologically relevant?

## 1.7 References

1. X. Chen, H. A. R. d. S., M.J. Pettenati, P.N. Rao, P. St. George-Hyslop, A.D. Roses, Y. Xia, K. Horsburgh, K. Ueda, T. Saitoh (1995) The human NACP/ $\alpha$ -synuclein gene chromosome assignment to 4q21.3-q22 and TaqI RFLP analysis, *Genomics*. **26**, 425-427.
2. Spillantini, M. G., Divane, A. & Goedert, M. (1995) Assignment of human alpha-synuclein (SNCA) and beta-synuclein (SNCB) genes to chromosomes 4q21 and 5q35, *Genomics*. **27**, 379-81.
3. Maroteaux, L., Campanelli, J. T. & Scheller, R. H. (1988) Synuclein: a neuron-specific protein localized to the nucleus and presynaptic nerve terminal, *J Neurosci*. **8**, 2804-15.
4. Polymeropoulos, M., Lavedan, C., Leroy, E., Ide, S., Dehejia, A., Dutra, A., Pike, B., Root, H., Rubenstein, J., Boyer, R., Stenroos, E., Chandrasekharappa, S., Athanassiadou, A., Papapetropoulos, T., Johnson, W., Lazzarini, A., Duvoisin, R., Di Iorio, G., Golbe, L. & Nussbaum, R. (1997) Mutation in the alpha-synuclein gene identified in families with Parkinson's disease, *Science*. **276**, 2045 - 2047.
5. Ozansoy, M. & Basak, A. N. (2013) The central theme of Parkinson's disease: alpha-synuclein, *Mol Neurobiol*. **47**, 460-5.
6. Cannon, J. R. & Greenamyre, J. T. (2011) The role of environmental exposures in neurodegeneration and neurodegenerative diseases, *Toxicol Sci*. **124**, 225-50.
7. Spillantini MG, S. M., Lee VM, Trojanowski JQ, Jakes R, & M, G. (1997) Alpha-synuclein in Lewy bodies, *Nature*. **388**, 839-840.
8. Wolters, E. C. (2009) Non-motor extranigral signs and symptoms in Parkinson's disease, *Parkinsonism Relat Disord*. **15S3**, S6-12.
9. Gasser, T., Hardy, J. & Mizuno, Y. (2011) Milestones in PD genetics, *Movement Disorders*. **26**, 1042-1048.
10. Bekris, L. M., Mata, I. F. & Zabetian, C. P. (2010) The genetics of Parkinson disease, *J Geriatr Psychiatry Neurol*. **23**, 228-42.
11. Cookson, M. R. (2009) alpha-Synuclein and neuronal cell death, *Mol Neurodegener*. **4**, 9.

12. Gasser, T. (2009) Molecular pathogenesis of Parkinson disease: insights from genetic studies, *Expert Rev Mol Med.* **11**, e22.
13. Sellbach, A. N., Boyle, R. S., Silburn, P. A. & Mellick, G. D. (2006) Parkinson's disease and family history, *Parkinsonism Relat Disord.* **12**, 399-409.
14. Polymeropoulos, M. H. (1997) Mutation in the  $\alpha$ -Synuclein Gene Identified in Families with Parkinson's Disease, *Science.* **276**, 2045-2047.
15. Kruger, R., Kuhn, W., Muller, T., Woitalla, D., Graeber, M., Kosel, S., Przuntek, H., Epplen, J. T., Schols, L. & Riess, O. (1998) Ala30Pro mutation in the gene encoding alpha-synuclein in Parkinson's disease, *Nature Genetics.* **18**, 106-108.
16. Zarranz, J. J., Alegre, J., Gomez-Esteban, J. C., Lezcano, E., Ros, R., Ampuero, I., Vidal, L., Hoenicka, J., Rodriguez, O., Atares, B., Llorens, V., Gomez Tortosa, E., del Ser, T., Munoz, D. G. & de Yebenes, J. G. (2004) The new mutation, E46K, of alpha-synuclein causes Parkinson and Lewy body dementia, *Ann Neurol.* **55**, 164-73.
17. Proukakis, C., Dudzik, C. G., Brier, T., MacKay, D. S., Cooper, J. M., Millhauser, G. L., Houlden, H. & Schapira, A. H. (2013) A novel alpha-synuclein missense mutation in Parkinson disease, *Neurology.* **80**, 1062-4.
18. Appel-Cresswell, S., Vilarino-Guell, C., Encarnacion, M., Sherman, H., Yu, I., Shah, B., Weir, D., Thompson, C., Szu-Tu, C., Trinh, J., Aasly, J. O., Rajput, A., Rajput, A. H., Jon Stoessel, A. & Farrer, M. J. (2013) Alpha-synuclein p.H50Q, a novel pathogenic mutation for Parkinson's disease, *Mov Disord.*
19. Kiely, A. P., Asi, Y. T., Kara, E., Limousin, P., Ling, H., Lewis, P., Proukakis, C., Quinn, N., Lees, A. J., Hardy, J., Revesz, T., Houlden, H. & Holton, J. L. (2013) alpha-Synucleinopathy associated with G51D SNCA mutation: a link between Parkinson's disease and multiple system atrophy?, *Acta Neuropathol.* **125**, 753-69.
20. Lesage, S., Anheim, M., Letournel, F., Bousset, L., Honore, A., Rozas, N., Pieri, L., Madiona, K., Durr, A., Melki, R., Verny, C., Brice, A. & French Parkinson's Disease Genetics Study, G. (2013) G51D alpha-synuclein mutation causes a novel parkinsonian-pyramidal syndrome, *Ann Neurol.* **73**, 459-71.
21. Iwai, A., Masliah, E., Yoshimoto, M., Ge, N., Flanagan, L., de Silva, H. A., Kittel, A. & Saitoh, T. (1995) The precursor protein of non-A beta component of Alzheimer's disease amyloid is a presynaptic protein of the central nervous system, *Neuron.* **14**, 467-75.
22. Perrin, R. J., Woods, W. S., Clayton, D. F. & George, J. M. (2000) Interaction of human alpha-Synuclein and Parkinson's disease variants with phospholipids. Structural analysis using site-directed mutagenesis, *J Biol Chem.* **275**, 34393-8.
23. Jo, E., Fuller, N., Rand, R. P., St George-Hyslop, P. & Fraser, P. E. (2002) Defective membrane interactions of familial Parkinson's disease mutant A30P alpha-synuclein, *J Mol Biol.* **315**, 799-807.
24. Giasson, B. I., Murray, I. V., Trojanowski, J. Q. & Lee, V. M. (2001) A hydrophobic stretch of 12 amino acid residues in the middle of alpha-synuclein is essential for filament assembly, *J Biol Chem.* **276**, 2380-6.
25. Uversky, V. N., Lee, H. J., Li, J., Fink, A. L. & Lee, S. J. (2001) Stabilization of partially folded conformation during alpha-synuclein oligomerization in both purified and cytosolic preparations, *J Biol Chem.* **276**, 43495-8.
26. Uversky, V. N. (2007) Neuropathology, biochemistry, and biophysics of alpha-synuclein aggregation, *J Neurochem.* **103**, 17-37.
27. Souza, J. M., Giasson, B. I., Chen, Q., Lee, V. M. & Ischiropoulos, H. (2000) Dityrosine cross-linking promotes formation of stable alpha -synuclein polymers. Implication of nitrative and oxidative stress in the pathogenesis of neurodegenerative synucleinopathies, *J Biol Chem.* **275**, 18344-9.
28. Giehm, L., Svergun, D. I., Otzen, D. E. & Vestergaard, B. (2011) Low-resolution structure of a vesicle disrupting  $\alpha$ -synuclein oligomer that accumulates during fibrillation, *Proc Natl Acad Sci U S A.* **108**, 3246-51.
29. Horvath, I., Weise, C. F., Andersson, E. K., Chorell, E., Sellstedt, M., Bengtsson, C., Olofsson, A., Hultgren, S. J., Chapman, M., Wolf-Watz, M., Almqvist, F. & Wittung-Stafshede, P. (2012)

## Chapter 1

Mechanisms of protein oligomerization: inhibitor of functional amyloids templates alpha-synuclein fibrillation, *J Am Chem Soc.* **134**, 3439-44.

30. Kaye, R., Head, E., Thompson, J. L., McIntire, T. M., Milton, S. C., Cotman, C. W. & Glabe, C. G. (2003) Common structure of soluble amyloid oligomers implies common mechanism of pathogenesis, *Science*. **300**, 486-9.

31. Danzer, K. M., Haasen, D., Karow, A. R., Moussaoui, S., Habeck, M., Giese, A., Kretschmar, H., Hengerer, B. & Kostka, M. (2007) Different species of alpha-synuclein oligomers induce calcium influx and seeding, *J Neurosci.* **27**, 9220-32.

32. Cappai, R., Leck, S. L., Tew, D. J., Williamson, N. A., Smith, D. P., Galatis, D., Sharples, R. A., Curtain, C. C., Ali, F. E., Cherny, R. A., Culvenor, J. G., Bottomley, S. P., Masters, C. L., Barnham, K. J. & Hill, A. F. (2005) Dopamine promotes alpha-synuclein aggregation into SDS-resistant soluble oligomers via a distinct folding pathway, *FASEB J.* **19**, 1377-9.

33. Lashuel, H. A., Petre, B. M., Wall, J., Simon, M., Nowak, R. J., Walz, T. & Lansbury, P. T. (2002)  $\alpha$ -Synuclein, Especially the Parkinson's Disease-associated Mutants, Forms Pore-like Annular and Tubular Protofibrils, *J Mol Biol.* **322**, 1089-1102.

34. Nasstrom, T., Wahlberg, T., Karlsson, M., Nikolajeff, F., Lannfelt, L., Ingelsson, M. & Bergstrom, J. (2009) The lipid peroxidation metabolite 4-oxo-2-nonenal cross-links alpha-synuclein causing rapid formation of stable oligomers, *Biochem Biophys Res Commun.* **378**, 872-6.

35. Koutsopoulos, S., Outeiro, T. F., Putcha, P., Tetzlaff, J. E., Spoelgen, R., Koker, M., Carvalho, F., Hyman, B. T. & McLean, P. J. (2008) Formation of Toxic Oligomeric  $\alpha$ -Synuclein Species in Living Cells, *PLoS ONE.* **3**, e1867.

36. Danzer, K. M., Ruf, W. P., Putcha, P., Joyner, D., Hashimoto, T., Glabe, C., Hyman, B. T. & McLean, P. J. (2011) Heat-shock protein 70 modulates toxic extracellular alpha-synuclein oligomers and rescues trans-synaptic toxicity, *FASEB J.* **25**, 326-36.

37. van Rooijen, B. D., Claessens, M. M. & Subramaniam, V. (2009) Lipid bilayer disruption by oligomeric alpha-synuclein depends on bilayer charge and accessibility of the hydrophobic core, *Biochim Biophys Acta.* **1788**, 1271-8.

38. van Rooijen, B. D., van Leijenhorst-Groener, K. A., Claessens, M. M. & Subramaniam, V. (2009) Tryptophan fluorescence reveals structural features of  $\alpha$ -synuclein oligomers, *J Mol Biol.* **394**, 826-33.

39. Wright, J. A., Wang, X. & Brown, D. R. (2009) Unique copper-induced oligomers mediate alpha-synuclein toxicity, *FASEB J.* **23**, 2384-93.

40. Rose, F., Hodak, M. & Bernholc, J. (2011) Mechanism of copper(II)-induced misfolding of Parkinson's disease protein, *Sci Rep.* **1**, 11.

41. Bharathi, Indi, S. S. & Rao, K. S. (2007) Copper- and iron-induced differential fibril formation in alpha-synuclein: TEM study, *Neurosci Lett.* **424**, 78-82.

42. Camponeschi, F., Valensin, D., Tessari, I., Bubacco, L., Dell'Acqua, S., Casella, L., Monzani, E., Gaggelli, E. & Valensin, G. (2013) Copper(I)-alpha-synuclein interaction: structural description of two independent and competing metal binding sites, *Inorg Chem.* **52**, 1358-67.

43. Ostrerova-Golts, N., Petrucelli, L., Hardy, J., Lee, J. M., Farer, M. & Wolozin, B. (2000) The A53T alpha-synuclein mutation increases iron-dependent aggregation and toxicity, *J Neurosci.* **20**, 6048-54.

44. Jiang, T. F., Zhang, Y. J., Zhou, H. Y., Wang, H. M., Tian, L. P., Liu, J., Ding, J. Q. & Chen, S. D. (2013) Curcumin ameliorates the neurodegenerative pathology in A53T alpha-synuclein cell model of Parkinson's disease through the downregulation of mTOR/p70S6K signaling and the recovery of macroautophagy, *J Neuroimmune Pharmacol.* **8**, 356-69.

45. Felix Schmidt, J. L., Frits Kamp, Hans Kretschmar, Armin Giese, Kai Bötzel (2012) Single-Channel Electrophysiology Reveals a Distinct and Uniform Pore Complex Formed by  $\alpha$ -Synuclein Oligomers in Lipid Membranes, *PLoS ONE.* **7**, e424545.

46. Lowe, R., Pountney, D. L., Jensen, P. H., Gai, W. P. & Voelcker, N. H. (2004) Calcium(II) selectively induces alpha-synuclein annular oligomers via interaction with the C-terminal domain, *Protein Sci.* **13**, 3245-52.

47. Leong, S. L., Pham, C. L., Galatis, D., Fodero-Tavoletti, M. T., Perez, K., Hill, A. F., Masters, C. L., Ali, F. E., Barnham, K. J. & Cappai, R. (2009) Formation of dopamine-mediated alpha-synuclein-soluble oligomers requires methionine oxidation, *Free Radic Biol Med.* **46**, 1328-37.
48. Leong, S. L., Cappai, R., Barnham, K. J. & Pham, C. L. (2009) Modulation of alpha-synuclein aggregation by dopamine: a review, *Neurochem Res.* **34**, 1838-46.
49. Nasstrom, T., Fagerqvist, T., Barbu, M., Karlsson, M., Nikolajeff, F., Kasrayan, A., Ekberg, M., Lannfelt, L., Ingelsson, M. & Bergstrom, J. (2011) The lipid peroxidation products 4-oxo-2-nonenal and 4-hydroxy-2-nonenal promote the formation of alpha-synuclein oligomers with distinct biochemical, morphological, and functional properties, *Free Radic Biol Med.* **50**, 428-37.
50. Shamoto-Nagai, M., Maruyama, W., Hashizume, Y., Yoshida, M., Osawa, T., Riederer, P. & Naoi, M. (2007) In parkinsonian substantia nigra, alpha-synuclein is modified by acrolein, a lipid-peroxidation product, and accumulates in the dopamine neurons with inhibition of proteasome activity, *J Neural Transm.* **114**, 1559-67.
51. Ibanez, P., Bonnet, A. M., Debarges, B., Lohmann, E., Tison, F., Pollak, P., Agid, Y., Durr, A. & Brice, A. (2004) Causal relation between alpha-synuclein gene duplication and familial Parkinson's disease, *Lancet.* **364**, 1169-71.
52. Ibanez, P., Lesage, S., Janin, S., Lohmann, E., Durif, F., Destee, A., Bonnet, A. M., Brefel-Courbon, C., Heath, S., Zelenika, D., Agid, Y., Durr, A. & Brice, A. (2009) Alpha-synuclein gene rearrangements in dominantly inherited parkinsonism: frequency, phenotype, and mechanisms, *Arch Neurol.* **66**, 102-8.
53. Ozansoy, M. & Başak, A. N. (2012) The Central Theme of Parkinson's Disease:  $\alpha$ -Synuclein, *Mol Neurobiol.* **47**, 460-465.
54. Singleton, A. B., Farrer, M., Johnson, J., Singleton, A., Hague, S., Kachergus, J., Hulihan, M., Peuralinna, T., Dutra, A., Nussbaum, R., Lincoln, S., Crawley, A., Hanson, M., Maraganore, D., Adler, C., Cookson, M. R., Muenter, M., Baptista, M., Miller, D., Blancato, J., Hardy, J. & Gwinn-Hardy, K. (2003) alpha-Synuclein locus triplication causes Parkinson's disease, *Science.* **302**, 841.
55. Chartier-Harlin, M.-C., Kachergus, J., Roumier, C., Mouroux, V., Douay, X., Lincoln, S., Levecque, C., Larvor, L., Andrieux, J., Hulihan, M., Waucquier, N., Defebvre, L., Amouyel, P., Farrer, M. & Destée, A. (2004)  $\alpha$ -synuclein locus duplication as a cause of familial Parkinson's disease, *The Lancet.* **364**, 1167-1169.
56. Zijlstra, N., Blum, C., Segers-Nolten, I. M., Claessens, M. M. & Subramaniam, V. (2012) Molecular composition of sub-stoichiometrically labeled alpha-synuclein oligomers determined by single-molecule photobleaching, *Angew Chem Int Ed Engl.* **51**, 8821-4.
57. Lashuel, H. A., Hartley, D., Petre, B. M., Walz, T. & Lansbury, P. T. (2002) Neurodegenerative disease: Amyloid pores from pathogenic mutations, *Nature.* **418**, 291-291.
58. Lorenzen, N., Nielsen, S. B., Buell, A. K., Kaspersen, J. D., Arosio, P., Vad, B. S., Paslawski, W., Christiansen, G., Valnickova-Hansen, Z., Andreassen, M., Enghild, J. J., Pedersen, J. S., Dobson, C. M., Knowles, T. P. & Otzen, D. E. (2014) The role of stable alpha-synuclein oligomers in the molecular events underlying amyloid formation, *J Am Chem Soc.* **136**, 3859-68.
59. Castellani, R. J., Siedlak, S. L., Perry, G. & Smith, M. A. (2000) Sequestration of iron by Lewy bodies in Parkinson's disease, *Acta Neuropathol.* **100**, 111-4.
60. Pall, H. S., Williams, A. C., Blake, D. R., Lunec, J., Gutteridge, J. M., Hall, M. & Taylor, A. (1987) Raised cerebrospinal-fluid copper concentration in Parkinson's disease, *Lancet.* **2**, 238-41.
61. Wright, J. A., Wang, X. & Brown, D. R. (2009) Unique copper-induced oligomers mediate alpha-synuclein toxicity, *The FASEB Journal.* **23**, 2384-2393.
62. Rasia, R. M., Bertocini, C. W., Marsh, D., Hoyer, W., Cherny, D., Zweckstetter, M., Griesinger, C., Jovin, T. M. & Fernandez, C. O. (2005) Structural characterization of copper(II) binding to alpha-synuclein: Insights into the bioinorganic chemistry of Parkinson's disease, *Proc Natl Acad Sci U S A.* **102**, 4294-9.
63. Abeliovich, A., Schmitz, Y., Farinas, I., Choi-Lundberg, D., Ho, W. H., Castillo, P. E., Shinsky, N., Verdugo, J. M., Armanini, M., Ryan, A., Hynes, M., Phillips, H., Sulzer, D. & Rosenthal, A. (2000) Mice lacking alpha-synuclein display functional deficits in the nigrostriatal dopamine system, *Neuron.* **25**, 239-52.



## Chapter 1

64. Yavich, L., Tanila, H., Vepsalainen, S. & Jakala, P. (2004) Role of alpha-synuclein in presynaptic dopamine recruitment, *J Neurosci.* **24**, 11165-70.
65. Mosharov, E. V., Larsen, K. E., Kanter, E., Phillips, K. A., Wilson, K., Schmitz, Y., Krantz, D. E., Kobayashi, K., Edwards, R. H. & Sulzer, D. (2009) Interplay between cytosolic dopamine, calcium, and alpha-synuclein causes selective death of substantia nigra neurons, *Neuron.* **62**, 218-29.
66. Lee, H. J., Baek, S. M., Ho, D. H., Suk, J. E., Cho, E. D. & Lee, S. J. (2011) Dopamine promotes formation and secretion of non-fibrillar alpha-synuclein oligomers, *Exp Mol Med.* **43**, 216-22.
67. Conway, K. A., Rochet, J. C., Bieganski, R. M. & Lansbury, P. T., Jr. (2001) Kinetic stabilization of the alpha-synuclein protofibril by a dopamine-alpha-synuclein adduct, *Science.* **294**, 1346-9.
68. Li, J., Zhu, M., Manning-Bog, A. B., Di Monte, D. A. & Fink, A. L. (2004) Dopamine and L-dopa disaggregate amyloid fibrils: implications for Parkinson's and Alzheimer's disease, *FASEB J.* **18**, 962-4.
69. Ha, Y., Yang, A., Lee, S., Kim, K., Liew, H., Lee, S. H., Lee, J. E., Lee, H. I., Suh, Y. H., Park, H. S. & Churchill, D. G. (2014) Dopamine and Cu<sup>+2</sup> can induce oligomerization of alpha-synuclein in the absence of oxygen: Two types of oligomerization mechanisms for alpha-synuclein and related cell toxicity studies, *J Neurosci Res.* **92**, 359-68.
70. Curzio, M., Esterbauer, H., Di Mauro, C., Cecchini, G. & Dianzani, M. U. (1986) Chemotactic activity of the lipid peroxidation product 4-hydroxynonenal and homologous hydroxyalkenals, *Biol Chem Hoppe Seyler.* **367**, 321-9.
71. Curzio, M. (1988) Interaction between neutrophils and 4-hydroxyalkenals and consequences on neutrophil motility, *Free Radic Res Commun.* **5**, 55-66.
72. Curzio, M., Esterbauer, H., Dimauro, C. & Dianzani, M. U. (1990) Influence of the lipid-peroxidationproduct 4-hydroxynonenal on human neutrophil migration *Int J Immunother.* **6**, 13-18.
73. Esterbauer, H., Schaur, R. J. & Zollner, H. (1991) Chemistry and biochemistry of 4-hydroxynonenal, malonaldehyde and related aldehydes, *Free Radic Biol Med.* **11**, 81-128.
74. Benedetti, A., Comporti, M., Fulceri, R. & Esterbauer, H. (1984) Cytotoxic aldehydes originating from the peroxidation of liver microsomal lipids. Identification of 4,5-dihydroxydecenal, *Biochim Biophys Acta.* **792**, 172-81.
75. Koster, J. F., Slee, R. G., Montfoort, A., Lang, J. & Esterbauer, H. (1986) Comparison of the inactivation of microsomal glucose-6-phosphatase by in situ lipid peroxidation-derived 4-hydroxynonenal and exogenous 4-hydroxynonenal, *Free Radic Res Commun.* **1**, 273-87.
76. Uchida, K. (2003) 4-Hydroxy-2-nonenal: a product and mediator of oxidative stress, *Prog Lipid Res.* **42**, 318-43.
77. Lee, S. H. & Blair, I. A. (2000) Characterization of 4-oxo-2-nonenal as a novel product of lipid peroxidation, *Chem Res Toxicol.* **13**, 698-702.
78. Xiang, W., Schlachetzki, J. C., Helling, S., Bussmann, J. C., Berlinghof, M., Schaffer, T. E., Marcus, K., Winkler, J., Klucken, J. & Becker, C. M. (2013) Oxidative stress-induced posttranslational modifications of alpha-synuclein: specific modification of alpha-synuclein by 4-hydroxy-2-nonenal increases dopaminergic toxicity, *Mol Cell Neurosci.* **54**, 71-83.
79. Qin, Z., Hu, D., Han, S., Reaney, S. H., Di Monte, D. A. & Fink, A. L. (2007) Effect of 4-hydroxy-2-nonenal modification on alpha-synuclein aggregation, *J Biol Chem.* **282**, 5862-70.
80. Nieva, J., Shafton, A., Altobelli, L. J., 3rd, Tripuraneni, S., Rogel, J. K., Wentworth, A. D., Lerner, R. A. & Wentworth, P., Jr. (2008) Lipid-derived aldehydes accelerate light chain amyloid and amorphous aggregation, *Biochemistry.* **47**, 7695-705.
81. Siegel, S. J., Bieschke, J., Powers, E. T. & Kelly, J. W. (2007) The oxidative stress metabolite 4-hydroxynonenal promotes Alzheimer protofibril formation, *Biochemistry.* **46**, 1503-10.
82. Lind, S., Trostchansky, A., Hodara, R., Oe, T., Blair, Ian A., Ischiropoulos, H., Rubbo, H. & Souza, José M. (2006) Interaction with phospholipids modulates  $\alpha$ -synuclein nitration and lipid-protein adduct formation, *Biochemical Journal.* **393**, 343.
83. Jo, E., McLaurin, J., Yip, C. M., St George-Hyslop, P. & Fraser, P. E. (2000) alpha-Synuclein membrane interactions and lipid specificity, *J Biol Chem.* **275**, 34328-34.
84. Eliezer, D., Kutluay, E., Bussell, R., Jr. & Browne, G. (2001) Conformational Properties of alpha-Synuclein in its Free and Lipid-associated States, *J Mol Biol.* **307**, 1061-73.

85. Davidson, W. S., Jonas, A., Clayton, D. F. & George, J. M. (1998) Stabilization of alpha-synuclein secondary structure upon binding to synthetic membranes, *J Biol Chem.* **273**, 9443-9.
86. Jao, C. C., Hegde, B. G., Chen, J., Haworth, I. S. & Langen, R. (2008) Structure of membrane-bound alpha-synuclein from site-directed spin labeling and computational refinement, *Proc Natl Acad Sci U S A.* **105**, 19666-71.
87. Akihiko Iwai, E. M., Makoto Yoshimoto,, Nianfeng Ge, L. F., H. A. Rohan de Silva, & Agnes Kitte, a. T. S. (1995) The precursor protein of non-A $\beta$  component of Alzheimer's disease amyloid is a presynaptic protein of the central nervous system, *Neuron.* **14**, 467-475.
88. Zigoneanu, I. G., Yang, Y. J., Krois, A. S., Haque, E. & Pielak, G. J. (2012) Interaction of alpha-synuclein with vesicles that mimic mitochondrial membranes, *Biochim Biophys Acta.* **1818**, 512-9.
89. Chandra, S., Chen, X., Rizo, J., Jahn, R. & Sudhof, T. C. (2003) A broken alpha-helix in folded alpha-Synuclein, *J Biol Chem.* **278**, 15313-8.
90. Bartels, T., Ahlstrom, L. S., Leftin, A., Kamp, F., Haass, C., Brown, M. F. & Beyer, K. (2010) The N-terminus of the intrinsically disordered protein alpha-synuclein triggers membrane binding and helix folding, *Biophys J.* **99**, 2116-24.
91. Rhoades, E., Ramlall, T. F., Webb, W. W. & Eliezer, D. (2006) Quantification of alpha-synuclein binding to lipid vesicles using fluorescence correlation spectroscopy, *Biophys J.* **90**, 4692-700.
92. Trexler, A. J. & Rhoades, E. (2009) Alpha-synuclein binds large unilamellar vesicles as an extended helix, *Biochemistry.* **48**, 2304-6.
93. Middleton, E. R. & Rhoades, E. (2010) Effects of curvature and composition on alpha-synuclein binding to lipid vesicles, *Biophys J.* **99**, 2279-88.
94. Pandey, A. P., Haque, F., Rochet, J. C. & Hovis, J. S. (2009) Clustering of alpha-synuclein on supported lipid bilayers: role of anionic lipid, protein, and divalent ion concentration, *Biophys J.* **96**, 540-51.
95. Stockl, M., Fischer, P., Wanker, E. & Herrmann, A. (2008) Alpha-synuclein selectively binds to anionic phospholipids embedded in liquid-disordered domains, *J Mol Biol.* **375**, 1394-404.
96. Zhu, M., Li, J. & Fink, A. L. (2003) The association of alpha-synuclein with membranes affects bilayer structure, stability, and fibril formation, *J Biol Chem.* **278**, 40186-97.
97. Pfefferkorn, C. M. & Lee, J. C. (2010) Tryptophan Probes at the  $\alpha$ -Synuclein and Membrane Interface, *J Phys Chem B.* **114**, 4615-22.
98. Shvadchak, V. V., Falomir-Lockhart, L. J., Yushchenko, D. A. & Jovin, T. M. (2011) Specificity and kinetics of alpha-synuclein binding to model membranes determined with fluorescent excited state intramolecular proton transfer (ESIPT) probe, *J Biol Chem.* **286**, 13023-32.
99. van Rooijen, B. D., Claessens, M. M. & Subramaniam, V. (2010) Membrane Permeabilization by Oligomeric alpha-Synuclein: In Search of the Mechanism, *PLoS One.* **5**, e14292.
100. Stockl, M. T., Zijlstra, N. & Subramaniam, V. (2013) alpha-Synuclein oligomers: an amyloid pore? Insights into mechanisms of alpha-synuclein oligomer-lipid interactions, *Mol Neurobiol.* **47**, 613-21.
101. Stockl, M., Claessens, M. M. & Subramaniam, V. (2012) Kinetic measurements give new insights into lipid membrane permeabilization by  $\alpha$ -synuclein oligomers, *Mol Biosyst.* **8**, 338-45.
102. van Rooijen, B. D., Claessens, M. M. & Subramaniam, V. (2008) Membrane binding of oligomeric alpha-synuclein depends on bilayer charge and packing, *FEBS Lett.* **582**, 3788-92.
103. van Rooijen, B. D., Claessens, M. M. & Subramaniam, V. (2010) Membrane interactions of oligomeric alpha-synuclein: potential role in Parkinson's disease, *Curr Protein Pept Sci.* **11**, 334-42.
104. Kaye, R., Sokolov, Y., Edmonds, B., McIntire, T. M., Milton, S. C., Hall, J. E. & Glabe, C. G. (2004) Permeabilization of lipid bilayers is a common conformation-dependent activity of soluble amyloid oligomers in protein misfolding diseases, *J Biol Chem.* **279**, 46363-6.
105. Volles, M. J., Lee, S. J., Rochet, J. C., Shtilerman, M. D., Ding, T. T., Kessler, J. C. & Lansbury, P. T., Jr. (2001) Vesicle Permeabilization by Protofibrillar alpha-Synuclein: Implications for the Pathogenesis and Treatment of Parkinson's Disease, *Biochemistry.* **40**, 7812-19.
106. Volles, M. J. & Lansbury, P. T. (2002) Vesicle Permeabilization by Protofibrillar  $\alpha$ -Synuclein Is Sensitive to Parkinson's Disease-Linked Mutations and Occurs by a Pore-like Mechanism, *Biochemistry.* **41**, 4595-4602.

## Chapter 1

107. Quist, A., Doudevski, I., Lin, H., Azimova, R., Ng, D., Frangione, B., Kagan, B., Ghiso, J. & Lal, R. (2005) Amyloid ion channels: a common structural link for protein-misfolding disease, *Proc Natl Acad Sci U S A.* **102**, 10427-32.
108. Kaye, R., Pensalfini, A., Margol, L., Sokolov, Y., Sarsoza, F., Head, E., Hall, J. & Glabe, C. (2009) Annular protofibrils are a structurally and functionally distinct type of amyloid oligomer, *J Biol Chem.* **284**, 4230-7.
109. Sparr, E., Engel, M. F. M., Sakharov, D. V., Sprong, M., Jacobs, J., de Kruijff, B., Höppener, J. W. M. & Antoinette Killian, J. (2004) Islet amyloid polypeptide-induced membrane leakage involves uptake of lipids by forming amyloid fibers, *FEBS Letters.* **577**, 117-120.
110. Zhao, H. X., Tuominen, E. K. J. & Kinnunen, P. K. J. (2004) Formation of amyloid fibers triggered by phosphatidylserine-containing membranes, *Biochemistry.* **43**, 10302-10307.

## Chapter 2

# **$\alpha$ S oligomer binding to bilayers with increasingly complex lipid compositions**

### **2.1 Abstract**

Membranes are considered a major site at which  $\alpha$ -synuclein oligomers cause damage in Parkinson's disease. However, not all biological membranes are damaged by oligomer-membrane interactions. An important parameter defining whether certain membranes are affected is the binding affinity of the oligomers to the relevant membrane. In order to explain damage to specific membranes in more detail we qualitatively investigated how membrane binding of  $\alpha$ S oligomers depends on the lipid composition and overall membrane charge of membranes with more than two components. Cholesterol does not prevent the binding of oligomers to membranes but makes them less vulnerable to permeabilization. With increasingly complex lipid compositions  $\alpha$ S oligomer binding decreases. We conclude that, as observed for 2-component membranes, the membranes with a more complex lipid composition should contain at least 20% negatively charged lipids to bind  $\alpha$ S oligomers.

### **2.2 Introduction**

Although the exact function of the protein  $\alpha$ -synuclein ( $\alpha$ S) is still under investigation, it has become apparent over the years that membrane binding is an important aspect of  $\alpha$ S function. Some early studies on  $\alpha$ S from *Torpedo Californica* demonstrated  $\alpha$ S to be localized in close proximity of the nuclear membrane [1]. Others studies showed that  $\alpha$ S is associated with synaptic membranes and suggested that a fraction of the cellular  $\alpha$ S pool binds to these membranes [2, 3]. Additionally  $\alpha$ S has been found near presynaptic terminals [4] and is reported to interact with plasma membranes [5] and mitochondrial membranes [6, 7]. Together these studies indicate that  $\alpha$ S likely has a membrane-associated function.

The ability of  $\alpha$ S to bind membranes is thought to contribute to cell death in PD. Binding of amyloidogenic proteins, such as  $\alpha$ S, to membranes can cause permeabilization of the bilayers, which is toxic for cells [8]. Besides binding to

## Chapter 2

membranes,  $\alpha$ S can self-assemble into oligomers and amyloid fibrils. Oligomeric  $\alpha$ S is thought to be the main toxic species that causes membrane damage in PD. Mitochondrial membranes have been indicated as the site of  $\alpha$ S oligomer-induced damage [7, 9, 10]. It has also been reported that the plasma membrane can be a target of  $\alpha$ S oligomer-induced permeabilization [11].

The different membrane systems in cells differ in lipid and protein composition. Additionally, the inner and outer membrane leaflets in cells are asymmetric in lipid composition. The inner leaflet of the plasma membrane is mainly composed of the phospholipids PS, PG, PI, PA and PE, while the outer leaflet contains the zwitterionic phospholipid PC and sphingolipid sphingomyelin [12]. The lipids found in synaptic vesicle membranes are mainly phospholipids (PC, PE, PS, PI), sphingolipids (sphingomyelin) and sterols (cholesterol) [12-14]. The weight ratio between total phospholipid and cholesterol concentration in synaptic vesicles is 1:1 [14]. The mitochondrial membrane is the only membrane that contains cardiolipin [15]. Cardiolipin is mainly localized in the inner mitochondrial membrane and in contact sites. Nuclear membranes are rich in PI; the PI content of this membrane amounts to 15% of the total phospholipids [14]. These differences in lipid composition of the membranes of cellular compartments most likely influences  $\alpha$ S oligomer localization and thus determines which membranes are damaged by oligomers.

The first study of  $\alpha$ S binding to membranes, done on model membranes more than 15 years ago [16], showed that monomeric  $\alpha$ S preferentially binds to negatively charged membranes. Electrostatic interactions represent the first step in binding of monomeric  $\alpha$ S to membranes [17]. Monomeric  $\alpha$ S binds to negatively charged membranes by folding into an amphipathic  $\alpha$ -helix. The binding of  $\alpha$ S to negatively charged lipids is mediated by lysines present in the N-terminal part of the protein [18]. Oligomeric  $\alpha$ S species seem to have a similar preference for the negatively charged bilayers [19-22]. Increasing the fraction of negatively charged lipids in vesicle membranes encourages the binding of  $\alpha$ S monomers [23, 24] and oligomers [20]. Binding of monomeric and oligomeric  $\alpha$ S to charged phospholipids not only depends on charge but also on other headgroup characteristics (e.g.  $\alpha$ S binds with higher affinity to membranes that contain PS headgroup with polyunsaturated fatty acyl chain rather than with the oleoyl side chain); it decreases in the order PA>PI>PS [20, 24-28]. A study with GUVs showed that oligomers show higher binding affinity to POPC:DOPA and POPC:POPG mixtures than to POPC:POPS, which suggested a specificity for lipid headgroups in membrane

binding [20]. Besides charge density, and possibly headgroup specificity, lipid packing affects  $\alpha$ S binding. Confocal microscopy on negatively charged GUVs showed that monomeric  $\alpha$ S preferentially binds to liquid disordered phases ( $l_d$ ) over liquid ordered ( $l_o$ ) ones [24].

However, model membranes composed of one or two lipid species are not representative for the complex lipid compositions found in cells. Little is known on the binding of  $\alpha$ S oligomers to natural membranes, and subsequent membrane permeabilization. In this chapter, I will therefore study the binding of  $\alpha$ S oligomers to GUVs with an increasingly complex lipid composition. The results obtained here will enable us to choose relevant model systems that mimic membranes found in cells. These specific membrane compositions would be further used for more detailed study.

## **2.3 Materials and Methods**

### **2.3.1 Expression and purification of $\alpha$ -synuclein**

Expression and purification of human wild-type (WT)  $\alpha$ S and the cysteine (Cys) mutant  $\alpha$ S-A140C was performed as previously described [29]. The protein concentration was determined by measuring the absorbance on a Shimadzu spectrophotometer at 276 nm, using molar extinction coefficients of  $5600 \text{ M}^{-1}\text{cm}^{-1}$  for WT and  $5745 \text{ M}^{-1}\text{cm}^{-1}$  for A140C [30, 31].

### **2.3.2 Labeling of alpha-synuclein**

The cysteine mutant  $\alpha$ S-A140C was used for labeling the protein with an Alexa Fluor 488 C5 maleimide dye (A488), which was obtained from Invitrogen (Carlsbad, California). Prior to labeling a six-fold molar excess of dithiothreitol (DTT) was added to  $\alpha$ S-A140C to reduce disulfide bonds. After 30 minutes of incubation, DTT was removed using Zeba Spin desalting columns, and a two-fold excess of A488 was added. After 1 hour incubation, excess of free dye was removed using two desalting steps. To determine the protein and A488 concentration the absorbance at 276 nm was measured assuming a molar extinction coefficient of  $5745 \text{ M}^{-1}\text{cm}^{-1}$  for the protein and at 495 nm using a molar extinction

## Chapter 2

coefficient of  $72000 \text{ M}^{-1} \text{ cm}^{-1}$  for the dye. The labeling efficiency was estimated to be between 90-100 %.

### 2.3.3 Preparation of labeled $\alpha$ S oligomers

Briefly, oligomers were obtained by incubating  $\alpha$ S monomers at high concentrations (1 mM) in the absence of any additional factors [19]. Alexa 488 labeled oligomers with 7.5 % labeling density, achieved by mixing appropriate quantities of labeled and unlabeled protein, were prepared for membrane binding studies by confocal microscopy. Oligomers were purified and separated from monomers using size-exclusion chromatography. To confirm the presence of oligomers a native PAGE gradient gel was used with a polyacrylamide gradient between 3 and 16%. Monomers could not be detected in the oligomer preparation.

### 2.3.4 Qualitative oligomer binding assay

Giant unilamellar vesicles (GUVs) were prepared as previously described by Angelova [32] and Stöckl [33] on indium tin oxide (ITO) covered glass slides. 1% DOPE-Rhodamine was included in the lipid mixtures to facilitate visualization of the lipid bilayer. Electroswellling of GUVs was done using a constant frequency of 10 Hz and increasing the voltage from 0.1 to 1.1 V during 48 minutes. This voltage was held for another 100 min. To separate GUVs from the ITOs slides, a voltage of 1.3 V was applied using frequency of 4 Hz for 30 min. Vesicles were stored at 4°C and used within one week after preparation.

GUVs were equilibrated with fluorescently-labeled oligomers for 30 minutes before imaging. In all experiments DOPG vesicles were used as a positive control for binding of oligomers to membranes. Binding of fluorescently-labeled  $\alpha$ S oligomers to GUV membranes was assessed using the green 488 nm imaging channel of a confocal Zeiss LSM 510 microscope. Imaging conditions (objective 63X, pixel dwell, pinhole size, image size, digital offset and digital gain) were the same for both red (543 nm) and green (488 nm) channel. However, the master gain of the green (488 nm) channel is different and is given for each specific type of GUVs in **Table 2.1**.

**Table 2.1: Master gain for the green (488 nm) channel according to the type of membrane that was imaged**

<b>Lipid</b>	<b>Master gain for the 488 nm channel</b>
DOPG	1087
DOPG:DPPG	794
DOPG:DPPG:ch	930
DOPG:DPPG:sm:ch	919
DOPA:sm:ch	769
POPG:sm:ch	931
POPS:sm:ch	1087
CL:POPC	794
CL:POPE:POPC	1087
CL:POPE:POPC	1100
CL:soyPI:POPE:POPC	1100
CL:brain PE	1100
POPC:DOPA	1087
POPS:ch	1087
brain PS:brain PE	1087
brain PS:brain PE:ch	1087

## 2.4 Results

### 2.4.1 The effect of cholesterol and sphingomyelin on $\alpha$ S oligomer binding in the presence of negatively charged lipids

$\alpha$ S oligomers are reported to bind to bilayers composed of negatively charged phospholipids [19]. When fluorescently labeled GUVs composed of the negatively charged phospholipid DOPG are incubated with labeled oligomers we indeed observe colocalization of these oligomers with the GUV membrane (**Figure 2.1A**). The fluorescence signal from oligomers, visible in the green channel, shows that in excess of oligomers, not all oligomers are bound to the lipid bilayer. Oligomers are also found in both the vesicle interior and in the exterior solution. This suggests that oligomers are, at some point, able to penetrate the bilayer. In DOPG both the fatty acid chains contain an unsaturation which may render the bilayers particularly vulnerable to oligomer-induced membrane damage and subsequent diffusion of the



## Chapter 2

oligomers through the membrane. Decreasing the amount of unsaturated lipids by replacing half of the unsaturated lipids with saturated DPPG does not change the result. Oligomers are able to bind DOPG:DPPG membranes and the presence of oligomers in the vesicle interior again suggest that they can diffuse over the DOPG:DPPG membrane (**Figure 2.1B**). Cholesterol (ch) plays an important role in maintaining the structural integrity of membranes. When cholesterol was added to a DOPG:DPPG mixture, oligomers were still able to bind the membrane (**Figure 2.1C**). The increased structural integrity resulting from the incorporation of cholesterol has decreased vulnerability of the membrane to oligomer-induced disruption. Besides phospholipids and sterols, sphingolipids such as sphingomyelin (sm) are important membrane building blocks. Sphingomyelin has a high phase transition temperature and interacts with cholesterol. These properties are thought to be responsible for the formation of more ordered microdomains, also called rafts, in the membrane. This phase separation in microdomains is not visible in GUVs composed of a 1:1:1:1 ratio of DOPG:DPPG:ch:sm (**Figure 2.1D**). The DOPE-Rhodamine in the bilayer has a preference for disordered phases and the equal distribution of DOPE-Rhodamine over the vesicle surface suggests that the membrane does not phase separate on length scales visible with confocal microscopy. Although the surface charge density of the bilayer has decreased with the incorporation of sm, this does not appear to interfere with oligomer binding. The fluorescence signal from the oligomers is found to colocalize with the membrane fluorescence. As observed for DOPG:DOPC:ch GUVs the vesicle interior and exterior of the DOPG:DOPC:ch:sm vesicles do not contain equal amounts of oligomers (**Figure 2.1D**). The interaction between sm and ch and the possible formation of small domains has not decreased the structural integrity of the membrane. Oligomers can bind but cannot pass the DOPG:DOPC:ch:sm bilayer.

$\alpha$ S oligomer binding to bilayers with increasingly complex lipid compositions

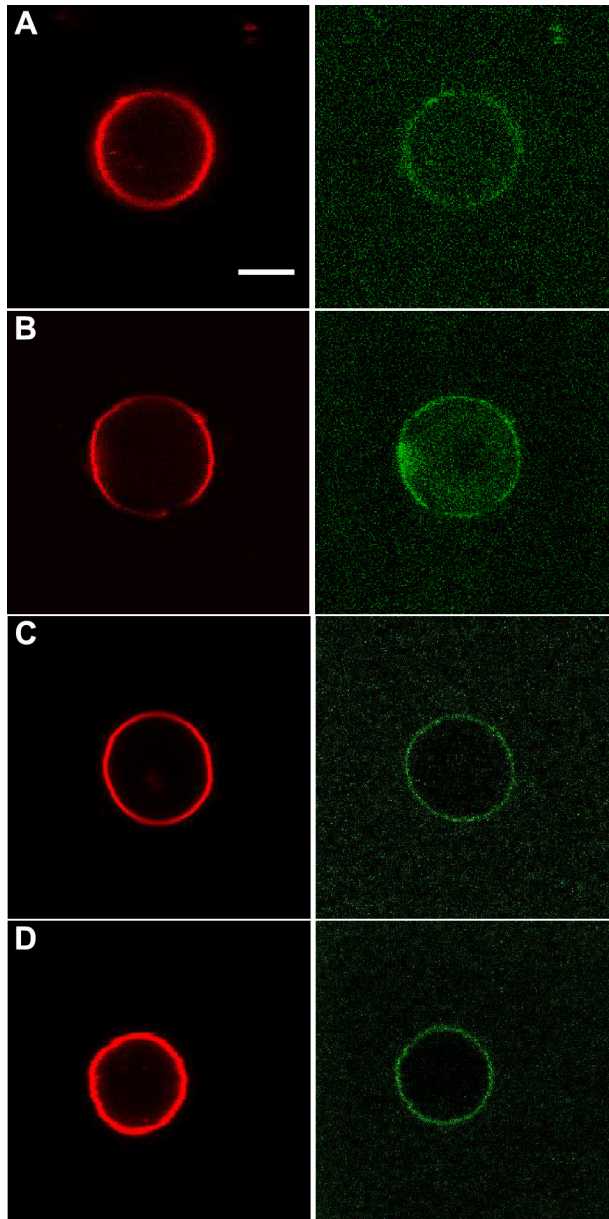


**Figure 2.1:** Representative confocal microscopy images of DOPE-Rhodamine labeled GUVs negatively charged phospholipid(s) (red channel) and  $\alpha$ S wt-140C-A488 oligomers (green channel). A) DOPG, B) DOPG:DPPG (1:1), C), DOPG:DPPG:ch (1:1:1) and D) DOPG:DPPG:ch:sm (1:1:1:1). Imaging conditions of the red (543 nm) and the green (488 nm) channel were the same for all the images, except the master gain of the green channel which is given in Table 2.1. Scale bar corresponds 5  $\mu$ m.

### 2.4.2 The effect of lipid headgroup on oligomer binding

Besides the different lipid species that are present in physiological membranes there is also a variation in the composition of a single lipid species. The different headgroups found in phospholipids is an example of this variation. The headgroups of naturally occurring phospholipids are either negatively charged or zwitterionic. The phospholipids PS, PG, PA and PI have a negatively charged headgroup and are common in biological membranes. In order to determine the influence of negatively-charged lipid headgroups on  $\alpha$ S oligomer membrane binding we have investigated the effect of different negatively charged headgroups in lipid bilayers containing cholesterol and sphingomyelin (**Figure 2.2**). We have used three different lipid compositions: DOPA:ch:sm (1:1:1), POPG:ch:sm (1:1:1) and POPS:ch:sm (1:1:1). The distribution of DOPE-Rhodamine in the DOPA:ch:sm (1:1:1) lipid vesicles shows that this membrane phase separates (**Figure 2.2A**). When  $\alpha$ S oligomers were added in excess to these membranes, oligomers tended to bind to both the disordered and ordered lipid domains. However, the higher fluorescence intensity in the green channel indicates more  $\alpha$ S oligomers are bound to the disordered domains which also favor DOPE-Rhodamine localization (**Figure 2.2A**). POPG:ch:sm membranes do not show signs of phase separation (**Figure 2.2B**). Moreover, when the oligomers were incubated with POPG:ch:sm GUVs, no oligomer binding could be observed. Images of DOPE-Rhodamine in POPS:ch:sm GUVs do not show any phase separation or oligomer binding (**Figure 2C**). From this experiment we conclude that the binding of oligomers to membranes that contain negatively charged lipids, sphingomyelin and cholesterol does not depend only on the charge of the lipids or the charge density of the membrane. Vesicles containing DOPA bind oligomers, while no association of oligomers with vesicles containing POPG or POPS is observed. This may indicate that oligomers preferentially bind PA. We cannot however exclude that the observed effect is due to differences in packing of the lipids, since the used hydrophobic tails (fatty acids) DO versus PO of the phospholipids were different during these experiments.

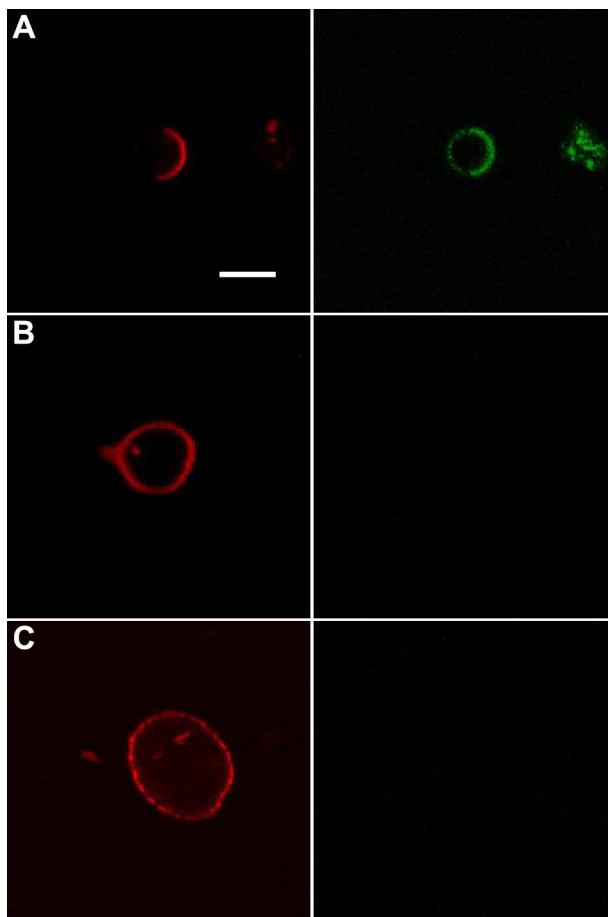


**Figure 2.2: Representative confocal microscopy images of DOPE-Rhodamine labeled GUVs that contain sm, ch and negatively charged phospholipids (red channel) and  $\alpha$ S wt-140C-A488 oligomers (green channel).** The following mixtures were used: A) DOPA:sm:ch, B) POPG:ch:sm and C) POPS:ch:sm, where the binding was only observed with DOPA:sm:ch. Scale bar indicates 5  $\mu$ m.

### 2.4.3 The effect of Cardiolipin on $\alpha$ S oligomer binding

In eukaryotic cells, mitochondrial membranes, especially the inner mitochondrial membrane and mitochondrial contact sites, are very rich in cardiolipin, a negatively charged diphosphatidylglycerol. Cardiolipin represents 20% of the total lipid composition of the mitochondrial inner membrane, while in mitochondrial contact sites that percentage is somewhat higher and lies between 20 and 25%. In

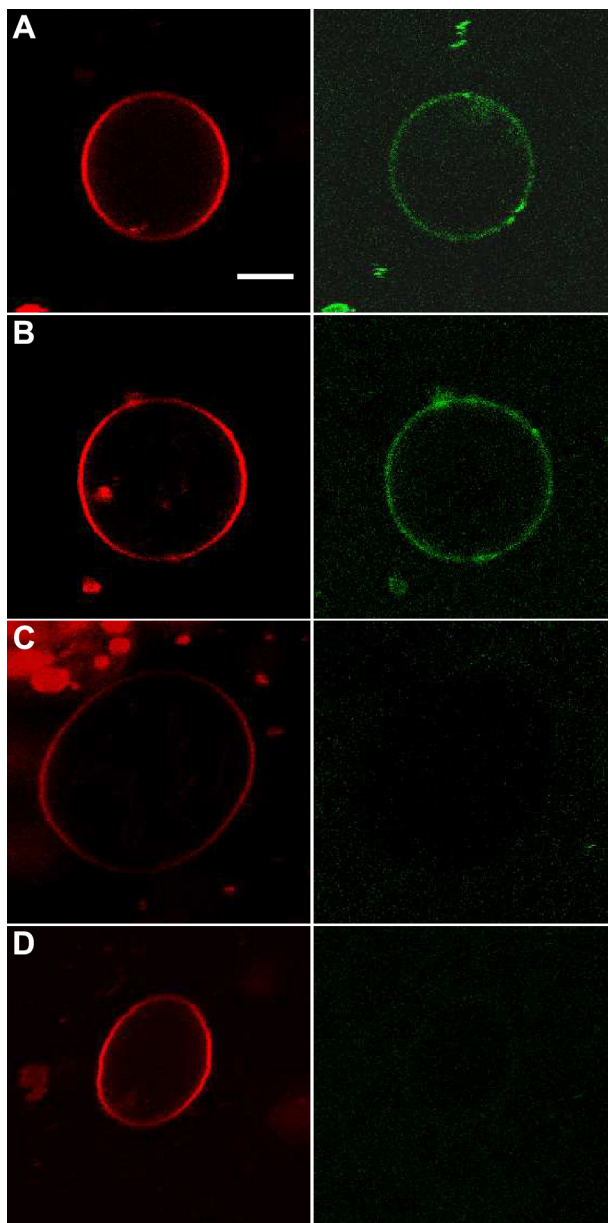


**Figure 2.3:** Representative confocal microscopy images of DOPE-Rhodamine labeled GUVs that contain CL (red channel) and  $\alpha$ S wt-140C-A488 oligomers (green channel).  $\alpha$ S shows higher affinity to these membranes that contain higher percentage of negatively charged CL: A) CL:POPC (1:1), B) CL:POPE:POPC (33:25:42), C) CL:POPE:POPC (14:36:50) and D) CL:soy PI:POPE:POPC (17:17:25:41). Scale bar indicates 5  $\mu$ m.

order to test the binding of oligomeric  $\alpha$ S to a model system that is closer to the lipid composition of mitochondrial membranes, GUVs composed of CL and zwitterionic POPC are tested (Figure 2.3A). Oligomers are observed to bind to CL:POPC vesicles. The presence of oligomers in the vesicle interior suggest that they can diffuse through the CL:POPC membrane. CL has apparently made the membrane more permeable to oligomers, which is in agreement with the literature [19]. Decreasing the amount of CL in the membrane to 33% and introducing the unsaturated phosphatidylethanolamine POPE gives similar binding of oligomers as CL:POPC membranes (Figure 2.3B). When the amount of CL is further decreased (< 15%) oligomers are not able to bind to the CL:POPE:POPC membranes anymore (Figure 2.3C). Oligomers are not able to bind to membranes that contain <20% CL, but they can also not diffuse through this membrane. Here the charge of CL plays an important role in oligomer binding, since CL carries double negative charge. Another important negatively charged lipid in the mitochondrial membrane is PI. However when the negative charge of the membranes is increased by introducing soy PI, negligible effect on oligomer binding is observed. For lipid bilayers composed of CL:soy PI:POPE:POPC 17:17:15:41 no colocalization of oligomers with the vesicle membrane can be seen (Figure 2.3D).

### **2.4.4 The effect of brain lipids on oligomers binding**

In order to further assess the effect of an increase of the complexity of the membranes, phospholipids derived from brain lipid extract were included in the lipid mixture. The brain derived extract contains phospholipids consisting of a certain headgroup and a variety of fatty acid tails. We imaged the binding of oligomers to membranes that contain at least one type of brain lipids. Vesicles formed from CL and brain PE in a 4:3 ratio bind oligomers. The presence of almost 60 % of double negatively charged CL made the membrane more vulnerable to permeabilization by oligomers resulting in the presence of oligomers in the interior of the vesicles (**Figure 2.4A**). When we exchanged CL with negatively charged brain PS and increase the fraction of charged lipids to 90 %, we have observed a similar effect upon incubation with oligomers (**Figure 2.4B**). Oligomers tend to colocalize on the GUVs composed of brain PS:brain PE (9:1) which possibly results in membrane permeabilization. The plasma membrane is reported to be one of the possible sites of  $\alpha$ S oligomer-induced permeabilization. In order to examine the binding of  $\alpha$ S to a model system mimicking the plasma membrane inner leaflet,

## Chapter 2

GUVs composed of brain PS:brain PE:ch were made (**Figure 2.4C**). Upon the incubation with oligomers, we observe weak binding to these PS:brain PE:ch membranes. We also observed that not all brain PS:brain PE:ch bound oligomers; ~50 % of brain PS:brain PE:ch bound oligomers. Based on confocal microscopy images it is hard to judge if the oligomers are localized on both inner and outer solution of the membranes. This can be attributed to the complexity of the membranes. A more quantitative analysis of the permeabilization of these membranes will be given in **Chapter 3**.

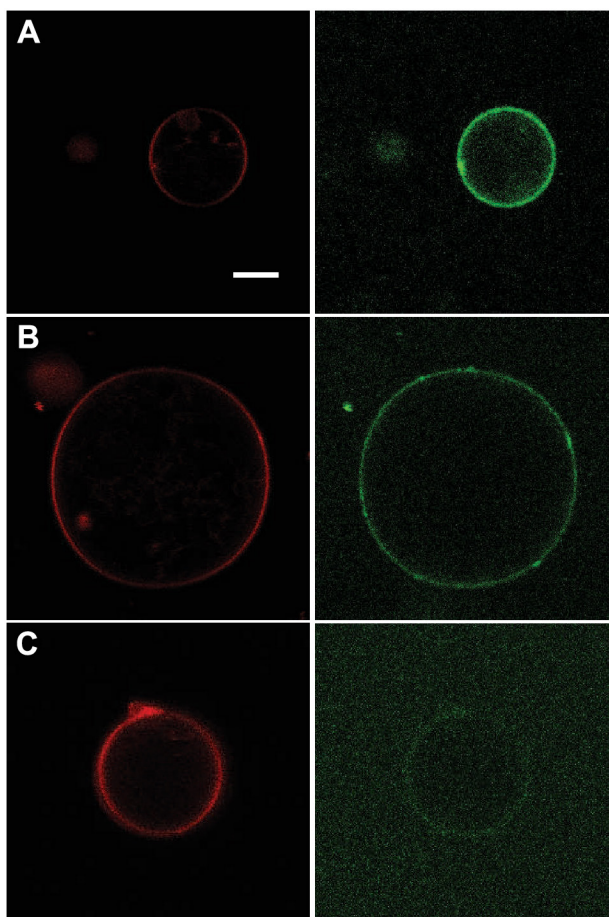


**Figure 2.4: Representative confocal microscopy images of DOPE-Rhodamine labeled GUVs composed of at least one brain lipid (red channel) and  $\alpha$ S wt-140C-A488 oligomers (green channel). Binding of  $\alpha$ S oligomers to A) CL:brain PE (4:3) B) brain PS:brain PE (9:1) and C) brain PS:brain PE:ch (2:5:3) is depicted. The scale bar indicates 5  $\mu$ m.**

## 2.5 Discussion

$\alpha$ S oligomers preferentially bind negatively charged membranes [20, 21, 34-36]. It has also been reported that, in excess,  $\alpha$ S oligomers do not only bind but can also cause permeabilization of such membranes [19, 36]. When oligomers were incubated with negatively charged vesicles (DOPG and DOPG:DPPG), we observed that oligomers can indeed permeabilize these membranes. This permeabilization is detected by oligomer fluorescence from the vesicle interior. The permeabilization of DOPG membranes by oligomers agrees with a previously published report [37]. When cholesterol was added to vesicles that contain negatively-charged DOPG:DPPG lipids we still observe that the fluorescence signal from the oligomers is colocalized with the membrane fluorescence. Model membranes composed of zwitterionic lipids and cholesterol bind  $\alpha$ S with less affinity than membranes that contain only negatively-charged lipids [28]. The membranes that we have tested and that contain at least 25% DOPG bind oligomers. Both sphingomyelin and cholesterol are known to stabilize membranes [38, 39], which agrees with our observation that the oligomers cannot cross membranes with a more physiological ch and sm content.

To test the effect of the negatively charged phospholipid headgroup (DOPA, POPS, POPG) on oligomer binding, GUVs were prepared of these phospholipids in combination with sphingomyelin and cholesterol. In these experiments we observed that oligomers only bind to DOPA:ch:sm GUVs. Binding of oligomers to membranes is apparently not only dependent on the bilayer charge. Others observed that  $\alpha$ S monomers have a 60 times higher affinity for PA membranes compared to PS and PG membranes [27], and this specificity for the PA headgroup was also suggested for oligomer binding [20]. However, from our results we cannot conclude which factor plays a more important role in a membrane binding -the binding to DOPC:ch:sm membranes can either be due to headgroup specificity or packing of the lipids in the membrane.

Because the mitochondrial inner membrane and the plasma membrane inner leaflet are proposed sites of oligomer-induced damage [11, 40-42] in PD, we wanted to further study complex membranes that bind oligomers and mimic the composition of these membranes in the next chapters. Binding studies have shown that  $\alpha$ S interacts with the mitochondrial inner membrane [15], probably due to the high content of the negatively charged lipid CL. Under physiological conditions,  $\alpha$ S is mainly localized in mitochondrial inner membrane [6, 43], although some other



## Chapter 2

authors claim that  $\alpha$ S is present in the outer membrane of mitochondria [9]. We confirmed the possible binding of  $\alpha$ S oligomers to the inner mitochondrial membrane in a model system consisting of CL:POPE:POPC (33:25:42) (**Figure 2.3B**). Binding of  $\alpha$ S to CL-containing vesicles does not occur only based on charge. When half or the CL was replaced by the negatively charged phospholipid PI only a minor fraction of the oligomers was observed to bind to the mitochondrial model membrane system. Because we observed a clear binding of oligomers to CL:POPE:POPC (33:25:42) membranes using confocal microscopy, this model system that mimics the mitochondrial inner membrane was chosen for performing the further binding and permeabilization studies. This will be described in more detail in the next chapters of the thesis.

Because  $\alpha$ S is an intracellular protein we decided to mimic the inner leaflet of the plasma membrane and study oligomer binding to GUVs composed of brain PS:brain PE:ch. This model membrane is chosen because not much data is available on  $\alpha$ S oligomer binding to these membranes made of physiologically relevant lipids. Moreover most studies on model plasma membranes do not take into the account the asymmetry between the membranes [16]. Others have shown that upon internalization,  $\alpha$ S colocalizes with the inner leaflet of the plasma membrane [40]. We show that oligomers bind to brain PS:brain PE:ch membranes. However in order to confirm if the oligomers are inside the vesicles by permeabilizing these physiologically relevant membranes a more detailed analysis will have to be done in the future. A possible experiment for the future could be to add a membrane-impermeable quencher (DPX) to the solution after the addition and incubation of fluorescently-labeled oligomers. The quencher molecule should then effectively quench fluorophores in the exterior solution and on the membrane, but should leave those on oligomers inside the vesicles unaffected.

**$\alpha$ S oligomer binding to bilayers with increasingly complex lipid compositions**

**Table 2.2: Summarized data on binding of oligomeric  $\alpha$ S to GUVs of different lipid compositions.**

<b>Lipid</b>	<b>ratio</b>	<b>binding</b>	<b>experiments</b>
DOPG	1	+	n = 14, N = 1
DOPG:DPPG	1:1	+	n = 15, N = 1
DOPG:DPPG:ch	1:1:1	+	n = 10, N = 1
DOPG:DPPG:sm:ch	1:1:1:1	+	n = 15, N = 1
DOPA:sm:ch	1:1:1	+	n = 13, N = 1
POPG:sm:ch	1:1:1	-	n = 10, N = 1
POPS:sm:ch	1:1:1	-	n = 12, N = 1
CL:POPC	1:1	+	n = 20, N = 2
CL:POPE:POPC	33:25:42:	+	n = 30, N = 3
CL:POPE:POPC	14:36:50	-	n = 10, N = 1
CL:soyPI:POPE:POPC	17:17:25:41	-	n = 11, N = 1
CL:brain PE	4:3	+	n = 29, N = 4
POPC:DOPA	1:1	+	n = 100, N = 9
POPS:ch	5:1	+	n = 29, N = 3
brain PS:brain PE	9:1	+	n = 15, N = 1
brain PS:brain PE:ch	2:5:3	+	n = 35, N = 4

**binding** – binding to oligomers is qualitatively represented as follows:

+ means that oligomers bind to these types of vesicles

– means no binding of oligomers to the vesicles

**experiments**- number of experiments is performed for the given lipid mixture:

**n** represents number of imaged vesicles

**N** represents on how many different days the experiment was repeated

## 2.6 References

1. Maroteaux, L., Campanelli, J. & Scheller, R. (1988) Synuclein: a neuron-specific protein localized to the nucleus and presynaptic nerve terminal, *The Journal of Neuroscience*. **8**, 2804-2815.
2. Akihiko Iwai, E. M., Makoto Yoshimoto,, Nianfeng Ge, L. F., H. A. Rohan de Silva, & Agnes Kitte, a. T. S. (1995) The precursor protein of non-A $\beta$  component of Alzheimer's disease amyloid is a presynaptic protein of the central nervous system, *Neuron*. **14**, 467-475.
3. Clayton, D. F. & George, J. M. (1999) Synucleins in synaptic plasticity and neurodegenerative disorders, *J Neurosci Res*. **58**, 120-9.
4. McLean, P. J., Kawamata, H., Ribich, S. & Hyman, B. T. (2000) Membrane association and protein conformation of alpha-synuclein in intact neurons - Effect of Parkinson's disease-linked mutations, *J Biol Chem*. **275**, 8812-8816.
5. Fiske, M., White, M., Valtierra, S., Herrera, S., Solvang, K., Konnikova, A. & DebBurman, S. (2011) Familial Parkinson's Disease Mutant E46K  $\alpha$ -synuclein Localizes to Membranous Structures, Forms Aggregates, and Induces Toxicity in Yeast Models, *ISRN Neurology*. **2011**, 14.
6. Liu, G., Zhang, C., Yin, J., Li, X., Cheng, F., Li, Y., Yang, H., Ueda, K., Chan, P. & Yu, S. (2009) alpha-Synuclein is differentially expressed in mitochondria from different rat brain regions and dose-dependently down-regulates complex I activity, *Neurosci Lett*. **454**, 187-92.
7. Meratan, A. A., Ghasemi, A. & Nemat-Gorgani, M. (2011) Membrane integrity and amyloid cytotoxicity: a model study involving mitochondria and lysozyme fibrillation products, *J Mol Biol*. **409**, 826-38.
8. Butterfield, S. M. & Lashuel, H. A. (2010) Amyloidogenic protein-membrane interactions: mechanistic insight from model systems, *Angew Chem Int Ed Engl*. **49**, 5628-54.
9. Nakamura, K., Nemani, V. M., Azarbal, F., Skibinski, G., Levy, J. M., Egami, K., Munishkina, L., Zhang, J., Gardner, B., Wakabayashi, J., Sesaki, H., Cheng, Y., Finkbeiner, S., Nussbaum, R. L., Masliah, E. & Edwards, R. H. (2011) Direct membrane association drives mitochondrial fission by the Parkinson disease-associated protein alpha-synuclein, *J Biol Chem*. **286**, 20710-26.
10. Yong-Kee, C. J., Sidorova, E., Hanif, A., Perera, G. & Nash, J. E. (2012) Mitochondrial dysfunction precedes other sub-cellular abnormalities in an in vitro model linked with cell death in Parkinson's disease, *Neurotox Res*. **21**, 185-94.
11. Pacheco, C., Aguayo, L. G. & Opazo, C. (2012) An extracellular mechanism that can explain the neurotoxic effects of alpha-synuclein aggregates in the brain, *Front Physiol*. **3**, 297.
12. Takamori, S., Holt, M., Stenius, K., Lemke, E. A., Gronborg, M., Riedel, D., Urlaub, H., Schenck, S., Brugger, B., Ringler, P., Muller, S. A., Rammner, B., Gräter, F., Hub, J. S., De Groot, B. L., Mieskes, G., Moriyama, Y., Klingauf, J., Grubmuller, H., Heuser, J., Wieland, F. & Jahn, R. (2006) Molecular anatomy of a trafficking organelle, *Cell*. **127**, 831-46.
13. Michaelson, D. M., Barkai, G. & Barenholz, Y. (1983) Asymmetry of lipid organization in cholinergic synaptic vesicle membranes, *Biochem J*. **211**, 155-62.
14. van Meer, G., Voelker, D. R. & Feigenson, G. W. (2008) Membrane lipids: where they are and how they behave, *Nat Rev Mol Cell Biol*. **9**, 112-24.
15. Ardail, D., Privat, J. P., Egret-Charlier, M., Levrat, C., Lerme, F. & Louisot, P. (1990) Mitochondrial contact sites. Lipid composition and dynamics, *J Biol Chem*. **265**, 18797-802.
16. Davidson, W. S., Jonas, A., Clayton, D. F. & George, J. M. (1998) Stabilization of alpha-synuclein secondary structure upon binding to synthetic membranes, *J Biol Chem*. **273**, 9443-9.
17. Berthelot, K., Cullin, C. & Lecomte, S. (2013) What does make an amyloid toxic: morphology, structure or interaction with membrane?, *Biochimie*. **95**, 12-9.
18. Madine, J., Doig, A. J. & Middleton, D. A. (2006) A Study of the Regional Effects of  $\alpha$ -Synuclein on the Organization and Stability of Phospholipid Bilayers†, *Biochemistry*. **45**, 5783-5792.
19. van Rooijen, B. D., Claessens, M. M. & Subramaniam, V. (2009) Lipid bilayer disruption by oligomeric alpha-synuclein depends on bilayer charge and accessibility of the hydrophobic core, *Biochim Biophys Acta*. **1788**, 1271-8.

## **$\alpha$ S oligomer binding to bilayers with increasingly complex lipid compositions**

20. van Rooijen, B. D., Claessens, M. M. & Subramaniam, V. (2008) Membrane binding of oligomeric alpha-synuclein depends on bilayer charge and packing, *FEBS Lett.* **582**, 3788-92.
21. Stefanovic, A. N., Stockl, M. T., Claessens, M. M. & Subramaniam, V. (2014) alpha-Synuclein oligomers distinctively permeabilize complex model membranes, *FEBS J.* **281**, 2838-50.
22. Volles, M. J., Lee, S. J., Rochet, J. C., Shtilerman, M. D., Ding, T. T., Kessler, J. C. & Lansbury, P. T., Jr. (2001) Vesicle permeabilization by protofibrillar alpha-synuclein: implications for the pathogenesis and treatment of Parkinson's disease, *Biochemistry.* **40**, 7812-9.
23. Kjaer, L., Giehm, L., Heimburg, T. & Otzen, D. (2009) The influence of vesicle size and composition on alpha-synuclein structure and stability, *Biophys J.* **96**, 2857-70.
24. Stockl, M., Fischer, P., Wanker, E. & Herrmann, A. (2008) Alpha-synuclein selectively binds to anionic phospholipids embedded in liquid-disordered domains, *J Mol Biol.* **375**, 1394-404.
25. Jo, E., McLaurin, J., Yip, C. M., St George-Hyslop, P. & Fraser, P. E. (2000) alpha-Synuclein membrane interactions and lipid specificity, *J Biol Chem.* **275**, 34328-34.
26. Rhoades, E., Ramlall, T. F., Webb, W. W. & Eliezer, D. (2006) Quantification of alpha-synuclein binding to lipid vesicles using fluorescence correlation spectroscopy, *Biophys J.* **90**, 4692-700.
27. Middleton, E. R. & Rhoades, E. (2010) Effects of curvature and composition on alpha-synuclein binding to lipid vesicles, *Biophys J.* **99**, 2279-88.
28. Shvadchak, V. V., Falomir-Lockhart, L. J., Yushchenko, D. A. & Jovin, T. M. (2011) Specificity and kinetics of alpha-synuclein binding to model membranes determined with fluorescent excited state intramolecular proton transfer (ESIPT) probe, *J Biol Chem.* **286**, 13023-32.
29. van Raaij, M. E., Segers-Nolten, I. M. & Subramaniam, V. (2006) Quantitative morphological analysis reveals ultrastructural diversity of amyloid fibrils from alpha-synuclein mutants, *Biophys J.* **91**, L96-8.
30. Pace, C. N., Vajdos, F., Fee, L., Grimsley, G. & Gray, T. (1995) How to measure and predict the molar absorption coefficient of a protein, *Protein Sci.* **4**, 2411-23.
31. Zijlstra, N., Blum, C., Segers-Nolten, I. M., Claessens, M. M. & Subramaniam, V. (2012) Molecular composition of sub-stoichiometrically labeled alpha-synuclein oligomers determined by single-molecule photobleaching, *Angew Chem Int Ed Engl.* **51**, 8821-4.
32. M.I. Angelova & Dimitrov, D. S. (1986) Liposome electroformation, *Faraday Discuss Chem Soc.* **81**, 303-311.
33. Stöckl, M., Nikolaus, J. & Herrmann, A. (2010) Visualization of Lipid Domain-Specific Protein Sorting in Giant Unilamellar Vesicles in *Liposomes* (Weissig, V., ed) pp. 115-126, Humana Press.
34. Stockl, M., Claessens, M. M. & Subramaniam, V. (2012) Kinetic measurements give new insights into lipid membrane permeabilization by alpha-synuclein oligomers, *Mol Biosyst.* **8**, 338-45.
35. Stockl, M. T., Zijlstra, N. & Subramaniam, V. (2013) alpha-Synuclein oligomers: an amyloid pore? Insights into mechanisms of alpha-synuclein oligomer-lipid interactions, *Mol Neurobiol.* **47**, 613-21.
36. Lorenzen, N., Nielsen, S. B., Buell, A. K., Kaspersen, J. D., Arosio, P., Vad, B. S., Paslawski, W., Christiansen, G., Valnickova-Hansen, Z., Andreasen, M., Enghild, J. J., Pedersen, J. S., Dobson, C. M., Knowles, T. P. & Otzen, D. E. (2014) The role of stable alpha-synuclein oligomers in the molecular events underlying amyloid formation, *J Am Chem Soc.* **136**, 3859-68.
37. van Rooijen, B. D., Claessens, M. M. & Subramaniam, V. (2010) Membrane Permeabilization by Oligomeric alpha-Synuclein: In Search of the Mechanism, *PLoS One.* **5**, e14292.
38. Maxfield, F. R. & van Meer, G. (2010) Cholesterol, the central lipid of mammalian cells, *Curr Opin Cell Biol.* **22**, 422-9.
39. van Meer, G. & Hoetzel, S. (2010) Sphingolipid topology and the dynamic organization and function of membrane proteins, *FEBS Lett.* **584**, 1800-5.
40. Fauvet, B., Fares, M. B., Samuel, F., Dikiy, I., Tandon, A., Eliezer, D. & Lashuel, H. A. (2012) Characterization of semisynthetic and naturally Nalpha-acetylated alpha-synuclein in vitro and in intact cells: implications for aggregation and cellular properties of alpha-synuclein, *J Biol Chem.* **287**, 28243-62.
41. Gitler, A. D., Bevis, B. J., Shorter, J., Strathearn, K. E., Hamamichi, S., Su, L. J., Caldwell, K. A., Caldwell, G. A., Rochet, J. C., McCaffery, J. M., Barlowe, C. & Lindquist, S. (2008) The

## Chapter 2

Parkinson's disease protein alpha-synuclein disrupts cellular Rab homeostasis, *Proc Natl Acad Sci U S A.* **105**, 145-50.

42. Devi, L. & Anandatheerthavarada, H. K. (2010) Mitochondrial trafficking of APP and alpha synuclein: Relevance to mitochondrial dysfunction in Alzheimer's and Parkinson's diseases, *Biochim Biophys Acta.* **1802**, 11-9.

43. Devi, L., Raghavendran, V., Prabhu, B. M., Avadhani, N. G. & Anandatheerthavarada, H. K. (2008) Mitochondrial import and accumulation of alpha-synuclein impair complex I in human dopaminergic neuronal cultures and Parkinson disease brain, *J Biol Chem.* **283**, 9089-100.

## Chapter 3

# Alpha-synuclein oligomers distinctively permeabilize complex model membranes

### 3.1 Abstract

Alpha-synuclein oligomers are increasingly considered to be responsible for the death of dopaminergic neurons in Parkinson's disease. The toxicity mechanism of alpha-synuclein oligomers likely involves membrane permeabilization. Even though it is well established that alpha-synuclein oligomers bind and permeabilize vesicles composed of negatively charged lipids, little attention has been given to the interaction of oligomers with bilayers of physiologically relevant lipid compositions. We investigated the interaction of alpha-synuclein with bilayers composed of lipid mixtures that mimic those of plasma and mitochondrial membranes. Here we show that monomeric and oligomeric alpha-synuclein bind to these membranes. The resulting membrane leakage differs from what is observed for simple artificial model bilayers. While the addition of oligomers to negatively charged lipid vesicles displays fast content release in a bulk permeabilization assay, adding oligomers to vesicles with compositions mimicking mitochondrial membranes shows a much slower loss of content. Oligomers are not able to induce leakage in the artificial plasma membranes even after long-term incubation. Circular dichroism experiments indicate that binding to lipid bilayers initially induces conformational changes in both oligomeric and monomeric alpha-synuclein, that show little change upon long-term incubation of oligomers with membranes. Our results show that the mitochondrial model membranes are more vulnerable to permeabilization by oligomers than model plasma membranes reconstituted from brain-derived lipids; this preference may imply that increasingly complex membrane components, such as those in the plasma membrane mimic used here, are less vulnerable to damage by oligomers.

## 3.2 Introduction

Parkinson's disease (PD) is one of the most common human neurodegenerative diseases, involving the progressive loss of dopaminergic neurons in the *substantia nigra* in the midbrain [1]. The appearance of Lewy bodies (LB) is characteristic of the pathology of PD. The main component of these LBs is the protein alpha-synuclein ( $\alpha$ S), which is present as amyloid fibrils.  $\alpha$ S is a 140 amino acid intrinsically disordered protein of as yet unknown function. In PD, aggregation of  $\alpha$ S causes the protein to lose its putative function and gain toxicity [2-8] (**Figure 3.1.A**).  $\alpha$ S consists of a positively charged N-terminal region (residues 1-60) containing imperfect KTKEGV repeats, a hydrophobic NAC region (residues 61-95) and a negatively charged C-terminal region (residues 96-140). For membrane binding the N-terminal part of  $\alpha$ S plays a key role. Upon binding to phospholipid membranes the protein adopts an  $\alpha$ -helical structure [9]. Interactions of monomeric  $\alpha$ S with lipid vesicles of different compositions and size have been studied [10-15]. Current thinking suggests that intermediate species in the fibril formation pathway of  $\alpha$ S are the toxic species involved in cell death in PD [4, 16-18]. In spite of structural differences between  $\alpha$ S oligomers and monomers, they both show high affinity for negatively charged membranes. We have previously shown that oligomer binding induces leakage of artificial negatively charged lipid vesicles. Although several studies [19-21] have shown that isolated oligomers can decrease the integrity of simple negatively charged lipid vesicles, little is known on how these species bind and permeabilize natural membranes. Mitochondrial damage has been observed in PD and mitochondrial membranes are therefore thought to be a likely target for oligomer-induced damage [22-24]. Mitochondrial membranes are enriched in cardiolipin [25], a unique negatively charged diphosphatidylglycerol lipid (**Figure 3.1.B**). Monomeric  $\alpha$ S shows a high binding affinity to cardiolipin-containing membranes [26, 27]. Quantitative correlation between  $\alpha$ S in mitochondria and cytosol confirmed that monomeric  $\alpha$ S interacts with mitochondrial membranes [28]. Moreover, it has been reported that  $\alpha$ S is present on mitochondrial membranes in functional dopaminergic neurons of the *substantia nigra* [29, 30], where, at physiological concentrations  $\alpha$ S is mainly localized at the mitochondrial inner membrane and only a small fraction is found at the outer membrane [28, 31] (**Figure 3.1.B**). However, a contrasting report suggests  $\alpha$ S is localized in the outer mitochondrial membrane [23]. Mitochondria of dopaminergic neurons in brains of PD patients contain a higher concentration of  $\alpha$ S than normal

## Alpha-synuclein oligomers distinctively permeabilize complex model membranes

brains [32]. A recent study has suggested that WT  $\alpha$ S is mainly localized in mitochondria-associated endoplasmic reticulum (ER) membranes and modulates the morphology of mitochondria [33]. Besides these membranes, the plasma membrane has been indicated as a site of oligomer-induced damage. Upon internalization,  $\alpha$ S colocalizes with the inner leaflet of the plasma membrane [34, 35]. In a yeast model it was found that  $\alpha$ S binds to plasma membranes [36]. Finally, a recent report suggests that  $\alpha$ S can interact with lipids in the plasma membrane increasing the membrane permeability as a potential mechanism of extracellular neurotoxicity [37].

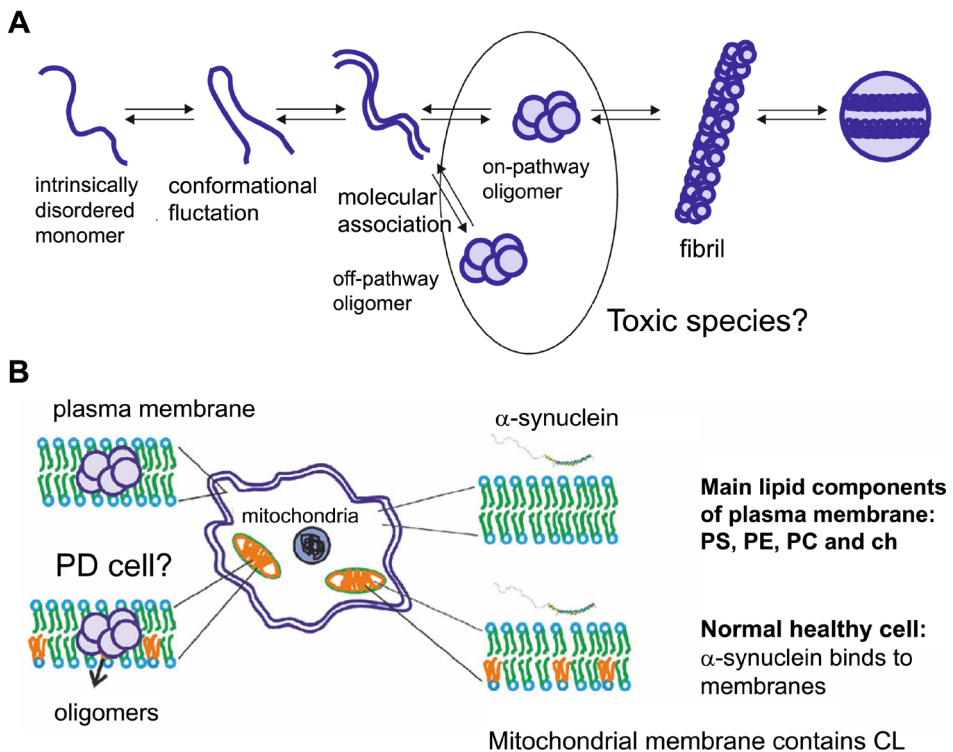


**Figure 3.1: (A) Schematic aggregation pathway of  $\alpha$ S and (B) schematic of interaction of  $\alpha$ S monomers and oligomers with membranes.**

In the present study, we investigate the binding of specific, well-characterized, oligomeric  $\alpha$ S species to lipid membranes made of physiologically relevant mitochondrial and plasma membrane lipid mixtures. We show that these oligomers cause slow permeabilization of mitochondrial inner membrane mimics, whereas



they bind to, but could not induce leakage in, plasma membrane inner leaflet model systems.

### 3.3 Materials and methods

#### 3.3.1 Expression and purification of $\alpha$ S

Expression and purification of human wild-type (WT)  $\alpha$ S and the cysteine (cys) mutant  $\alpha$ S-A140C, where alanine at position 140 was replaced with a cysteine, was done as previously described [38]. The protein concentration was determined by measuring the absorbance on a Shimadzu spectrophotometer at 276 nm, using molar extinction coefficients of  $5600 \text{ M}^{-1} \text{ cm}^{-1}$  for wt and  $5745 \text{ M}^{-1} \text{ cm}^{-1}$  for A140C [39, 40]. The protein was stored at  $-80^\circ \text{C}$  until further use.

#### 3.3.2 Labeling of $\alpha$ S

The cys mutant  $\alpha$ S-A140C was used for labeling the protein with an Alexa Fluor 488 C5 maleimide dye (A488) (Invitrogen, Carlsbad, CA, USA). Prior to labeling, a six-fold molar excess of dithiothreitol (DTT) was added to  $\alpha$ S-A140C to reduce disulfide bonds. After 30 minutes of incubation, DTT was removed using Zeba Spin desalting columns (Pierce, Rockford, IL, USA), and a two-fold excess of A488 was added. After 1 hour incubation, excess of free dye was removed using two desalting steps. The labeling efficiency was estimated to be between 90-100% from absorption spectra. To determine the protein and A488 concentration the absorbance at 276 nm was measured using a molar extinction coefficient of  $5745 \text{ M}^{-1} \text{ cm}^{-1}$  for the protein and at 495 nm using a molar extinction coefficient of  $72000 \text{ M}^{-1} \text{ cm}^{-1}$  for the dye.

#### 3.3.3 Preparation of unlabeled and labeled $\alpha$ S oligomers

Briefly, oligomers were obtained by incubating  $\alpha$ S at high concentrations in the absence of additional factors [19]. Alexa 488 labeled oligomers with 7.5 % labeling density, achieved by mixing appropriate quantities of labeled protein ( $\alpha$ S-A140C) with unlabeled protein (WT), were prepared for membrane binding studies by confocal microscopy. Oligomers were purified and separated from monomers using

size-exclusion chromatography on a Superdex™ 200 10/300 GL column (GE Healthcare Bio-Sciences AB, Uppsala, Sweden). Separation of oligomers from monomers is based on size, where larger particles (oligomers) elute first. To confirm the presence of oligomers a native PAGE gradient gel was used [19] with a polyacrylamide gradient between 3 and 16%. We have previously demonstrated that oligomers prepared in this manner are composed of ~ 30 monomers, and are stable [40]. Monomers could not be detected in the oligomer preparation (data not shown).

### **3.3.4 LUVs preparation and calcein release assay**

All lipids were purchased from Avanti Polar Lipids (Alabaster, AL, USA). In the experiments the following lipids were used: 1-Palmitoyl-2-oleoylphosphatidylcholine (POPC), 1,2-dioleoylphosphatidylglycerol (DOPG), 1-Palmitoyl-2-oleoylphosphatidylethanolamine (POPE), 1',3'-bis[1,2-dioleoyl-sn-glycero-3-phospho]-sn-glycerol (18:1 Cardiolipin, CL), porcine brain L- $\alpha$ -phosphatidylserine (Brain PS), porcine brain L- $\alpha$ -phosphatidylethanolamine (Brain PE) and cholesterol (ch).

To mimic the lipid composition of neuronal plasma membranes we used mixtures of brain PS:brain PE:cholesterol in a molar ratio of 2:5:3, which corresponds to 20% of negatively charged lipids. However, no elaborative data of brain lipid composition are available. The neuronal membrane has approximately 10% negatively charged lipids, mainly PS, while the main components of these membranes are neutral PC and PE phospholipids [41]. However, this estimation of the lipid composition does not take into account asymmetry between the inner and outer leaflets of the membrane [42]. Because  $\alpha$ S is an intracellular protein, we chose to mimic the inner leaflet of the plasma membrane, which is enriched in PS.  $\alpha$ S has also been implicated in interactions with mitochondrial membranes. Literature data suggests that  $\alpha$ S preferentially binds to the mitochondrial inner membrane [25]. To mimic the mitochondrial inner membrane we used a lipid composition that contains CL:POPE:POPC in a molar ratio 4:3:5 [25].

Specific lipid compositions were prepared by mixing 650  $\mu$ M of lipids in chloroform. The solvent was removed by drying under nitrogen flow. The resulting lipid films were then hydrated for 1 hour using 50 mM calcein, 10 mM HEPES (4-(2-Hydroxyethyl)piperazine-1-ethanesulfonic acid), 60 mM NaCl to obtain an osmolality (Cryoscopic osmometer, Gonotec, Berlin, Germany) of 320 mOsm/kg.

## Chapter 3

The sample was then subjected to 5 freeze-thaw cycles using liquid nitrogen and a water bath. The temperature of the water bath was kept above the transition temperature of the lipid mixture. The solution was subsequently extruded 11 times through 100 nm pore size filters (Whatman, Maidstone, UK) and finally unencapsulated calcein was removed using PD-10 columns filled with Sephadex G-100 (GE Healthcare Bio-Sciences AB, Uppsala, Sweden).

Long-term calcein release kinetics of the model membranes was followed on a Varian Cary Eclipse fluorometer (Varian Inc., Palo Alto, CA, USA). We used lipid concentrations of 40  $\mu$ M. The emission intensity was recorded at 515 nm for excitation at 495 nm. TritonX (0.5%) was added to completely lyse the vesicles. All the data points were normalized using the intensity after TritonX treatment as 100 % leakage.

### 3.3.5 Semi-quantitative $\alpha$ S monomer and oligomer binding assay

Giant unilamellar vesicles (GUVs) were prepared in sucrose solution as previously described by Angelova [43]. The sucrose concentration was equiosmolar to the 10mM HEPES, 150mM NaCl solution in which the proteins were dissolved. 1% DOPE-Rhodamine was included in the previously mentioned lipid mixtures to facilitate visualization of the lipid membrane.

GUVs mimicking natural lipid compositions were equilibrated with fluorescently labeled oligomers for 30 minutes before imaging. DOPG vesicles were used as a positive control for binding of monomers and oligomers to membranes.

We used the ImageJ (NIH, Bethesda, MD, USA) script plot profile to extract semi-quantitative fluorescence values reporting on the binding of monomers and oligomers to membranes. The amount of  $\alpha$ S bound to GUV membranes was estimated from the peak values of the Alexa 488 intensity profiles and averaged for at least 15 vesicles on five random cross sections using the same imaging settings (master gain, digital offset and laser power).

### 3.3.6 SUVs preparation and binding of $\alpha$ S oligomers to SUVs

Lipid mixtures that contain 3.8 mM of lipids in chloroform were prepared. After removing traces of chloroform a thin lipid film was dissolved in 10 mM K-phosphate buffer. SUVs were prepared from this solution by sonicating for half an hour using a tip sonicator (Labsonic, Branson Ultrasonics, Danbury, CT, USA) at 38

maximum amplitude on ice. Binding-induced conformational changes of oligomeric and monomeric alpha-synuclein were investigated using CD spectroscopy [44]. Both protein and lipids samples were prepared in 10 mM K-phosphate buffer. Spectra were recorded from 190 to 260 nm with a step size of 0.2 nm in 1 mm quartz cuvettes. Monomer and oligomer concentrations were 16  $\mu\text{M}$  and 10  $\mu\text{M}$  of equivalent monomer concentration respectively, keeping the lipid to protein ratio 260:1 for oligomer binding to SUVs and 170:1 for monomers binding to SUVs. A lipid concentration of 2.72 mM gave us the above-mentioned lipid to protein ratio. These ratios were chosen to obtain complete binding of the protein [42, 45]. Mean residue ellipticities (MRE,  $\text{deg dmol}^{-1} \text{cm}^2$ ) were calculated using Equation 1, where  $c$  is the protein concentration,  $l$  is the pathlength cuvette and  $n_{\text{residues}}$  is the number of residues (amino acids).

$$MRE = \frac{\text{recorded value} - \text{buffer value}}{l(\text{cm}) \times n_{\text{residues}} \times 10 \times c(M)} \quad (1)$$

In principle the MRE at any wavelength is a combination of  $\alpha$ -helical structure,  $\beta$ -sheet and random coil content of the sample [46]. The  $\alpha$ -helical content was estimated by measuring the CD signal at 222 nm; at this wavelength the contribution of random coil structure is relatively small [47].

At 222 nm the  $\alpha$ -helical content was obtained using Equations 2-4:

$$\% \text{helicity} = \frac{\theta_{222} - \theta_{\text{coil}}}{\theta_{\text{helix}} - \theta_{\text{coil}}} \times 100 \quad (2)$$

where  $\theta_{\text{helix}}$  and  $\theta_{\text{coil}}$  could be calculated:

$$\theta_{\text{coil}} = 640 - 45 \times \vartheta \quad (3)$$

$$\theta_{\text{helix}} = -40000 \times \left(1 - \frac{2.5}{n}\right) + 100 \times \vartheta \quad (4)$$

$\Theta_{222}$  is the measured mean residue ellipticity at 222 nm,  $\theta_{\text{helix}}$  and  $\theta_{\text{coil}}$  are mean residue ellipticities at 222 nm of idealized  $\alpha$ -helix and random coil proteins,  $n=140$  amino acids, and  $\vartheta$  is temperature in  $^{\circ}\text{C}$ .

## 3.4 Results

### 3.4.1 Binding of $\alpha$ S monomers to bilayers that mimic lipid composition of natural membranes

Electrostatic interactions play a key role in binding of monomers to negatively charged membranes. Membrane binding of monomers is mainly associated with positive charges on the N-terminal part of the protein [15]. Upon binding to negatively charged lipid bilayers, monomers adopt an amphipathic  $\alpha$ -helical structure. Fluorescently labeled monomers colocalize with the control DOPG vesicles (**Figure 3.2.A**) and with GUVs composed of both the plasma and mitochondrial membrane mimicking lipid mixtures (**Figure 3.2.B** and **3.2.C**). Analysis of the Alexa 488-fluorescence intensity at GUV membranes showed that the highest amount of monomers was bound at DOPG membranes (**Figure 3.2.D**). Surprisingly not all brain PS:brain PE:ch vesicles bound monomers, with  $\sim 50\%$  of the vesicles not showing any colocalization of labeled monomers and GUVs. It should be noted that in **Figure 3.2.D** only vesicles that bind  $\alpha$ S were taken into account.

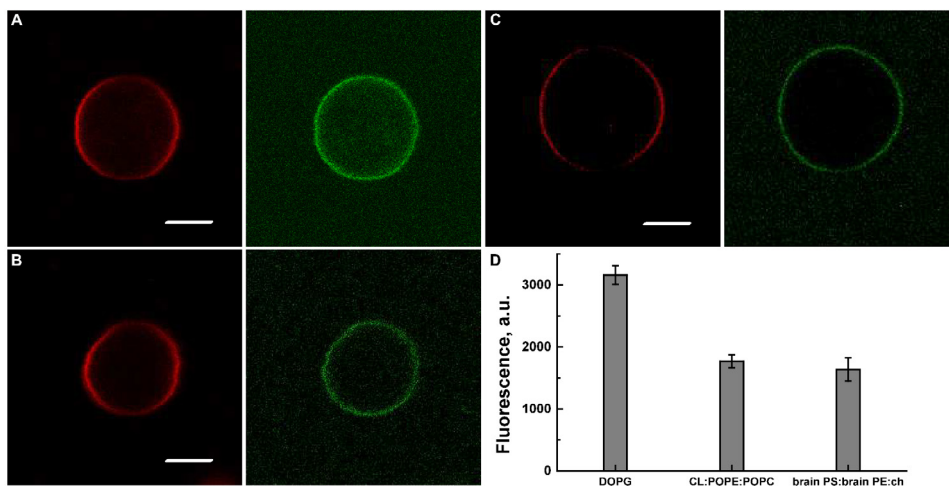


**Figure 3.2: Representative confocal microscopy images of DOPE-Rhodamine labeled GUVs (red channel) and  $\alpha$ S wt-140C-A488 monomers (green channel).** Binding of  $\alpha$ S monomers to A) DOPG, B) CL:POPE:POPC (4:3:5), C) Brain PS:brain PE:cholesterol (2:5:3) membranes is depicted. D) Quantitative analysis of fluorescently labeled  $\alpha$ S bound to vesicles ( $n = 15$ ). The error bars represent standard deviation. The scale bars indicate  $5 \mu\text{m}$ .

CD spectroscopy was used to assess whether binding of monomers to vesicles of all lipid compositions resulted in conformational changes in the protein. Monomers in solution showed CD spectra typical for an intrinsically disordered protein with a negative peak at 198 nm. As previously reported,  $\alpha$ -synuclein monomers form an  $\alpha$ -helix upon binding to SUVs [42, 45]. Upon binding membranes mimicking plasma or mitochondrial lipid compositions, monomers adopt an  $\alpha$ -helical structure that is characterized by two negative bands at 208 and 222 nm in the CD spectrum. The  $\alpha$ -helical content of the protein upon binding was estimated from the MRE at 222 nm as explained in the Materials and Methods section below. Binding of monomers to control DOPG vesicles resulted in an  $\alpha$ -helical content of  $65.1 \pm 1.2$  %. Monomers binding to CL:POPE:POPC membranes or membranes composed of brain PS:brain PE:cholesterol adopted a comparable amount of  $\alpha$ -helix ( $59.0 \pm 0.4$  % and  $61.1 \pm 0.3$  % respectively) (**Figure 3.3**).

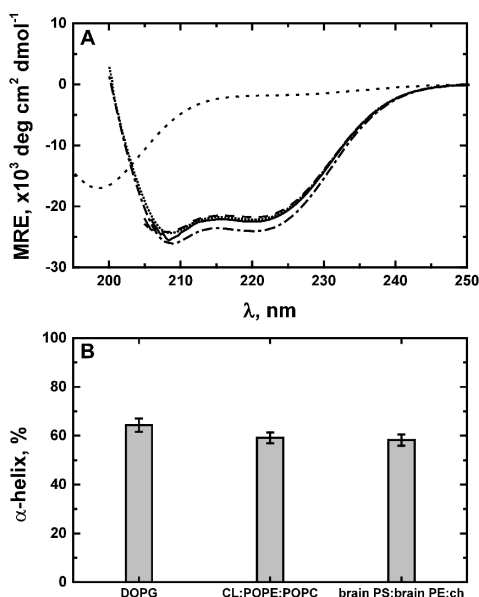


**Figure 3.3:** Circular dichroism measurements of conformational changes of  $\alpha$ S monomers ( $\cdots$ ) upon binding to membranes. A) Binding of  $\alpha$ S to DOPG ( $-\cdot-$ ), CL:POPE:POPC ( $\cdots$ ) and brain PS:brain PE:ch ( $-$ ) vesicles showed increase of  $\alpha$ -helical content. There is no change in  $\alpha$ -helical content of  $\alpha$ S monomers bound to brain PS:brain PE:ch vesicles with time when comparing CD spectra 10 minutes ( $--$ ) after binding or after 20h of incubation ( $-$ ). B) Percentage of  $\alpha$ -helix formed for  $\alpha$ S monomers bound to vesicles with the lipid compositions tested above. Data are the average of 3 different measurements. Error bars represent standard deviations.

The similarity of the CD spectra suggests that  $\alpha$ S monomers were fully bound and in a predominantly  $\alpha$ -helical conformation at saturating lipid concentrations for all types of natural membranes tested. There were no changes in  $\alpha$ -helical content of  $\alpha$ S monomers bound to brain PS:brain PE:ch vesicles when comparing CD spectra immediately after binding or after 20h of incubation (**Figure 3.3.A**). CD data points below 205 nm were not taken into account because of the high noise, likely due to a presence of some other organic compounds in the lipid mixtures of brain lipids.

### 3.4.2 Do $\alpha$ S oligomers bind to bilayers mimicking the lipid composition of natural membranes and does this binding result in conformational changes?

We have previously shown that  $\alpha$ S oligomers can bind to lipid membranes composed of negatively charged lipids such as DOPG or POPG [48]. The binding of fluorescently labeled oligomers to GUVs with a lipid composition mimicking either negatively charged, neuronal or mitochondrial membranes was studied using confocal microscopy.

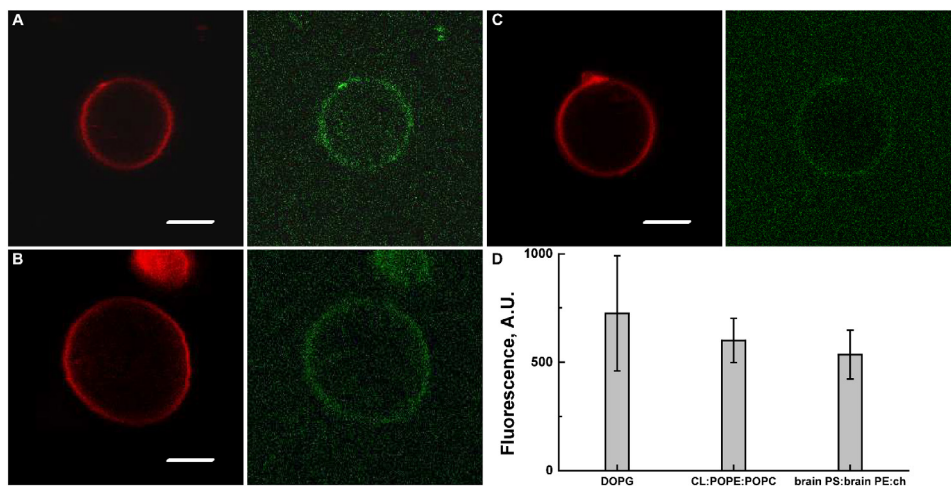


**Figure 3.4:** Representative confocal microscopy images of DOPE-Rhodamine labeled GUVs (red channel) and  $\alpha$ S wt-140C-A488 oligomers (green channel). Binding of  $\alpha$ S oligomers to A) DOPG, B) CL:POPE:POPC, C) brain PS:brain PE:ch vesicles is depicted. D) Quantitative analysis of fluorescently labeled oligomers bound to vesicles ( $n = 15$ ). The error bars represent standard deviation. The scale bars indicate 5  $\mu$ m.

We observed that oligomers bind to bilayers mimicking the lipid composition of both the plasma membrane inner leaflet and the mitochondrial inner membrane (Figure 3.4.B and 3.4.C). Semi-quantitative comparison of oligomer membrane binding was done in the same manner as for monomers. Oligomers showed comparable binding to DOPG, CL:POPE:POPC and brain PS:brain PE:ch GUVs (Figure 3.4.D). As for monomer binding, we also observed that not all brain PS:brain PE:ch membranes bound oligomers.

We further investigated if the membrane binding caused conformational changes in the oligomers similar to those observed for monomeric  $\alpha$ S using CD spectroscopy. In solution, oligomers showed some  $\beta$ -sheet conformation (Figure 3.5). Binding of oligomers to vesicles resulted in a small change in protein conformation for both lipid mixtures. Oligomers showed an increase in  $\alpha$ -helical content upon addition of SUVs. The  $\alpha$ -helical content of the oligomers was comparable for all lipid membranes studied, and did not change in time. Oligomers bound to brain PS:brain PE:cholesterol membranes showed similar CD spectra immediately after the addition of protein to membranes and after 20h of incubation (Figure 3.5).

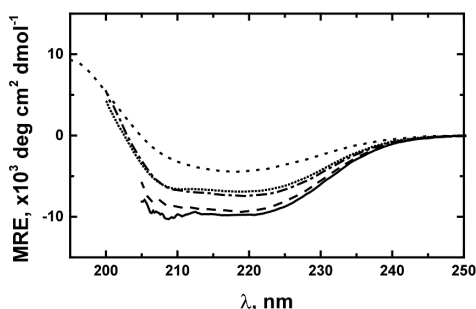


**Figure 3.5: Circular dichroism measurements of conformational changes of  $\alpha$ S oligomers upon binding to membranes.** Oligomers partially adopted  $\alpha$ -helical structure upon addition of SUVs. No difference in changes of protein conformation was observed after 20h for  $\alpha$ S oligomers binding to brain PS:brain PE:ch vesicles. Legend:  $\alpha$ S oligomers ( $\cdot\cdot\cdot$ ), DOPG ( $-\cdot-$ ), CL:POPE:POPC ( $\cdots$ ) and brain PS:brain PE:ch after 10 minutes ( $-\cdot-$ ) and 20 h of incubation ( $-$ ).

We investigated the membrane disrupting properties of oligomers by studying the kinetics of membrane permeabilization using a dye release assay.



### 3.4.3 Kinetics of membrane permeabilization (Dye release assay)

Oligomers have been shown to disrupt membranes composed of negatively charged lipid vesicles [19]. After the addition of oligomers to a solution of calcein-filled DOPG LUVs a rapid release of encapsulated dye was observed (**Figure 3.6.A**). We have previously shown that monomers and fibrils also could cause membrane permeabilization of negatively charged PG vesicles, but that much higher concentrations of the protein are necessary to get comparable leakage [19]. Comparing the oligomer-induced leakage kinetics of the dye from DOPG LUVs with dye encapsulated in vesicles of lipid bilayers that mimic physiologically relevant membrane compositions revealed large differences. Although oligomer binding was observed after 30 minutes of incubation, little oligomer-induced vesicle leakage of membranes that mimic natural membranes was observed at these timescales. For LUVs composed of a mixture of CL:POPE:POPC a slow dye leakage was observed which was still increasing after 18h (**Figure 3.6.B**). For these LUVs the oligomer-induced leakage was concentration dependent; higher oligomer concentrations showed more leakage. In contrast, even after 18 hour incubation, oligomer concentrations as high as 4  $\mu\text{M}$  did not result in more than 2% membrane leakage for bilayers composed of brain PS:brain PE:cholesterol (**Figure 3.6.C**).

## Alpha-synuclein oligomers distinctively permeabilize complex model membranes

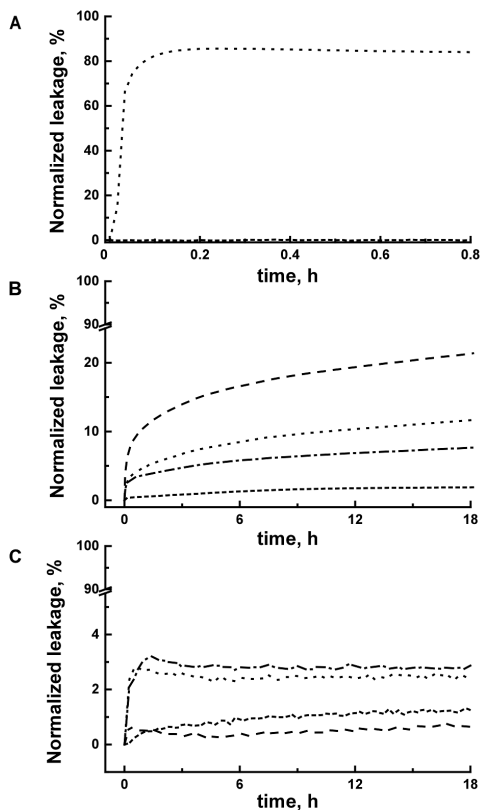


**Figure 3.6: Dye release kinetics from vesicles of different lipid composition after addition of  $\alpha$ S oligomers.** A) with DOPG vesicles 1  $\mu$ M oligomers showed almost complete leakage and fast kinetics which reached a plateau after 12 minutes. B) CL:POPE:POPC vesicles did not result in comparable leakage after 18 hours even with 4  $\mu$ M oligomer concentration. C) Oligomers did not induce appreciable leakage in brain PS:brain PE:ch model membranes even on a long time scale. Legend: 4  $\mu$ M oligomers (---), 1  $\mu$ M oligomers (···), 0.5  $\mu$ M oligomers (-·-·) and lipids alone (···).

To obtain a better understanding of the observed slow release kinetics, we used the diffusion equation assuming steady state release to fit the data. In the absence of oligomers the change in concentration,  $c$ , of dye in the vesicles was assumed to follow the expression  $c = c(0)(1 - e^{-kt})$  where the rate constant  $k = P_c \times A/V$ ,  $V$  is the volume of the vesicle,  $P_c$  the membrane permeability for calcein and  $A$  the area over which diffusion takes place. To fit the data in presence of oligomers, we expect the rate constant to change or more exponents to be required to better describe the dye release kinetics.

## Chapter 3

**Table 3.1: Fitting parameters for oligomer-induced calcein leakage from CL:POPE:POPC vesicles<sup>a, b</sup>.**

Concentration	$A$	$B$	$C$	$k_1$	$k_2$	$k_3$
$\mu\text{M}$				$\text{h}^{-1}$	$\text{h}^{-1}$	$\text{h}^{-1}$
4	6.4±0.17	7.8±0.13	86	10.87±0.59	0.47±0.02	0.004
3	6.33±0.14	7.39±0.12	86	10.15±0.47	0.45±0.02	0.004
2	5.8±0.1	7.5±0.08	85.5	12.59±0.47	0.47±0.012	0.004
1	2.87±0.06	4.79±0.07	92	10.58±0.48	0.34±0.01	0.002
0.5	2.69±0.04	2.69±0.07	94.03	13.88±0.47	0.31±0.01	0.001
0.25	2.52±0.04	1.31±0.03	96.4	13.28±0.4	0.37±0.03	<0.001

<sup>a</sup> Fits were determined using  $y = A \times (1 - e^{-k_1 \times t}) + B \times (1 - e^{-k_2 \times t}) + C \times (1 - e^{-k_3 \times t}) + y_0$ ,  $A$  and  $B$ , preexponential factors associated with oligomer-induced leakage,  $k_1$  and  $k_2$ , rate constant of oligomer-induced leakage;  $C$ , preexponential factor of bare membrane leakage,  $k_3$ , rate constant bare vesicle leakage,  $y_0$ , the offset.

<sup>b</sup> We present calcein release kinetics measured for 6 different oligomer concentrations: 4  $\mu\text{M}$ , 3  $\mu\text{M}$ , 2  $\mu\text{M}$ , 1  $\mu\text{M}$ , 0.5  $\mu\text{M}$  0.25  $\mu\text{M}$ . At least three exponentials were necessary for adequate fits of our data.

When oligomers were added, fast leakage was observed for DOPG LUVs. This is not the case for membranes composed of CL:POPE:POPC. Oligomer-induced leakage from these vesicles required a fit with at least three exponentials. One of these exponents is comparable for all oligomer concentrations (the exponent associated with amplitude  $C$  in **Table 3.1**). This amplitude ( $C$ ) decreases with increasing oligomer concentration and was attributed to the calcein permeability of the bare bilayer. With increasing oligomer concentration a decreasing fraction of vesicles is not affected by oligomers and show leakage comparable to bare membranes. From the slow exponent attributed to the bare membrane, the calcein permeability  $P_c$  of the CL:POPE:POPC membrane was calculated to be  $\sim 10^{-13}$  cm/s. The amplitudes of the other two exponents increase with increasing oligomer concentration indicating that these contributions result from the presence of oligomers. Both oligomer-related rate constants were observed to increase with increasing oligomer concentration (**Table 3.1**).

### 3.5 Discussion

It is well established that binding of  $\alpha$ S to lipid bilayers is accompanied by an increase in  $\alpha$ -helical content [42]. The binding of  $\alpha$ S to lipid bilayers strongly depends on the presence of negatively charged lipids [10, 15, 27, 42, 49, 50]. However although most reports suggest that neutral membranes do not bind  $\alpha$ S [42, 51], others claim differently [10, 52]. The amount of  $\alpha$ S bound to lipid bilayers is proportional to the number of available binding sites and therefore to the fraction of negatively charged lipids in the bilayer [10, 15]. Earlier studies with brain derived lipids showed no binding of  $\alpha$ S to lipid bilayers that contained only 10-15% of PS lipids indicating that the 20% used in our experiments is close to the minimal amount required for  $\alpha$ S binding [42]. Variations in composition of the brain PS:brain PE:ch GUVs may explain why monomers did not bind to all brain PS:brain PE:ch GUVs. This variation in composition is possibly caused by the presence of brain PS in the lipid mixture. It has been claimed that brain PS can interfere with the electroformation of GUVs resulting in variation in lipid composition of the resulting vesicles [53].

In the presence of excess vesicles of all lipid compositions (DOPG or natural lipids),  $\alpha$ S showed comparable results in CD binding studies. The maximal  $\alpha$ -helical content of the protein did not depend on the negatively charged lipid species. Interactions of CL containing vesicles with  $\alpha$ S monomers have been

characterized by  $^{19}\text{F}$ -NMR [27]. It was proposed that the positively charged N-terminal region is involved in binding via interaction between positively charged lysines and negatively charged CL [27]. The protein binds to lipid surfaces through an amphipathic  $\alpha$ helix adopted by 100 amino acid residues on the N-terminal part of the protein, while the acidic C-terminal tail of the protein remains in solution [54]. According to the literature,  $\alpha\text{S}$  monomers adopt 41%  $\alpha$ -helix in the presence of 1 mM of SDS [55], while upon the binding to DPPC:DPPG vesicles 61% of the protein adopted  $\alpha$ -helical conformation [56], which is comparable to our observations.

Similar to  $\alpha\text{S}$  monomers, oligomers were found to bind lipid bilayers of all compositions studied. However, compared to observations on  $\alpha\text{S}$  monomers, the helical content observed in the presence of oligomers was much lower [19]. It is possible that only the monomers in the oligomer facing the bilayer bind the membrane and adopt an  $\alpha$ -helical conformation. Alternatively, the interactions between  $\alpha\text{S}$  monomers in the oligomer may be too strong to permit further conformational changes upon lipid binding.

Oligomers interacting with simple negatively charged lipid bilayers composed of e.g. DOPG or POPG immediately permeabilize these lipid membranes [21]. Fast content release was also observed for vesicles containing POPC:DOPA lipids [19, 48]. The binding of oligomers to lipid bilayers has been reported to not always result in membrane permeabilization [19, 21]. Even 30 minutes after addition of the oligomers POPG:POPC bilayers remained intact [48, 57]. For the two component lipid mixture CL:POPC (1:3), a lipid composition that comes close to that of mitochondrial membranes, no leakage was observed at short time scales [19]. Here we show that interaction of oligomers with bilayers does not necessarily result in a fast loss of membrane integrity. Membranes with a lipid composition (CL:POPE:POPC (4:3:5)) similar to that reported earlier [19] show some dye release over 18 hours (**Figure 3.6.B**). However, even on these long time scales oligomer binding did not result in permeabilization of the plasma membrane mimicking lipid bilayers (brain PS:brain PE:cholesterol) (**Figure 3.6.C**). To describe the oligomer-induced calcein release kinetics from CL:POPE:POPC vesicles at least three exponentials, and therefore at least three rate constants, were necessary. The presence of more than one rate constant suggests that subpopulations of vesicles are differently affected by the addition of oligomers. The value of one of the rate constants ( $k_3$  in **Table 3.1**) describing the calcein flux as a function of oligomer concentration is comparable to that observed for lipid

bilayers in the absence of oligomers [58, 59]. This suggests that a fraction of the vesicles is not affected by the oligomers. Oligomers either did not bind or did not affect the calcein permeability of this fraction. As expected, the fraction of unaffected vesicles becomes smaller with increasing oligomer concentration. The amplitude of the other two exponents increases with the oligomer concentration. The dye release kinetics described by these two exponents is therefore attributed to the presence of oligomers in or on the lipid bilayer. Surprisingly both rate constants are observed to increase with increasing oligomer concentrations (See **Table 3.1**). The oligomer-dependent exponents are expected to contain contributions of both the lipid bilayer and the oligomers. Because the leakage is much faster in the presence of oligomers we assume that the contribution of oligomers is very large compared to the contribution of the bare bilayer. As indicated in the Results section the value of  $k$  does not only depend on the permeability coefficient  $P$  but also on the volume of the vesicle and the area over which diffusion takes place. With increasing oligomer concentrations, the area covered by oligomers is expected to become larger. In contrast to our observation this increase in oligomer area should give rise to an increase in the rate constants contributed to oligomers. The observed decrease in the rate constants may result from an increase in vesicle volume, i.e. by incorporation of oligomers in the lipid bilayer. Dynamic light scattering experiments indicate that CL:POPE:POPC LUVs indeed become larger upon incubation with oligomers supporting the hypothesis that the decrease in rate constants corresponding to oligomer-induced leakage results from a volume increase. The observed change in CL:POPE:POPC vesicles diameter of approximately 30 nm corresponds to the expected volume change resulting from oligomer incorporation (**Figure 3.7**). The decrease in leakage observed for brainPS:brainPE:ch bilayers in the presence of oligomers possibly results from the binding of oligomers and blocking of the membrane surface. The permeability of the oligomer-covered surface is low compared to the permeability of the bare membrane surface.

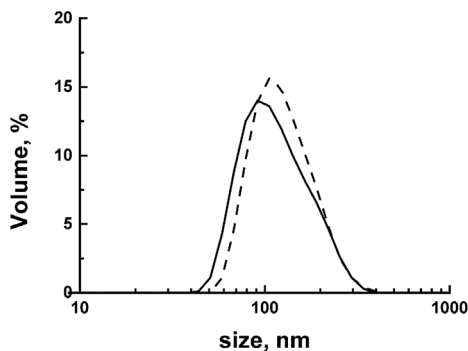


**Figure 3.7: Typical DLS graph for CL:POPE:POPC LUVs before and after addition of oligomers.** Parameters from DLS measurements are described as volume of particles (%) as a function of size (nm) ( $F(\text{size, nm}) = \text{volume of vesicles, \%}$ ) for vesicles alone (CL:POPE:POPC (-)) and vesicles + oligomers (---). Changes in diameter between membranes ( $144.1 \pm 6.0$ ) and membranes after addition of oligomers ( $177.8 \pm 15.1$ ) are  $\sim 30$  nm for CL:POPE:POPC membranes. Peak width changes were  $\sim 12$  nm; peak width of vesicles alone is  $50.2 \pm 6.5$  nm and peak width after 18h of incubation with oligomers is  $62.6 \pm 4.5$  nm.

Recent data on more physiologically relevant Brain Total Lipid Extract membranes (BTLEM) have shown that  $\alpha$ S causes bilayer defects [60]. We speculate that the brain PS: brain PE:ch model system we use may show lipid rearrangement similar to that proposed for BTLEM membranes. Cholesterol in complex model brain PS:brain PE:ch membranes can have an additional stabilizing effect on these membranes [19, 48, 52, 61] making them less vulnerable to oligomer-induced leakage. In our experimental system, the inclusion of cholesterol at a constant charge density does not appear to have any appreciable effect on the extent permeabilization (**Figure 3.8**). However it has been suggested that the amount of the cholesterol in the plasma membrane is important for the formation of amyloid channels [62, 63].

For the amyloid-forming protein Islet Amyloid Polypeptide, slow dye release from POPG:POPC vesicles was concluded to be caused by the formation of fibrils [64]. The experiments presented here were performed with stable oligomers [40]. We thus do not expect that conformational changes and further aggregation play a role in long-term leakage kinetics. Alternatively any conformational changes in the oligomer may be beyond our detection limit because they involve only a few proteins.

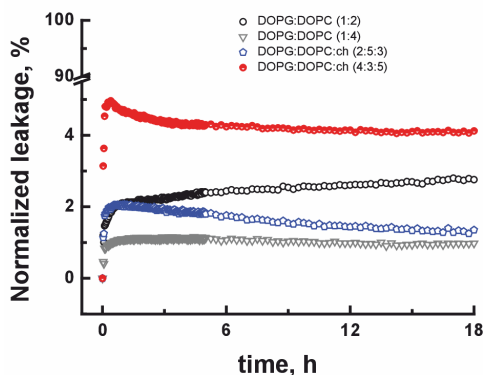


**Figure 3.8: Oligomer-induced leakage kinetics from vesicles of different lipid composition:** DOPG:DOPC (1:2, black circles), DOPG:DOPC (1:4, grey triangles), DOPG:DOPC:cholesterol (2:5:3, blue pentagons) and DOPG:DOPC:cholesterol (4:3:5, red circles). Oligomers at 1  $\mu$ M (equivalent monomer) concentration were incubated with the lipid membranes for 18 h. Oligomer-induced leakage was < 5%, which is comparable to the data observed with our plasma inner leaflet membrane mimics.

The reported membrane leakage data suggest that complex lipid membranes are less prone to oligomer-induced damage. The complexity of model plasma membranes lies in the composition of the membranes itself, consisting largely of combinations of long and polyunsaturated lipids in the brain lipid extracts used. The results of the present study show that mitochondrial model membranes are more prone to oligomer-induced damage at longer timescales while the more complex plasma membrane model systems do not show a concentration dependent permeabilization on the same time scale. Other *in vitro* studies have suggested that the mitochondria specific lipid CL is essential for  $\alpha$ S mitochondrial membrane interactions [27]. A recent study [64] confirmed a common mechanism of damage of mitochondrial membranes by amyloid induced species via direct interactions of these species with membrane phospholipids. Their proposed mechanism agrees very well with our data on mitochondrial model membranes, which is mediated by increased affinity of these species for CL.

### 3.6 Acknowledgments

We thank Kirsten van Leijenhorst-Groener and Nathalie Schilderink for assistance with the expression and purification of  $\alpha$ -synuclein. This work was financially



supported by the Nederlandse Organisatie voor Wetenschappelijk Onderzoek (NWO) via NWO-CW TOP grant number 700.58.302. M. T. S. and V. S. acknowledge support by NanoNextNL, a micro and nanotechnology consortium of the Government of the Netherlands and 130 partners. CD experiments were performed in the Molecular Nanofabrication group at the University of Twente. We thank Prof. Dr. Ir. Pascal Jonkheijm from the Molecular Nanofabrication group for help and useful inputs about CD.

### 3.7 References

1. Cookson, M. R. (2009) alpha-Synuclein and neuronal cell death, *Mol Neurodegener.* **4**, 9.
2. Uversky, V. N. (2007) Neuropathology, biochemistry, and biophysics of alpha-synuclein aggregation, *J Neurochem.* **103**, 17-37.
3. Auluck, P. K., Caraveo, G. & Lindquist, S. (2010) alpha-Synuclein: membrane interactions and toxicity in Parkinson's disease, *Annu Rev Cell Dev Biol.* **26**, 211-33.
4. Kayed, R., Head, E., Thompson, J. L., McIntire, T. M., Milton, S. C., Cotman, C. W. & Glabe, C. G. (2003) Common structure of soluble amyloid oligomers implies common mechanism of pathogenesis, *Science.* **300**, 486-9.
5. Kaye, R., Sokolov, Y., Edmonds, B., McIntire, T. M., Milton, S. C., Hall, J. E. & Glabe, C. G. (2004) Permeabilization of lipid bilayers is a common conformation-dependent activity of soluble amyloid oligomers in protein misfolding diseases, *J Biol Chem.* **279**, 46363-6.
6. Zanzoni, A., Marchese, D., Agostini, F., Bolognesi, B., Cirillo, D., Botta-Orfila, M., Livi, C. M., Rodriguez-Mulero, S. & Tartaglia, G. G. (2013) Principles of self-organization in biological pathways: a hypothesis on the autogenous association of alpha-synuclein, *Nucleic Acids Res.* **41**, 9987-98.
7. Breydo, L., Wu, J. W. & Uversky, V. N. (2012) Alpha-synuclein misfolding and Parkinson's disease, *Biochim Biophys Acta.* **1822**, 261-85.
8. Auluck, P. K., Caraveo, G. & Lindquist, S. (2010) alpha-Synuclein: membrane interactions and toxicity in Parkinson's disease, *Annu Rev Cell Dev Biol.* **26**, 211-33.
9. Jao, C. C., Hegde, B. G., Chen, J., Haworth, I. S. & Langen, R. (2008) Structure of membrane-bound alpha-synuclein from site-directed spin labeling and computational refinement, *Proc Natl Acad Sci U S A.* **105**, 19666-71.
10. Rhoades, E., Ramlall, T. F., Webb, W. W. & Eliezer, D. (2006) Quantification of alpha-synuclein binding to lipid vesicles using fluorescence correlation spectroscopy, *Biophys J.* **90**, 4692-700.
11. Middleton, E. R. & Rhoades, E. (2010) Effects of curvature and composition on alpha-synuclein binding to lipid vesicles, *Biophys J.* **99**, 2279-88.
12. Shvadchak, V. V., Yushchenko, D. A., Pievo, R. & Jovin, T. M. (2011) The mode of alpha-synuclein binding to membranes depends on lipid composition and lipid to protein ratio, *FEBS Lett.* **585**, 3513-9.
13. Kjaer, L., Giehm, L., Heimburg, T. & Otzen, D. (2009) The influence of vesicle size and composition on alpha-synuclein structure and stability, *Biophys J.* **96**, 2857-70.
14. Pandey, A. P., Haque, F., Rochet, J. C. & Hovis, J. S. (2009) Clustering of alpha-synuclein on supported lipid bilayers: role of anionic lipid, protein, and divalent ion concentration, *Biophys J.* **96**, 540-51.
15. Stockl, M., Fischer, P., Wanker, E. & Herrmann, A. (2008) Alpha-synuclein selectively binds to anionic phospholipids embedded in liquid-disordered domains, *J Mol Biol.* **375**, 1394-404.

## Alpha-synuclein oligomers distinctively permeabilize complex model membranes

16. Danzer, K. M., Haasen, D., Karow, A. R., Moussaud, S., Habeck, M., Giese, A., Kretschmar, H., Hengerer, B. & Kostka, M. (2007) Different species of alpha-synuclein oligomers induce calcium influx and seeding, *J Neurosci.* **27**, 9220-32.
17. Cappai, R., Leck, S. L., Tew, D. J., Williamson, N. A., Smith, D. P., Galatis, D., Sharples, R. A., Curtain, C. C., Ali, F. E., Cherny, R. A., Culvenor, J. G., Bottomley, S. P., Masters, C. L., Barnham, K. J. & Hill, A. F. (2005) Dopamine promotes alpha-synuclein aggregation into SDS-resistant soluble oligomers via a distinct folding pathway, *FASEB J.* **19**, 1377-9.
18. Lashuel, H. A., Petre, B. M., Wall, J., Simon, M., Nowak, R. J., Walz, T. & Lansbury, P. T., Jr. (2002) Alpha-synuclein, especially the Parkinson's disease-associated mutants, forms pore-like annular and tubular protofibrils, *J. Mol. Biol.* **322**, 1089-102.
19. van Rooijen, B. D., Claessens, M. M. & Subramaniam, V. (2009) Lipid bilayer disruption by oligomeric alpha-synuclein depends on bilayer charge and accessibility of the hydrophobic core, *Biochim Biophys Acta.* **1788**, 1271-8.
20. van Rooijen, B. D., Claessens, M. M. & Subramaniam, V. (2010) Membrane Permeabilization by Oligomeric alpha-Synuclein: In Search of the Mechanism, *PLoS One.* **5**, e14292.
21. Volles, M. J., Lee, S. J., Rochet, J. C., Shtilerman, M. D., Ding, T. T., Kessler, J. C. & Lansbury, P. T., Jr. (2001) Vesicle permeabilization by protofibrillar alpha-synuclein: implications for the pathogenesis and treatment of Parkinson's disease, *Biochemistry.* **40**, 7812-9.
22. Meratan, A. A., Ghasemi, A. & Nemat-Gorgani, M. (2011) Membrane integrity and amyloid cytotoxicity: a model study involving mitochondria and lysozyme fibrillation products, *J Mol Biol.* **409**, 826-38.
23. Nakamura, K., Nemani, V. M., Azarbal, F., Skibinski, G., Levy, J. M., Egami, K., Munishkina, L., Zhang, J., Gardner, B., Wakabayashi, J., Sesaki, H., Cheng, Y., Finkbeiner, S., Nussbaum, R. L., Masliah, E. & Edwards, R. H. (2011) Direct membrane association drives mitochondrial fission by the Parkinson disease-associated protein alpha-synuclein, *J Biol Chem.* **286**, 20710-26.
24. Yong-Kee, C. J., Sidorova, E., Hanif, A., Perera, G. & Nash, J. E. (2012) Mitochondrial dysfunction precedes other sub-cellular abnormalities in an in vitro model linked with cell death in Parkinson's disease, *Neurotox Res.* **21**, 185-94.
25. Ardail, D., Privat, J. P., Egret-Charlier, M., Levrat, C., Lerme, F. & Louisot, P. (1990) Mitochondrial contact sites. Lipid composition and dynamics, *J Biol Chem.* **265**, 18797-802.
26. Ramakrishnan, M., Jensen, P. H. & Marsh, D. (2003) Alpha-synuclein association with phosphatidylglycerol probed by lipid spin labels, *Biochemistry.* **42**, 12919-26.
27. Zigoneanu, I. G., Yang, Y. J., Krois, A. S., Haque, E. & Pielak, G. J. (2012) Interaction of alpha-synuclein with vesicles that mimic mitochondrial membranes in *Biochim Biophys Acta* pp. 512-9
28. Liu, G., Zhang, C., Yin, J., Li, X., Cheng, F., Li, Y., Yang, H., Ueda, K., Chan, P. & Yu, S. (2009) alpha-Synuclein is differentially expressed in mitochondria from different rat brain regions and dose-dependently down-regulates complex I activity, *Neurosci Lett.* **454**, 187-92.
29. Wen-Wei Li, R., J ing-Chun Guo, Hui-Min Ren, Xi-Liang Zha, Jie-Shi Cheng and Ding-Fang Cai (2007) Localization of a-synuclein to mitochondria within midbrain of mice, *NeuroReport.* **18**, 1543-1546.
30. Parihar, M. S., Parihar, A., Fujita, M., Hashimoto, M. & Ghafourifar, P. (2008) Mitochondrial association of alpha-synuclein causes oxidative stress, *Cell Mol Life Sci.* **65**, 1272-84.
31. Devi, L., Raghavendran, V., Prabhu, B. M., Avadhani, N. G. & Anandatheerthavarada, H. K. (2008) Mitochondrial import and accumulation of alpha-synuclein impair complex I in human dopaminergic neuronal cultures and Parkinson disease brain, *J Biol Chem.* **283**, 9089-100.
32. Devi, L. & Anandatheerthavarada, H. K. (2010) Mitochondrial trafficking of APP and alpha synuclein: Relevance to mitochondrial dysfunction in Alzheimer's and Parkinson's diseases, *Biochim Biophys Acta.* **1802**, 11-9.
33. Guardia-Laguarta, C., Area-Gomez, E., Rub, C., Liu, Y., Magrane, J., Becker, D., Voos, W., Schon, E. A. & Przedborski, S. (2014) alpha-Synuclein is localized to mitochondria-associated ER membranes, *J Neurosci.* **34**, 249-59.
34. Fauvet, B., Fares, M. B., Samuel, F., Dikiy, I., Tandon, A., Eliezer, D. & Lashuel, H. A. (2012) Characterization of semisynthetic and naturally Nalpha-acetylated alpha-synuclein in vitro and in

### Chapter 3

intact cells: implications for aggregation and cellular properties of alpha-synuclein, *J Biol Chem.* **287**, 28243-62.

35. Gitler, A. D., Bevis, B. J., Shorter, J., Strathearn, K. E., Hamamichi, S., Su, L. J., Caldwell, K. A., Caldwell, G. A., Rochet, J. C., McCaffery, J. M., Barlowe, C. & Lindquist, S. (2008) The Parkinson's disease protein alpha-synuclein disrupts cellular Rab homeostasis, *Proc Natl Acad Sci U S A.* **105**, 145-50.

36. Fiske, M., White, M., Valtierra, S., Herrera, S., Solvang, K., Konnikova, A. & DebBurman, S. (2011) Familial Parkinson's Disease Mutant E46K  $\alpha$ -synuclein Localizes to Membranous Structures, Forms Aggregates, and Induces Toxicity in Yeast Models, *ISRN Neurology.* **2011**, 14.

37. Pacheco, C., Aguayo, L. G. & Opazo, C. (2012) An extracellular mechanism that can explain the neurotoxic effects of alpha-synuclein aggregates in the brain, *Front Physiol.* **3**, 297.

38. van Raaij, M. E., Segers-Nolten, I. M. J. & Subramaniam, V. (2006) Quantitative Morphological Analysis Reveals Ultrastructural Diversity of Amyloid Fibrils from  $\alpha$ -Synuclein Mutants, *Biophys J.* **91**, L96-L98.

39. Pace, C. N., Vajdos, F., Fee, L., Grimsley, G. & Gray, T. (1995) How to measure and predict the molar absorption coefficient of a protein, *Protein Sci.* **4**, 2411-23.

40. Zijlstra, N., Blum, C., Segers-Nolten, I. M., Claessens, M. M. & Subramaniam, V. (2012) Molecular composition of sub-stoichiometrically labeled alpha-synuclein oligomers determined by single-molecule photobleaching, *Angew Chem Int Ed Engl.* **51**, 8821-4.

41. van Meer, G., Voelker, D. R. & Feigenson, G. W. (2008) Membrane lipids: where they are and how they behave, *Nat Rev Mol Cell Biol.* **9**, 112-124.

42. Davidson, W. S., Jonas, A., Clayton, D. F. & George, J. M. (1998) Stabilization of alpha-synuclein secondary structure upon binding to synthetic membranes, *J Biol Chem.* **273**, 9443-9.

43. Angelova, M. I. & Dimitrov, D. S. (1986) Liposome Electroformation, *Faraday Disc Chem Soc.* **81**, 303-311.

44. Barrow, C. J., Yasuda, A., Kenny, P. T. & Zagorski, M. G. (1992) Solution conformations and aggregational properties of synthetic amyloid beta-peptides of Alzheimer's disease, *J Mol Biol.* **225**, 1075-93.

45. Jo, E., McLaurin, J., Yip, C. M., St George-Hyslop, P. & Fraser, P. E. (2000) alpha-Synuclein membrane interactions and lipid specificity, *J Biol Chem.* **275**, 34328-34.

46. Chen, Y. H., Yang, J. T. & Chau, K. H. (1974) Determination of the Helix and beta Form of Proteins in Aqueous Solution by Circular Dichroism, *Biochemistry.* **13**, 3350-9.

47. Scholtz, J. M., Qian, H., York, E. J., Stewart, J. M. & Baldwin, R. L. (1991) Parameters of Helix-Coil Transition Theory for Alanine-Based Peptides of Varying Chain Lengths in Water, *Biopolymers.* **31**, 1463-1470.

48. van Rooijen, B. D., Claessens, M. M. & Subramaniam, V. (2008) Membrane binding of oligomeric alpha-synuclein depends on bilayer charge and packing, *FEBS Lett.* **582**, 3788-92.

49. Zhu, M., Li, J. & Fink, A. L. (2003) The association of alpha-synuclein with membranes affects bilayer structure, stability, and fibril formation, *J Biol Chem.* **278**, 40186-97.

50. Wang, G. F., Li, C. & Pielak, G. J. (2010) 19F NMR studies of alpha-synuclein-membrane interactions, *Protein Sci.* **19**, 1686-91.

51. Pfefferkorn, C. M. & Lee, J. C. (2010) Tryptophan probes at the alpha-synuclein and membrane interface, *J Phys Chem B.* **114**, 4615-22.

52. Shvadchak, V. V., Falomir-Lockhart, L. J., Yushchenko, D. A. & Jovin, T. M. (2011) Specificity and kinetics of alpha-synuclein binding to model membranes determined with fluorescent excited state intramolecular proton transfer (ESIPT) probe, *J Biol Chem.* **286**, 13023-32.

53. Schwiering, M. & Hellmann, N. (2012) Validation of liposomal lipid composition by thin-layer chromatography, *J Liposome Res.* **22**, 279-84.

54. Eliezer, D., Kutluay, E., Bussell, R., Jr. & Browne, G. (2001) Conformational properties of alpha-synuclein in its free and lipid-associated states, *J Mol Biol.* **307**, 1061-73.

55. Chandra, S., Chen, X., Rizo, J., Jahn, R. & Sudhof, T. C. (2003) A broken alpha-helix in folded alpha-synuclein, *J Biol Chem.* **278**, 15313-8.

## Alpha-synuclein oligomers distinctively permeabilize complex model membranes

56. Bartels, T., Ahlstrom, L. S., Leftin, A., Kamp, F., Haass, C., Brown, M. F. & Beyer, K. (2010) The N-terminus of the intrinsically disordered protein alpha-synuclein triggers membrane binding and helix folding, *Biophys J.* **99**, 2116-24.
57. Volles, M. & Lansbury, P. (2002) Vesicle permeabilization by protofibrillar alpha-synuclein is sensitive to Parkinson's disease-linked mutations and occurs by a pore-like mechanism, *Biochemistry.* **41**, 4595 - 4602.
58. Maherani, B., Arab-Tehrany, E., Kheiriloomoo, A., Geny, D. & Linder, M. (2013) Calcein release behavior from liposomal bilayer; influence of physicochemical/mechanical/structural properties of lipids, *Biochimie.* **95**, 2018-2033.
59. Shimanouchi, T., Ishii, H., Yoshimoto, N., Umakoshi, H. & Kuboi, R. (2009) Calcein permeation across phosphatidylcholine bilayer membrane: effects of membrane fluidity, liposome size, and immobilization, *Colloids Surf B Biointerfaces.* **73**, 156-60.
60. Ouberai, M. M., Wang, J., Swann, M. J., Galvagnion, C., Guilliams, T., Dobson, C. M. & Welland, M. E. (2013) alpha-Synuclein senses lipid packing defects and induces lateral expansion of lipids leading to membrane remodeling, *J Biol Chem.* **288**, 20883-95.
61. Leftin, A., Job, C., Beyer, K. & Brown, M. F. (2013) Solid-state (1)(3)C NMR reveals annealing of raft-like membranes containing cholesterol by the intrinsically disordered protein alpha-Synuclein, *J Mol Biol.* **425**, 2973-87.
62. Fantini, J., Carlus, D. & Yahi, N. (2011) The fusogenic tilted peptide (67-78) of alpha-synuclein is a cholesterol binding domain, *Biochim Biophys Acta.* **1808**, 2343-51.
63. Fantini, J. & Yahi, N. (2013) The driving force of alpha-synuclein insertion and amyloid channel formation in the plasma membrane of neural cells: key role of ganglioside- and cholesterol-binding domains, *Adv Exp Med Biol.* **991**, 15-26.
64. Camilleri, A., Zarb, C., Caruana, M., Ostermeier, U., Ghio, S., Hogen, T., Schmidt, F., Giese, A. & Vassallo, N. (2013) Mitochondrial membrane permeabilisation by amyloid aggregates and protection by polyphenols, *Biochim Biophys Acta.* **1828**, 2532-43.



## Chapter 4

# Characterization of oligomers formed from disease-related alpha-synuclein amino acid mutations

### 4.1 Abstract

Single amino acid mutations in the alpha-synuclein ( $\alpha$ S) protein are related to early onset Parkinson's disease. In addition to the well-known A30P, A53T, and E46K mutants, recently two new familial disease-related  $\alpha$ S mutations, H50Q (where Histidine 50 is replaced by Glutamine) and G51D (where Glycine 51 is replaced by Aspartic Acid) were discovered. How these mutations affect the putative physiological function of  $\alpha$ S and the disease pathology is still unknown. Here we show that like WT  $\alpha$ S, H50Q and G51D bind to negatively-charged membranes, form soluble partially-folded oligomers with an aggregation number of  $\sim$ 30 monomers, and can aggregate into amyloid fibrils. However, although the binding affinity of the monomeric protein and the aggregation number of the oligomers formed under our specific protocol are comparable for WT, H50Q and G51D, G51D oligomers cannot disrupt negatively-charged and physiologically-relevant model membranes. Replacement of the membrane immersed glycine by a negatively charged aspartic acid at position 51 prevents membrane destabilization whereas a mutation in the solvent exposed part of the membrane bound alpha helix such as found H50Q has little effect on the bilayer disrupting properties of oligomers.

\*Parts of this chapter represent content of a manuscript in preparation: Stefanovic, A. N., Lindhoud S., Semerdzhiev S.A., Claessens, M. M. A. E., & Subramaniam, V. Characterization of oligomers formed from disease-related alpha-synuclein amino acid mutations

## 4.2 Introduction

Alpha-synuclein is an intrinsically disordered protein involved in PD [1, 2]. 10-20% of all Parkinson's disease patients have a hereditary form of the disease. Disease-related mutations include gene duplications, triplications and point mutations in the SNCA (synuclein, alpha (non A4 component of amyloid precursor) gene encoding for  $\alpha$ S. In the last 20 years 5 different SNCA point mutations that results in an amino acid mutations in  $\alpha$ S and that are associated with PD have been identified: A30P [3], E46K [4], H50Q [5, 6], G51D [7, 8] and A53T [9]. The two recently-discovered mutations, H50Q and G51D result in early onset PD and rapid progression of the disease [5-8]. The pathology observed in patients with the G51D mutation is characterized by an early disease onset, moderate response to treatment with levodopa, rapid progression, loss of autonomy and frequent psychiatric symptoms [8]. The clinical pathology of the H50Q mutation is similar to the disease pathology of the E46K and A53T mutation [5].

All disease-related amino acid mutations are located in the N-terminal, membrane binding part of  $\alpha$ S. These mutations therefore directly affect  $\alpha$ S conformation and membrane binding. As observed for WT and other disease mutants, G51D and H50Q adopt an  $\alpha$ -helical conformation upon binding negatively charged membranes or SDS micelles [6, 8]. The affinity for membranes differs between the WT protein and the known  $\alpha$ S point mutants; A53T and E46K exhibit a higher binding affinity to negatively charged vesicles than A30P [10]. Not only membrane binding but also aggregation into amyloid fibrils is affected by the exchange of an amino acid. It was reported that A53T and E46K aggregate faster than WT, while A30P showed a slower aggregation rate [10, 11]. In comparison to WT the two newly discovered mutations H50Q and G51D have been reported to show respectively faster and slower kinetics of fibril formation [6, 8, 12-14]. Although membrane binding is an important aspect of the putative  $\alpha$ S function and fibrillization plays a role in the disease, monomers and fibrils are generally not thought to be responsible for a cell death in PD. Studies done in animals, cell systems and model membranes have identified soluble  $\alpha$ S oligomers as the potentially toxic species of PD [15-20]. To be able to relate possible toxicity to oligomer structure  $\alpha$ S oligomers have been characterized using various biophysical and biochemical techniques including circular dichroism [21, 22], single molecule photobleaching [23], small angle x-ray scattering (SAXS) [1, 24-26], atomic force microscopy (AFM) [27], NMR spectroscopy [28], confocal microscopy [29] and

electron microscopy [30]. These techniques have shown a variety of shapes and sizes, determined the molecular weight of the oligomers [31, 32] and established the aggregation number, or the number of monomers per oligomer [23, 24, 32]. Here we quantify the membrane binding affinity of the G51D and H50Q mutants, study their aggregation into amyloid fibrils and characterize the number of monomers per oligomer and the membrane disrupting properties of oligomers from all  $\alpha$ S disease mutants. SAXS studies show that all the oligomers (WT and disease-related mutants) are composed of a similar number of monomers. Compared to the other disease mutants, no differences in G51D membrane binding, fibril formation and oligomer structure were observed. However, G51D oligomers were not able to permeabilize membranes. We relate the inability of the G51D oligomers to permeabilize negatively charged DOPG and mitochondrial membrane mimics to the position of the amino acid mutation and its role in membrane binding.

## **4.3 Material and methods**

### **4.3.1 Preparation of oligomeric alpha-synuclein**

The expression and purification of human wild-type (WT) and disease-related  $\alpha$ S mutants were performed as previously described [21]. Oligomers from WT and disease-related mutants were prepared as described in the literature [21]. The protein concentration was determined by measuring the absorbance on a Shimadzu spectrophotometer at 276 nm, using a molar extinction coefficient of  $5600 \text{ M}^{-1}\text{cm}^{-1}$  [33]. Oligomers were purified and separated from monomers using size-exclusion chromatography on a Superdex<sup>TM</sup> 200 10/300 GL column (GE Healthcare Bio-Sciences AB, Uppsala, Sweden) using 10 mM Tris, 150 mM NaCl, 0.01% NaN<sub>3</sub> as an elution buffer. Separation of oligomers from monomers is based on size, where larger particles (oligomers) elute first. Based on size-exclusion elution profiles oligomer fractions were collected and concentrated up to  $\sim 100 \mu\text{M}$  equivalent monomer concentration for SAXS measurements and  $\sim$  up to  $50 \mu\text{M}$  equivalent monomer concentration for membrane leakage experiments.



### 4.3.2 SUVs preparation and binding of $\alpha$ S monomers to SUVs

Preparation of SUVs to study membrane binding of monomers using CD was done using the procedure described in **Chapter 3** with slight modifications. To test the binding affinities of  $\alpha$ S for DOPG and CL:POPE:POPC membranes, monomeric WT, G51D and H50Q  $\alpha$ S at a concentration of 4  $\mu$ M was titrated with an SUV solution. Lipid concentrations in the SUV solutions for the titration were between 0.004 and 1.2 mM. The following equation was applied to calculate the binding parameters [34]:

$$R = R_f + (R_0 - R_f) \left( \frac{-K_d + \sqrt{(K_d^2 + 4CK_d)}}{2C} \right) \quad (1)$$

where  $R$  is the measured signal at a given lipid concentration,  $C$  is the total lipid concentration,  $K_d$  is the dissociation equilibrium constant.  $R_f$  and  $R_0$  are the final and initial signals, respectively. To obtain the  $K_d$  values all the data are normalized.

### 4.3.4 LUV preparation and calcein release assay

LUVs of DOPG and CL:POPE:POPC for calcein release assays were prepared as described in **Chapter 3** of this thesis. A detailed protocol for the calcein release assay is given in **Chapter 3**.

### 4.3.5 Small-Angle X-ray Scattering

SAXS measurements on  $\alpha$ S oligomers were performed in triplicate, except for G51D oligomers, on samples containing a  $\sim 100$   $\mu$ M equivalent monomer concentration of  $\alpha$ S dissolved in 10 mM Tris, 150 mM NaCl, 0.01% NaN<sub>3</sub> buffer using the SAXS/WAXS setup in BM26 - DUBBLE - Dutch-Belgian Beamline, ESRF, Grenoble, France. Approximately 100  $\mu$ L of a sample was placed into 1.5 mm glass capillaries and 2D-images were collected using two Pilatus photon counting detectors. The sample-to-detector distance was 6.6 m. The wavelength for the incident X-ray was 0.1 nm and beam size  $2.5 \times 4.5$  mm<sup>2</sup> and the energy of the X-rays was 12 eV, resulting in a q-range of  $\sim 0.03$ -1.5 nm<sup>-1</sup>. For data reduction, buffer (background) scattering values were subtracted from the protein solution scattering values and standards were used to convert the scattering values to values on an absolute scale.

First we determined the radius of gyration,  $R_g$  and  $I(0)$ , using both Guinier's law:

$I(q) = I(0)\exp(-q^2R_g^2/3)$  and the Pair-Distance Distribution Function  $P(r)$ :

$$I(0) = 4\pi \int_0^{D_{max}} P(r)dr .$$

Guinier plots provide information about the average size of the particles in the solution. For spherical particles Guinier plots, where  $(\ln(I(q)))$  is plotted as a function of  $q^2$ , give a linear dependency for  $qR_g < 1.3$ . From the slope of this curve  $R_g$  was determined and  $I(0)$  was obtained by extrapolation to  $q = 0$ .

An alternative way to determine  $R_g$  is to use the  $P(r)$  function.  $P(r)$  within a protein is defined as the probable frequency of vector with interatomic distance ( $r$ ). It is sensitive to the changes in symmetry and structural domains. To obtain maximum linear dimension  $D_{max}$ , using  $P(r)$  function, it has to be assumed that  $P(r) = 0$  at  $r = 0$ .  $D_{max}$  depends on the quality of the scattering data and in theory the minimum  $q$  should satisfy the following relations for  $q_{min} : q_{min} \leq \pi D_{max}$  and  $q_{max} : q_{max} \geq 2\pi / D_{max}$  [35]. For data processing and determination of  $P(r)$  we have used the GNOM (ATSAS) indirect Fourier transform program [36]. From  $P(r)$  plots  $R_g$  and  $I(0)$  values can be obtained. A comparison of  $R_g$  values using both methods is presented in **Table 4.2**.

The aggregation numbers of the oligomers can be determined indirectly by an equation that describes the scattering of the particles in a solution:

$$I(q) = nV^2\Delta\rho_{rel.sol}^2P(q)S(q) \quad (2)$$

where  $n$  is the number of scattering particles per unit volume,  $V$  is the volume of the particle, and  $\Delta\rho_{rel.sol} = \rho_{particle} - \rho_{solvent}$  is the excess scattering length density or contrast,  $P(q)$  is the form factor of the particle and is related to the particle's shape,  $S(q)$  is the structure factor that defines inter-particle interactions in the solution.

When the SAXS intensities are extrapolated to  $q = 0$ , then  $I(0)$  is given by [37]:

$$I(0) = nV^2\Delta\rho_{rel.sol}^2 \quad (3)$$

## Chapter 4

In our case  $\Delta\rho_{\text{rel.sol}}$  was calculated to be  $0.0002864 \text{ nm}^{-2}$  using contrast calculator in SAXS utilities program (extension of Matlab) [38], using  $\rho_{\text{particle}} = 1.37 \text{ g/cm}^3$  as average protein density as was experimentally determined by [39, 40].

$I(0)$  and the volume  $V$  can be calculated using the  $R_g$  determined via the Guinier approximation or  $P(r)$  analysis.

For calculating  $M_w$  (molecular weight) of the particles/proteins following equation was applied [35]:

$$I(0) = N(\Delta\rho V)^2 = c\Delta\rho^2 v^2 M_w / N_A \quad (4)$$

where  $N_A$  is Avogadro's number and  $c$  is the protein or particle concentration.

The aggregation number  $N$  is extracted by dividing the  $M_w$  estimated from equation 3 by the molecular weight of the  $\alpha\text{S}$  monomer.

To visualize if disordered regions are present in the oligomer the obtained data is presented in a Kratky plot:  $I(q)q^2$  versus  $q$ . Rising Kratky plots are a characteristic of disordered regions [41].

### 4.3.6 Kinetics of aggregation

Solutions containing  $100 \mu\text{M}$   $\alpha\text{S}$  monomers of the different disease mutants in  $10 \text{ mM}$  Tris-HCl,  $100 \text{ mM}$  NaCl, pH 7.4 were incubated at  $37^\circ\text{C}$  under constant shaking in a Tecan SAFIRE II plate reader. Protein aggregation into amyloid fibrils was followed in a Thioflavin T (ThT) fluorescence assay. For this purpose  $5 \mu\text{M}$  ThT was used. Changes in ThT fluorescence were followed using an excitation wavelength of  $446 \text{ nm}$  and bandwidth  $10 \text{ nm}$  and the emission intensity at  $485 \text{ nm}$  was recorded with emission bandwidth of  $10 \text{ nm}$  as a function of time. Aggregation lag times were determined as previously described in [42].

### 4.3.7 Atomic force microscopy (AFM)

To visualize the amyloid fibrils, samples were prepared for AFM imaging. Samples of aggregated protein (after ThT assay) were placed on the mica substrate using the procedure described in [43]. The dried samples were visualized by AFM using tapping mode. During these experiments an NSC 36 tip B was used, with a force constant of  $1.75 \text{ N/m}$  (NanoAndMore GmbH, Wetzlar, Germany). All images

obtained during these experiments are 4 x 4  $\mu\text{m}$  in size, 512 pixels with a z-range of 20 nm.

## 4.4 Results

### 4.4.1 Binding of $\alpha\text{S}$ monomers to SUVs

To determine the membrane binding affinities of WT, H50Q and G51D  $\alpha\text{S}$  to SUVs composed of DOPG and CL:POPE:POPC we titrated  $\alpha\text{S}$  monomers with different SUVs concentrations. Conformational changes of WT, G51D and H50Q  $\alpha\text{S}$  monomers upon binding to the membranes were followed by recording CD spectra between 190 and 260 nm. To follow  $\alpha$ -helix formation and hence membrane binding, the mean residue ellipticities at 222 nm (MRE) are presented as a function of the lipid concentration in **Figure 4.1A** and **4.1B**. The binding affinities were determined from the changes in MRE at 222 nm as a function of lipid concentration (**Figure 4.1**). As described in the **Material and Methods** section, a simple binding model was used to calculate the equilibrium dissociation constant  $K_d$  from the titration of  $\alpha\text{S}$  monomers with DOPG (**Figure 4.1A**) and CL:POPE:POPC (**Figure 4.1B**).

**Table 4.1: Binding constants,  $K_d$ , of  $\alpha\text{S}$  monomers to SUVs**

Lipid	WT $K_d$ ( $\mu\text{M}$ )	H50Q $K_d$ ( $\mu\text{M}$ )	G51D $K_d$ ( $\mu\text{M}$ )
DOPG	54 $\pm$ 38	24 $\pm$ 6	32 $\pm$ 23
CL:POPE:POPC	199 $\pm$ 79	860 $\pm$ 391	368 $\pm$ 71

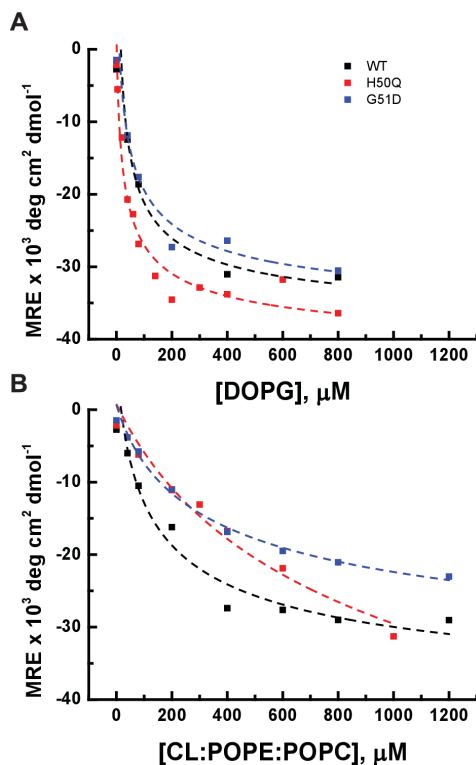


**Figure 4.1: Titration of  $\alpha\text{S}$  monomers by SUVs consisting of: A) DOPG and B) CL:POPE:POPC (4:3:5).** Conformational changes of WT, H50Q and G51D  $\alpha\text{S}$  were followed by CD spectroscopy. The membrane bound  $\alpha$ -helical conformation is characterized by a negative peak at 222 nm in the CD spectrum. The binding affinity was determined from the changes in mean residue ellipticity (MRE) at 222 nm as a function of the lipid concentration. For determination of  $K_d$  the data were normalized to 1. Experiments were performed at 25 °C for 4  $\mu\text{M}$  protein in 10 mM K-phosphate buffer, pH 7.4.

The dissociation constants obtained by fitting the titration curves for lipid mixtures and WT, G51D and H50Q  $\alpha\text{S}$  are given in **Table 4.1**. For all three  $\alpha\text{S}$  species the  $K_d$  values were of the same order of magnitude but the affinity for DOPG membranes was an order of magnitude higher than the affinity for the CL:POPE:POPC mitochondrial membrane mimics. The observed higher affinity for DOPG membranes is in agreement with previous studies on membrane binding of WT and the A30P, A53T, and E46K amino acid mutations in  $\alpha\text{S}$  [22, 44, 45].

#### 4.4.2 Aggregation studies

To further characterize the disease-related  $\alpha$ S mutants the aggregation of 100  $\mu$ M monomers into amyloid fibrils was studied in 10 mM Tris-HCl buffer at 100 mM NaCl, pH 7.4.

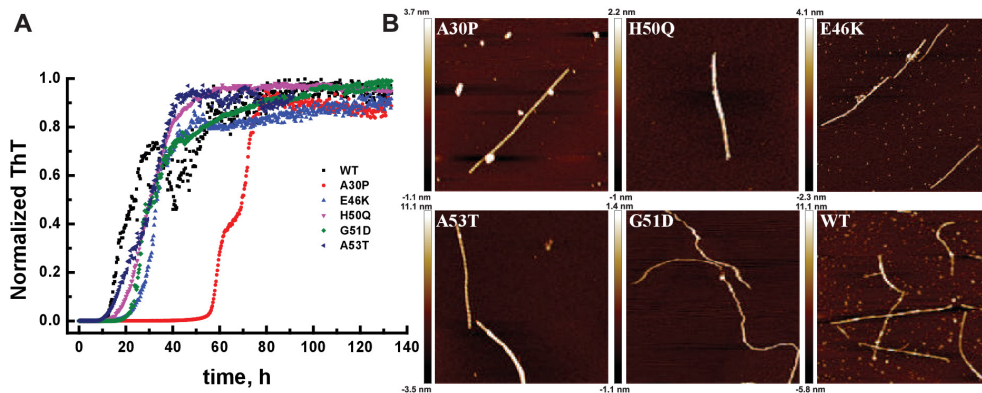


**Figure 4.2: Aggregation of disease-related  $\alpha$ S mutants.** Fibril formation was followed using a classical ThT assay (A) and the presence of fibrils at the ThT plateau is confirmed using AFM (B). Each curve in A) represents an average of 6 different samples. The ThT intensity was normalized to the maximal ThT fluorescence for each sample.

At these buffer conditions the aggregation lag times of most disease mutants were comparable to the lag time observed for WT protein, only A30P behaved significantly different (**Figure 4.2A**). With  $58 \pm 4$  hours the aggregation lag time of A30P was more than two-fold longer than for the other proteins. The fibrils that were obtained with the different disease mutants were visualized using AFM. This analysis confirmed that all disease mutants are able to form amyloid fibrils. The morphologies of the amyloid fibrils formed by WT and the disease-related mutants are qualitatively comparable (**Figure 4.2B**).

#### 4.4.3 Calcein release assay

The toxicity of  $\alpha$ S aggregation in PD has been related to oligomeric species that bind and permeabilize membranes. We performed a calcein release assay to test the ability of oligomers of disease-related  $\alpha$ S mutants to permeabilize negatively charged membranes and mitochondrial membrane mimics. LUVs were filled with calcein at a self-quenching concentration and upon incubation with oligomers an

increase of emission intensity results from dye dilution due to membrane permeabilization. When oligomers were added, they induced fast calcein leakage from DOPG LUVs which was not observed for LUVs in which the mitochondrial membrane composition was mimicked. In **Figure 4.3** the normalized leakage (%) measured 30 minutes after incubation with the respective oligomeric species is represented as a function of oligomer concentration (monomer equivalent). Except for oligomers composed of G51D, all oligomers tested were able to induce almost complete permeabilization of negatively charged DOPG membranes at the highest concentrations tested. The disease-related oligomers are slightly more efficient than WT oligomers in permeabilizing membranes; lower concentrations are required for comparable leakage (**Figure 4.3A**).

Oligomer induced calcein leakage from LUVs composed of a lipid mixture that mimics the mitochondrial membrane composition, CL:POPE:POPC, was very slow. Dye leakage reached a plateau approximately 18 hours after oligomer addition, which is presented in more detail for WT oligomers in **Chapter 4.3**. G51D, and E46K oligomers were not able to induce leakage from the CL:POPE:POPC LUVs (**Figure 4.3B**). Even for the A53T and A30P oligomers that were most efficient in permeabilizing LUVs of this membrane composition, the maximum leakage only reached 30 %.

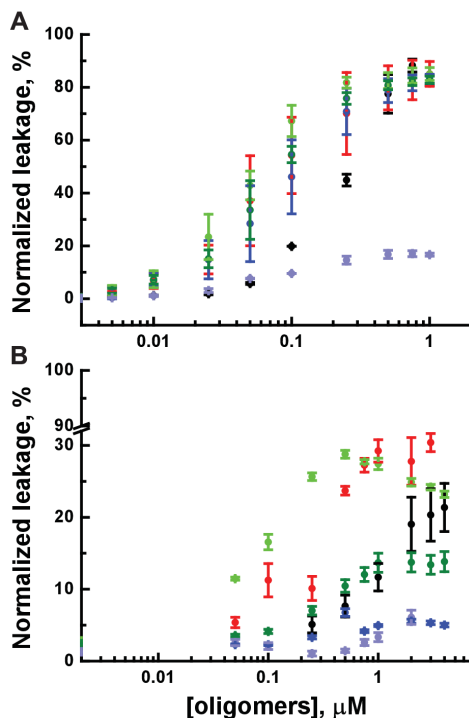


**Figure 4.3:** Calcein release from DOPG (A) and CL:POPE:POPC (B) LUVs as a function of the concentration of oligomeric WT (black circles) and disease-related  $\alpha$ S mutants: A30P (red), E46K (blue), A53T (light green), H50Q (dark green) and G51D (light purple circles). The oligomer concentration is given in equivalent monomer concentration.

#### 4.4.4 Aggregation number

Although the membrane binding affinity and aggregation kinetics of G51D, H50Q and WT  $\alpha$ S monomers are comparable, the ability of their oligomers to permeabilize membranes differs. With similar binding affinity of the monomers the different permeabilization propensity of the oligomers may result from differences in oligomer structure. The aggregation number and overall fold of the oligomers were therefore characterized by SAXS. **Figure 4.4** shows the scattering curves for the 6 different oligomers. The scattering curves look very similar in shape. From these scattering curves the aggregation numbers of the oligomers were estimated using the following procedure: First the  $R_g$  and  $I(0)$  were determined using the Guinier approximation and Pair Distance Distribution Function (PDDF or  $P(r)$ )



(**Figure 4.5**). To calculate the aggregation number, the molecular weight ( $M_w$ ) of protein oligomers has to be determined [46, 47]. We have used equations 3 and 4 to determine the aggregation numbers. The values determined, from the Guinier approximation and PDDF, for the aggregation numbers of the different oligomers can be found in **Figure 4.5B** and **Table 4.2**.

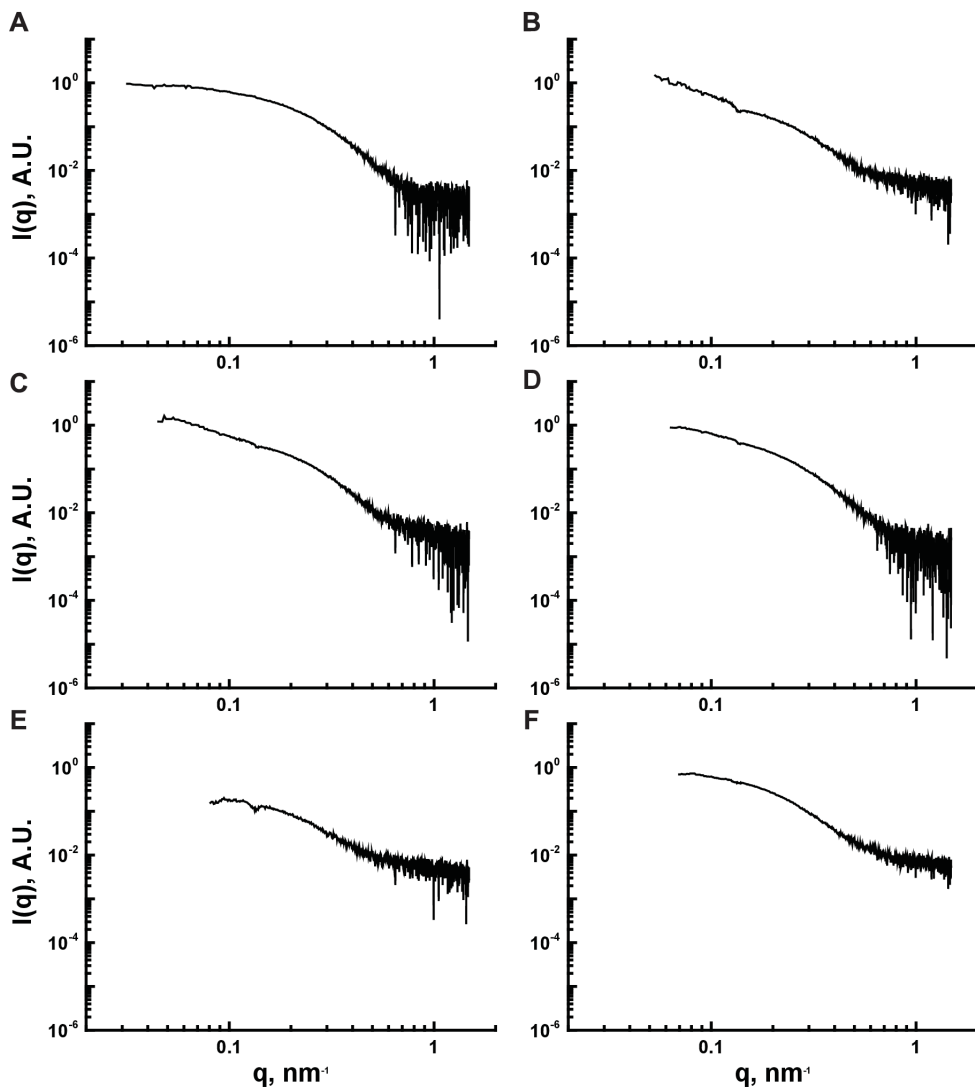


**Figure 4.4:** Experimentally obtained small-angle X-ray scattering curves of  $\alpha$ S oligomers. Representative scattered intensity profiles for: WT (A), A30P (B), E46K (C), H50Q (D), G51D (E) and A53T (F). Intensity of the buffer was subtracted from the intensity of the samples.

As we can observe in **Figure 4.5B** the aggregation number (number of monomers per oligomer,  $N_{m/1oli}$ ) estimated for the oligomers of each disease-related mutant was approximately 30 which agrees well with previously published data from our group on WT oligomers and dopamine-induced oligomers using a single molecule photobleaching approach [23, 48].

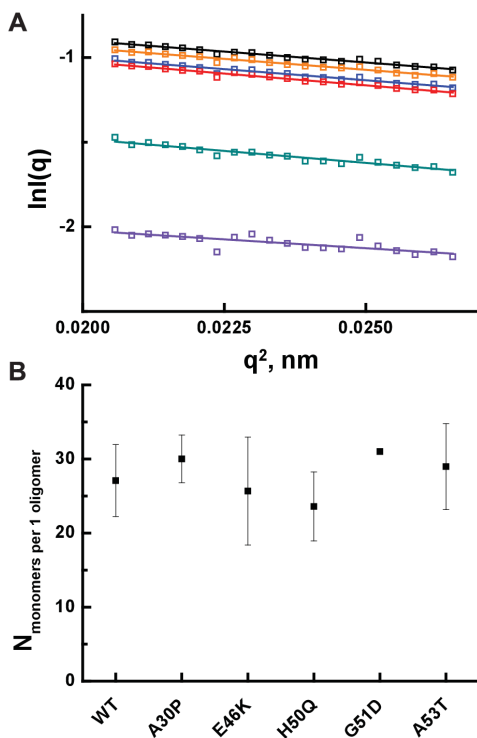


**Figure 4.5: Guinier plots (A) and calculation of number of monomers in the oligomers (B).** In (A) averaged Guinier plot is presented for all oligomers following the approximation  $qR_g < 1.3$ . Legend for Guinier plot in (A): WT (black squares) and  $\alpha$ S disease mutants oligomers A30P (dark cyan), E46K (blue), H50Q (red), G51D (purple) and A53T (orange squares).

In **Table 4.2** one can see that the  $R_g$  values obtained from the Guinier plots are consistently lower than the  $R_g$  values obtained from the PDDF. An explanation for this difference is that the  $P(r)$  function uses the whole data range for determination of  $R_g$  while only data from the low  $q$ -values are used to determine  $R_g$  from the Guinier plot [49]. However, much fewer assumptions about unknown

or not directly determined parameters are required to obtain  $R_g$  from the Guinier approximation. In the discussion we will therefore concentrate on the aggregation number obtained from the Guinier plots.

**Table 4.2: Summary of the parameters obtained from SAXS data by analysis of the Guinier plot and PDDF**

oligomers	Guinier plot			Pair-distance Distribution Function		
	$R_g$ , nm	$I(0)$ , $\text{cm}^{-1}$	$N_{m/1oli}$	$R_g$ , nm	$I(0)$ , $\text{cm}^{-1}$	$N_{m/1oli}$
<b>WT</b>	8.78±0.27	0.703±0.06	27±5	8.24±0.08	0.619±0.04	38±1
<b>A30P</b>	8.3±0.01	0.346±0.04	30±3	7.91±0.05	0.327±0.03	33±5
<b>E46K</b>	8.87±0.35	0.658±0.29	26±7	8.18±0.05	0.584±0.24	37±13
<b>H50Q</b>	9.13±0.24	0.629±0.09	24±4	8.09±0.08	0.525±0.06	41±8
<b>G51D*</b>	7.92	0.201	31	8.29	0.208	24
<b>A53T</b>	8.81±0.39	0.662±0.15	29±6	8.37±0.06	0.61±0.11	35±5

\*1 measurement

We further analyzed the data by plotting  $q^2I(q)$  versus  $q$  in Kratky plots. These Kratky plots are used to monitor the degree of the compactness of a protein in order to evaluate the extent of folding of proteins. Globular molecules follow Porod's law resulting in a bell-shaped curve whereas extended molecules, such as unfolded peptides, have a plateau or increase at higher  $q$ -ranges [50]. The Kratky plots presented in **Figure 4.6** show part of a bell shaped curve and increase of  $q^2I$  with increasing  $q$  which indicates that oligomers composed of WT and disease-related  $\alpha$ S mutants are composed of partially folded proteins.

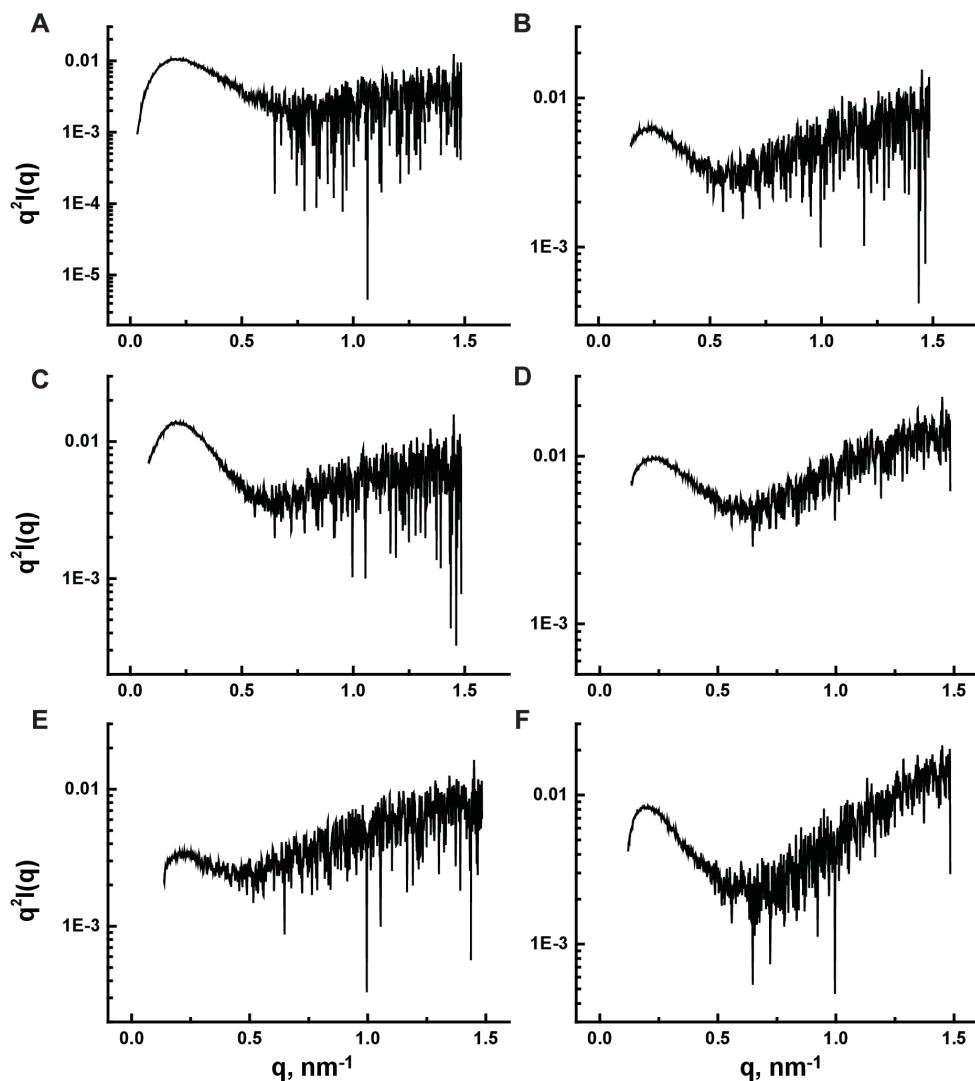


Figure 4.6: Kratky plots for oligomers composed of WT (A) and disease-related  $\alpha$ S mutants: A30P (B), E46K (C), H50Q (D), G51D (E) and A53T (G). The shape of the spectra indicates that all  $\alpha$ S oligomers are partially folded.

## 4.5 Discussion

The H50Q and G51D disease mutants have been reported to adopt an  $\alpha$ -helical conformation when binding membranes [6, 8]. Here we have determined the binding affinities of monomeric WT, G51D and H50Q to vesicles composed of negatively charged DOPG and a phospholipid composition mimicking the mitochondrial membrane. Our CD data show that WT, G51D and H50Q have comparable binding affinities to negatively charged DOPG membranes, while small differences between the mutants were visible on CL:POPE:POPC vesicles. In that case, an approximately 4 times higher binding affinity was observed for WT compared to H50Q. The membrane composition had a large effect on the observed  $K_d$ ;  $\alpha$ S has an order of magnitude higher affinity for DOPG than for CL:POPE:POPC membranes. It is known that a single amino-acid substitution can cause changes in binding affinity, with A30P monomers demonstrating a lower binding affinity than E46K, A53T and WT [10]. Whether and how  $\alpha$ S point mutations affect membrane binding most likely depends on the position of the amino-acid substitution. However, although in G51D a membrane immersed residue is replaced with a acidic amino acid, this change has only a small effect on  $K_d$ . The lack of a profound effect of the G51D point mutation on LUV binding may result from its proximity to the postulated break in the membrane bound  $\alpha$ -helix [51]. The replacement of H by Q in the H50Q mutation involves only a small change in the polarity of a solvent-exposed residue and has probably therefore little effect on membrane binding.

Under the conditions studied here, all the disease mutants form amyloid fibrils and only for A30P the aggregation lag time was significantly increased compared to WT and the other disease mutants (see **Figure 4.2A**). The shape of the aggregation profiles looks similar for all the mutants, suggesting that the fibril growth mechanism is comparable (**Figure 4.2A**). The morphologies of the fibrils in solution after a ThT aggregation experiment were studied by AFM, which confirmed that all mutants form qualitatively similar fibrils. Although it was previously reported that H50Q aggregated faster and G51D slower than WT [6, 8, 12, 13], we did not observe any difference in aggregation kinetics between these disease mutants and WT  $\alpha$ S. This difference could be caused by the experimental conditions used; both the buffer and  $\alpha$ S concentrations used in our experiments were different from the published reports. Whereas we studied the aggregation of

100  $\mu$ M  $\alpha$ S monomers in 10 mM Tris, 100 mM NaCl, pH 7.4 Ghosh et al. [6] used 3 times higher H50Q concentration in 20 mM Glycine-NaOH buffer, and reported a difference in aggregation kinetics between H50Q and WT. The slower aggregation kinetics of G51D compared to WT [8] was observed in 20 mM Tris, 150 mM KCl, pH 7.5  $\mu$ M which is similar to our aggregation conditions.

Current studies suggest that oligomers are the toxic species involved in PD [27, 52]. Oligomers are thought to disrupt the integrity of cellular membranes. Here we tested if oligomers of the different  $\alpha$ S disease mutants differ in their ability to induce membrane permeabilization. Our results showed a large difference in the permeabilization of DOPG membranes by G51D oligomers compared to the other oligomers. G51D oligomers could not induce more than 20% permeabilization of DOPG membranes. Oligomers of the newly discovered H50Q mutant showed similar permeabilization of DOPG vesicles as WT oligomers. However oligomers of both newly discovered mutants are less prone to induce permeabilization of mitochondrial model membranes than WT, where G51D oligomers showed almost no permeabilization (**Figure 4.3**).

WT, G51D and H51Q monomers do not differ much in membrane affinity (**Figure 4.1**). The differences in  $\alpha$ S oligomers ability to permeabilize membranes may therefore be related to differences in oligomer structure. SAXS has proven to be a very useful technique to obtain more detailed insights on the structure and size of protein oligomers [25, 32].

However, the size and aggregation number of the 6 different  $\alpha$ S oligomers studied are very similar. Moreover the Kratky plots show all oligomers are partially folded structures (**Figure 4.6**) that contain approximately 30 monomers (**Figure 4.5B**). CD measurements confirm the partially folded nature of the oligomer and show that oligomers contain  $\beta$ -sheets [21, 53]. The partially folded nature of the oligomer is also in good agreement with tryptophan quenching experiments which suggest that residues 4-90 make up the core of the aggregate while the C-terminus remains solvent exposed [54]. The similarities in aggregation number and structure observed by SAXS can however not exclude that differences exist. With SAXS an average size of the species in solution is probed and it is very difficult to distinguish between 2 or 3 different species. The mean aggregation number of this WT oligomer is comparable to the values found with SAXS [32] and single molecule photobleaching experiments [23]. Assuming that the aggregation number is correct, the difference in permeabilization cannot be attributed to the oligomer aggregation number and overall structure.

Although the binding affinity of WT and G51D monomers are comparable the exchange of a small neutral amino acid G with polar negatively charged D resulted in lower oligomer-induced permeabilization of DOPG membranes. The comparable binding affinity indicates that the G51D substitution does not result in large changes in the membrane binding  $\alpha$ -helical structure of the monomer. However with this substitution an acidic amino acid (D) would become exposed to a lipophilic environment [51]. Although  $\alpha$ S oligomers bind membranes, the partially folded structure of the oligomer may prevent binding of the complete  $\alpha$ -helix. When fewer residues per monomer are available, the relative contribution of position 51 may become more important. The oligomer may either not bind membranes or the G51D substitution may make it more difficult to distort the lipid bilayer because fewer amino acid residues are immersed in the bilayer.

## 4.6 Acknowledgments

SAXS experiments were performed in ESRF, Grenoble, France on the SAXS/WAXS configuration of BM26B (DUBBLE) experiment number 26-02-664. These experiments were performed in collaboration with S. Semerdzhiev and Dr. S. Lindhoud and were facilitated by an NWO grant for beamtime obtained by Dr. S. Lindhoud. We also thank Dr. G. Portale (Beamline Scientist) for the help in performing SAXS experiments.

## 4.7 References

1. Breydo, L., Wu, J. W. & Uversky, V. N. (2012) Alpha-synuclein misfolding and Parkinson's disease, *Biochim Biophys Acta*. **1822**, 261-85.
2. Uversky, V. N., Lee, H. J., Li, J., Fink, A. L. & Lee, S. J. (2001) Stabilization of partially folded conformation during alpha-synuclein oligomerization in both purified and cytosolic preparations, *J Biol Chem*. **276**, 43495-8.
3. Kruger, R., Kuhn, W., Muller, T., Woitalla, D., Graeber, M., Kosel, S., Przuntek, H., Epplen, J. T., Schols, L. & Riess, O. (1998) Ala30Pro mutation in the gene encoding alpha-synuclein in Parkinson's disease, *Nat Genet*. **18**, 106-8.
4. Zarranz, J. J., Alegre, J., Gomez-Esteban, J. C., Lezcano, E., Ros, R., Ampuero, I., Vidal, L., Hoenicka, J., Rodriguez, O., Atares, B., Llorens, V., Gomez Tortosa, E., del Ser, T., Munoz, D. G. & de Yebenes, J. G. (2004) The new mutation, E46K, of alpha-synuclein causes Parkinson and Lewy body dementia, *Ann Neurol*. **55**, 164-73.
5. Appel-Cresswell, S., Vilarino-Guell, C., Encarnacion, M., Sherman, H., Yu, I., Shah, B., Weir, D., Thompson, C., Szu-Tu, C., Trinh, J., Aasly, J. O., Rajput, A., Rajput, A. H., Jon Stoessel, A. & Farrer, M. J. (2013) Alpha-synuclein p.H50Q, a novel pathogenic mutation for Parkinson's disease, *Mov Disord*. **28**, 811-3.

## Characterization of oligomers formed from disease-related alpha-synuclein amino acid mutations

6. Ghosh, D., Mondal, M., Mohite, G. M., Singh, P. K., Ranjan, P., Anoop, A., Ghosh, S., Jha, N. N., Kumar, A. & Maji, S. K. (2013) The Parkinson's Disease-Associated H50Q Mutation Accelerates alpha-Synuclein Aggregation in Vitro, *Biochemistry*. **52**, 6925-7.
7. Kiely, A. P., Asi, Y. T., Kara, E., Limousin, P., Ling, H., Lewis, P., Proukakis, C., Quinn, N., Lees, A. J., Hardy, J., Revesz, T., Houlden, H. & Holton, J. L. (2013) alpha-Synucleinopathy associated with G51D SNCA mutation: a link between Parkinson's disease and multiple system atrophy?, *Acta Neuropathol*. **125**, 753-69.
8. Lesage, S., Anheim, M., Letournel, F., Bousset, L., Honore, A., Rozas, N., Pieri, L., Madiona, K., Durr, A., Melki, R., Verny, C., Brice, A. & French Parkinson's Disease Genetics Study, G. (2013) G51D alpha-synuclein mutation causes a novel parkinsonian-pyramidal syndrome, *Ann Neurol*. **73**, 459-71.
9. Polymeropoulos, M. H., Lavedan, C., Leroy, E., Ide, S. E., Dehejia, A., Dutra, A., Pike, B., Root, H., Rubenstein, J., Boyer, R., Stenroos, E. S., Chandrasekharappa, S., Athanassiadou, A., Papapetropoulos, T., Johnson, W. G., Lazzarini, A. M., Duvoisin, R. C., Di Iorio, G., Golbe, L. I. & Nussbaum, R. L. (1997) Mutation in the alpha-synuclein gene identified in families with Parkinson's disease, *Science*. **276**, 2045-7.
10. Choi, W., Zibace, S., Jakes, R., Serpell, L. C., Davletov, B., Crowther, R. A. & Goedert, M. (2004) Mutation E46K increases phospholipid binding and assembly into filaments of human alpha-synuclein, *FEBS Lett*. **576**, 363-8.
11. Lemkau, L. R., Comellas, G., Kloepper, K. D., Woods, W. S., George, J. M. & Rienstra, C. M. (2012) Mutant protein A30P alpha-synuclein adopts wild-type fibril structure, despite slower fibrillation kinetics, *J Biol Chem*. **287**, 11526-32.
12. Khalaf, O., Fauvet, B., Oueslati, A., Dikiy, I., Mahul-Mellier, A. L., Ruggeri, F. S., Mbefo, M. K., Vercruysse, F., Dietler, G., Lee, S. J., Eliezer, D. & Lashuel, H. A. (2014) The H50Q mutation enhances alpha-synuclein aggregation, secretion, and toxicity, *J Biol Chem*. **289**, 21856-76.
13. Rutherford, N. J., Moore, B. D., Golde, T. E. & Giasson, B. I. (2014) Divergent effects of the H50Q and G51D SNCA mutations on the aggregation of alpha-synuclein, *J Neurochem*.
14. Fares, M. B., Ait-Bouziad, N., Dikiy, I., Mbefo, M. K., Jovicic, A., Kiely, A., Holton, J. L., Lee, S. J., Gitler, A. D., Eliezer, D. & Lashuel, H. A. (2014) The novel Parkinson's disease linked mutation G51D attenuates in vitro aggregation and membrane binding of alpha-synuclein, and enhances its secretion and nuclear localization in cells, *Hum Mol Genet*. **23**, 4491-509.
15. Fredenburg, R. A., Rospigliosi, C., Meray, R. K., Kessler, J. C., Lashuel, H. A., Eliezer, D. & Lansbury, P. T. (2007) The Impact of the E46K Mutation on the Properties of  $\alpha$ -Synuclein in Its Monomeric and Oligomeric States, *Biochemistry*. **46**, 7107-7118.
16. Xilouri, M., Vogiatzi, T., Vekrellis, K., Park, D. & Stefanis, L. (2009) Abberant  $\alpha$ -Synuclein Confers Toxicity to Neurons in Part through Inhibition of Chaperone-Mediated Autophagy, *PLoS One*. **4**, e5515.
17. Cuervo, A. M., Stefanis, L., Fredenburg, R., Lansbury, P. T. & Sulzer, D. (2004) Impaired degradation of mutant alpha-synuclein by chaperone-mediated autophagy, *Science*. **305**, 1292-5.
18. Gureviciene, I., Gurevicius, K. & Tanila, H. (2007) Role of alpha-synuclein in synaptic glutamate release, *Neurobiol Dis*. **28**, 83-9.
19. Dimant, H., Kalia, S. K., Kalia, L. V., Zhu, L. N., Kibuuka, L., Ebrahimi-Fakhari, D., McFarland, N. R., Fan, Z., Hyman, B. T. & McLean, P. J. (2013) Direct detection of alpha synuclein oligomers in vivo, *Acta Neuropathol Commun*. **1**, 6.
20. Winner, B., Jappelli, R., Maji, S., Desplats, P., Boyer, L., Aigner, S., Hetzer, C., Loher, T., Vilar, M. & Campioni, S. (2011) In vivo demonstration that alpha-synuclein oligomers are toxic, *Proc Natl Acad Sci U S A*. **108**, 4194 - 4199.
21. van Rooijen, B. D., Claessens, M. M. & Subramaniam, V. (2009) Lipid bilayer disruption by oligomeric alpha-synuclein depends on bilayer charge and accessibility of the hydrophobic core, *Biochim Biophys Acta*. **1788**, 1271-8.
22. Davidson, W. S., Jonas, A., Clayton, D. F. & George, J. M. (1998) Stabilization of alpha-synuclein secondary structure upon binding to synthetic membranes, *J Biol Chem*. **273**, 9443-9.



## Chapter 4

23. Zijlstra, N., Blum, C., Segers-Nolten, I. M., Claessens, M. M. & Subramaniam, V. (2012) Molecular composition of sub-stoichiometrically labeled alpha-synuclein oligomers determined by single-molecule photobleaching, *Angew Chem Int Ed Engl.* **51**, 8821-4.
24. Giehm, L., Svergun, D. I., Otzen, D. E. & Vestergaard, B. (2011) Low-resolution structure of a vesicle disrupting &alpha;-synuclein oligomer that accumulates during fibrillation, *Proc Natl Acad Sci U S A.* **108**, 3246-51.
25. Pham, C. L., Kirby, N., Wood, K., Ryan, T., Roberts, B., Sokolova, A., Barnham, K. J., Masters, C. L., Knott, R. B., Cappai, R., Curtain, C. C. & Rekas, A. (2014) Guanidine hydrochloride denaturation of dopamine-induced alpha-synuclein oligomers: a small-angle X-ray scattering study, *Proteins.* **82**, 10-21.
26. Lorenzen, N., Lemminger, L., Pedersen, J. N., Nielsen, S. B. & Otzen, D. E. (2014) The N-terminus of alpha-synuclein is essential for both monomeric and oligomeric interactions with membranes, *FEBS Lett.* **588**, 497-502.
27. Danzer, K. M., Haasen, D., Karow, A. R., Moussaïd, S., Habeck, M., Giese, A., Kretzschmar, H., Hengerer, B. & Kostka, M. (2007) Different species of alpha-synuclein oligomers induce calcium influx and seeding, *J Neurosci.* **27**, 9220-32.
28. Bodner, C. R., Maltsev, A. S., Dobson, C. M. & Bax, A. (2010) Differential phospholipid binding of alpha-synuclein variants implicated in Parkinson's disease revealed by solution NMR spectroscopy, *Biochemistry.* **49**, 862-71.
29. van Rooijen, B. D., Claessens, M. M. & Subramaniam, V. (2008) Membrane binding of oligomeric alpha-synuclein depends on bilayer charge and packing, *FEBS Lett.* **582**, 3788-92.
30. Lashuel, H. A., Petre, B. M., Wall, J., Simon, M., Nowak, R. J., Walz, T. & Lansbury, P. T. (2002)  $\alpha$ -Synuclein, Especially the Parkinson's Disease-associated Mutants, Forms Pore-like Annular and Tubular Protofibrils, *J Mol Biol.* **322**, 1089-1102.
31. Rekas, A., Knott, R., Sokolova, A., Barnham, K., Perez, K., Masters, C., Drew, S., Cappai, R., Curtain, C. & Pham, C. L. (2010) The structure of dopamine induced  $\alpha$ -synuclein oligomers, *Eur Biophys J.* **39**, 1407-1419.
32. Lorenzen, N., Nielsen, S. B., Buell, A. K., Kaspersen, J. D., Arosio, P., Vad, B. S., Paslawski, W., Christiansen, G., Valnickova-Hansen, Z., Andreasen, M., Enghild, J. J., Pedersen, J. S., Dobson, C. M., Knowles, T. P. & Otzen, D. E. (2014) The role of stable alpha-synuclein oligomers in the molecular events underlying amyloid formation, *J Am Chem Soc.* **136**, 3859-68.
33. Pace, C. N., Vajdos, F., Fee, L., Grimsley, G. & Gray, T. (1995) How to measure and predict the molar absorption coefficient of a protein, *Protein Sci.* **4**, 2411-23.
34. Honda, S., Kobayashi, N., Munekata, E. & Uedaira, H. (1999) Fragment reconstitution of a small protein: folding energetics of the reconstituted immunoglobulin binding domain B1 of streptococcal protein G, *Biochemistry.* **38**, 1203-13.
35. Jacques, D. A. & Trewthella, J. (2010) Small-angle scattering for structural biology--expanding the frontier while avoiding the pitfalls, *Protein Sci.* **19**, 642-57.
36. Svergun, D. I. (1992) Determination of the Regularization Parameter in Indirect-Transform Methods Using Perceptual Criteria, *J Appl Crystallogr.* **25**, 495-503.
37. Fisher, C. K. & Stultz, C. M. (2011) Constructing ensembles for intrinsically disordered proteins, *Curr Opin Struct Biol.* **21**, 426-31.
38. Sztucki, M. & Narayanan, T. (2007) Development of an ultra-small-angle X-ray scattering instrument for probing the microstructure and the dynamics of soft matter, *J Appl Crystallogr.* **40**, s459-s462.
39. Gekko, K. & Noguchi, H. (1979) Compressibility of globular proteins in water at 25.degree.C, *J Phys Chem.* **83**, 2706-2714.
40. Fischer, H., Polikarpov, I. & Craievich, A. F. (2004) Average protein density is a molecular-weight-dependent function, *Protein Sci.* **13**, 2825-8.
41. Doniach, S. (2001) Changes in biomolecular conformation seen by small angle X-ray scattering, *Chem Rev.* **101**, 1763-1778.

## Characterization of oligomers formed from disease-related alpha-synuclein amino acid mutations

42. Willander, H., Presto, J., Askarieh, G., Biverstal, H., Frohm, B., Knight, S. D., Johansson, J. & Linse, S. (2012) BRICHOS domains efficiently delay fibrillation of amyloid beta-peptide, *J Biol Chem.* **287**, 31608-17.
43. Sweers, K., van der Werf, K., Bennink, M. & Subramaniam, V. (2011) Nanomechanical properties of alpha-synuclein amyloid fibrils: a comparative study by nanoindentation, harmonic force microscopy, and Peakforce QNM, *Nanoscale Res Lett.* **6**, 270.
44. Shvadchak, V. V., Falomir-Lockhart, L. J., Yushchenko, D. A. & Jovin, T. M. (2011) Specificity and kinetics of alpha-synuclein binding to model membranes determined with fluorescent excited state intramolecular proton transfer (ESIPT) probe, *J Biol Chem.* **286**, 13023-32.
45. Shvadchak, V. V., Yushchenko, D. A., Pievo, R. & Jovin, T. M. (2011) The mode of alpha-synuclein binding to membranes depends on lipid composition and lipid to protein ratio, *FEBS Lett.* **585**, 3513-9.
46. Fischer, H., de Oliveira Neto, M., Napolitano, H. B., Polikarpov, I. & Craievich, A. F. (2010) Determination of the molecular weight of proteins in solution from a single small-angle X-ray scattering measurement on a relative scale, *J Appl Cryst.* **43**, 101-109.
47. Bernado, P. & Svergun, D. I. (2012) Structural analysis of intrinsically disordered proteins by small-angle X-ray scattering, *Molecular BioSystems.* **8**, 151-167.
48. Zijlstra, N., Claessens, Mireille M. A. E., Blum, C. & Subramaniam, V. (2014) Elucidating the Aggregation Number of Dopamine-Induced  $\alpha$ -Synuclein Oligomeric Assemblies, *Biophys J.* **106**, 440-446.
49. Pilz, I., Glatter, O. & Kratky, O. (1979) Small-angle X-ray scattering, *Methods Enzymol.* **61**, 148-249.
50. Putnam, C. D., Hammel, M., Hura, G. L. & Tainer, J. A. (2007) X-ray solution scattering (SAXS) combined with crystallography and computation: defining accurate macromolecular structures, conformations and assemblies in solution, *Q Rev Biophys.* **40**, 191-285.
51. Shvadchak, V. V. & Subramaniam, V. (2014) A four-amino acid linker between repeats in the alpha-synuclein sequence is important for fibril formation, *Biochemistry.* **53**, 279-81.
52. Outeiro, T. F., Putcha, P., Tetzlaff, J. E., Spoelgen, R., Koker, M., Carvalho, F., Hyman, B. T. & McLean, P. J. (2008) Formation of toxic oligomeric alpha-synuclein species in living cells, *PLoS One.* **3**, e1867.
53. Stefanovic, A. N., Stockl, M. T., Claessens, M. M. & Subramaniam, V. (2014) alpha-Synuclein oligomers distinctively permeabilize complex model membranes, *FEBS J.* **281**, 2838-50.
54. van Rooijen, B. D., van Leijenhorst-Groener, K. A., Claessens, M. M. & Subramaniam, V. (2009) Tryptophan fluorescence reveals structural features of alpha-synuclein oligomers, *J Mol Biol.* **394**, 826-33.



## Chapter 5

### Are alpha-synuclein oligomers toxic species?

#### 5.1 Introduction

In protein aggregation diseases, including Parkinson's disease, oligomeric protein aggregates have been suggested to play a pivotal role in cytotoxicity. However different oligomeric species may exist and the toxicity of these species probably relates to their structure or structural plasticity [1]. In Parkinson's disease, oligomers of the membrane binding and amyloid forming protein  $\alpha$ -synuclein ( $\alpha$ S) are thought to be responsible for cell death.  $\alpha$ S oligomers were observed *in vitro* upon aggregation of recombinant  $\alpha$ S [2] and were later found *in vivo* in postmortem brain of patients with PD [3]. In post mortem tissue of patients suffering from familial PD the subcellular localization of oligomers was comparable to that observed in patients with sporadic PD [4]. Moreover the intracellular location of  $\alpha$ S oligomers was confirmed in both cultured cell lines [4-6] and neurons [7].

The toxicity  $\alpha$ S oligomers may be related to a specific oligomer species [8, 9] and probably depends on the levels of  $\alpha$ S oligomers [6, 7]. High oligomer levels have been associated with disease, but the toxic mechanism responsible for cell death is still under debate [3, 10]. There is evidence that accumulation of  $\alpha$ S oligomers within endoplasmic reticulum causes oxidative stress eventually leading to neurodegeneration [11]. Different types of oligomers have been observed and they possibly each contribute differently to toxicity in PD. Annular oligomers have been associated with the formation of membrane pores [8, 12], protofibrillar oligomers possibly promote cell death by entering from the extracellular matrix to intracellular spaces where they seed aggregation of the intracellular  $\alpha$ S pool [8], and globular oligomers may be involved in the impairment of synaptic functions [13].

Although there are a lot of toxicity studies done with  $\alpha$ S oligomers the toxic mechanism is still not understood at a molecular scale. Here we report on the toxicity of well-characterized  $\alpha$ S oligomers prepared at either elevated  $\alpha$ S concentrations (A-oligomers) [14], in the presence of dopamine (DA-oligomers) [15], or in the presence of HNE (HNE-oligomers) [16] in a cell model system.

Although all these oligomer species are able to disrupt the integrity of model membranes our data shows that extracellular addition of both A- and DA-oligomers is not toxic and does not cause cell death. Externally added HNE-oligomers show a concentration-dependent reduction in cell viability, but comparable effects are observed when cells are exposed to monomers obtained from the HNE-oligomer preparation. The toxicity of the externally added oligomers tested here seems to depend on the availability and toxicity of additional compounds rather than on the oligomers themselves. Although externally added  $\alpha$ S oligomers tested here were not toxic, we cannot draw any conclusions about the toxicity of oligomers produced intracellularly during aggregation of  $\alpha$ S.

## 5.2 Materials and Methods

### 5.2.1 Expression of $\alpha$ S and preparation of oligomers

The expression of  $\alpha$ S monomers is briefly described in **Chapter 3** of this thesis and in more detail by [14]. Oligomers are prepared in the way mentioned in **Chapter 3** for oligomers prepared at high protein concentrations (A-oligomers) [14] and for oligomers prepared in the presence Here we also prepared oligomers in the presence of dopamine (DA-oligomers) [15] and in the presence of HNE (4-hydroxy-2-nonenal; Cayman Chemicals, Ann Arbor, MI, USA) [17]. HNE is a lipid degradation product and effective protein modifier [18]. HNE is one of the most common aldehydes in the brain and has been shown to induce formation of oligomers [16]. The monomers that were used as control in the cell viability assays were obtained from the monomer fraction after oligomer purification by size exclusion chromatography.

### 5.2.2 Assay conditions

One 96-well plate was used for two assays: imaging (Labelling of SH-SY5Y cells) and cell viability (Cell viability in SH-SY5Y cells). Half of the plate is used for the first assay in order to observe changes in morphology upon incubation with oligomers and the other half of the 96-well plate is used for CTB (Cell titer blue) metabolic activity assay.

### 5.2.3 Labeling of SH-SY5Y cells

To observe if the oligomers can cause changes in cell morphology, SH-SY5Y cells were fixed and labeled using a previously described immunostaining protocol [19]. To fix cells, 4% paraformaldehyde (100  $\mu$ L) was added to each cell-containing well of the 96-well plate and incubated for 20 minutes. After washing with PBS, Triton X (0.1%) was added to permeabilize cells and ensure free access of antibody. In the next step, to prevent non-specific antibody binding, blocking buffer (0.1% TritonX, PBS, 5% fetal bovine serum) was added followed by incubation of 1 hour. As a primary antibody Monoclonal Anti- $\alpha$ -Tubulin antibody produced in mice (Sigma Aldrich, St. Louis, MO) was used. Before and after the addition of a secondary antibody (Alexa Fluor® 488 Goat Anti-Mouse IgG (H+L) Antibody; Invitrogen, Carlsbad, CA, USA) cells were washed with PBS. To be able to visualize the nucleus, cells were labeled with Hoechst dye. For imaging, an EVOS® FL Cell Imaging fluorescence microscope (Life Technologies, Carlsbad, CA, USA) was used at magnification of 20X.

### 5.2.4 Cell viability in SH-SY5Y cells

The Cell Titer-Blue (CTB, Promega, cat. G8080) assay is routinely used to test cellular toxicity of amyloid proteins [20, 21]. For toxicity studies of A-, DA- and HNE-oligomers, SH-SY5Y cells were cultured in Dulbecco's Modified Eagle Medium (DMEM) supplemented with 10 vol% fetal calf serum (FCS; Invitrogen, Carlsbad, CA, USA) and penicillin:streptomycin 1:100 in a 5% CO<sub>2</sub> humidified incubator at 37°C. Cells were used at a maximum total passage number of 20. A detailed protocol for testing cell viability in SH-SY5Y cells can be found in [20]. The cells were seeded in 96-well plates in 100  $\mu$ L medium at a density of ~30,000 cells per well. After ~2 hours of incubation, the old medium was replaced with a fresh medium that did not contain FCS. After 48 h in medium without FCS, cells were incubated with A-, DA- and HNE-oligomers for another 24 hours. The viability of cells in medium without FCS and staurosporine were used as negative and positive controls respectively. Additionally monomers from each oligomer preparation were used as a control to see if the reduced cell viability results from the presence of oligomers or from residues of additional factors (DA or HNE) used in the oligomer preparation protocol. For the CTB assay 10  $\mu$ l of the redox dye resazurin (prepared in PBS) was added to each well and the incubation was

continued for 3 hours. After 3 hours the conversion of resazurin by cells into the fluorescent resorufin was measured on a Perkin Elmer Wallac plate reader (Waltham, MA, USA) using an excitation wavelength of 560 nm and an emission wavelength of 590 nm. For each added component at least 6 wells were used and the experiment was repeated 3 times. Data are presented in histograms as mean values  $\pm$  standard deviation. Cell viability is expressed as % of formed resorufin compared to the control (66vol% FCS depleted medium and 33vol% buffer), which represents 100%.

### 5.3 Results and discussion

To observe if the presence of oligomers results in large scale reorganization in cell morphology, a subset of the 96-well plate is used for morphological imaging by staining for tubulin and counterstaining the cell nuclei. SH-SY5Y cell nuclei were labeled with Hoechst (blue nucleus labeling) and tubulin was visualized using antibody staining with an anti-tubulin primary antibody, and a secondary antibody labeled with Alexa Fluor® 488 (**Figure 5.1**). Our microscopy data shows no difference in cell morphology between the wells in which 12  $\mu$ M DA-oligomers or monomers were present compared to wells in which cells were only exposed to the medium without FCS. The metabolic activity assay shows that higher concentrations of oligomers are toxic to cells. In the presence of 100  $\mu$ M dopamine the morphology of the fixed cells is comparable to that of the controls, but the wells seem to contain much more cell debris (**Figure 5.1D**). This cell debris probably results from cell death. The fixation protocol involves several washing steps; detached dying cells are therefore not easily visualized.

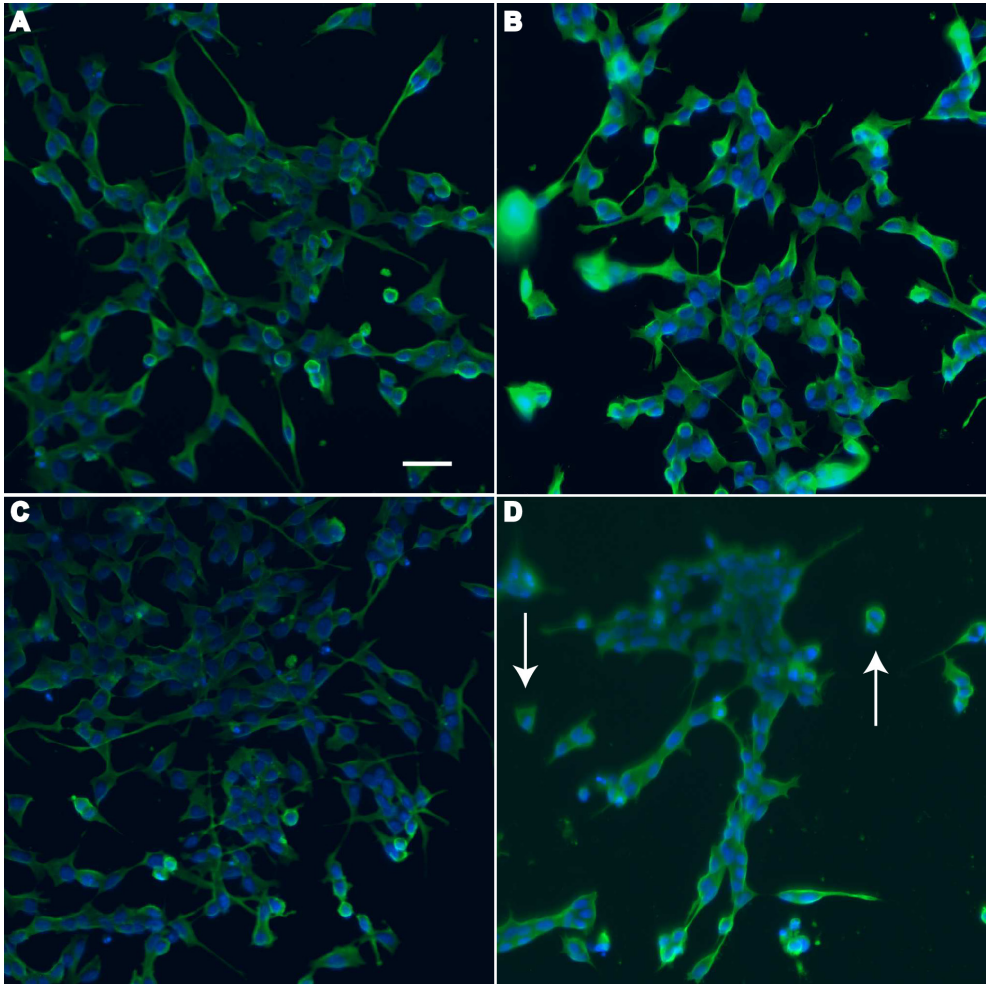


**Figure 5.1:** Representative fluorescence microscopy images of SH-5YSY cells incubated with 12  $\mu\text{M}$  DA-oligomers (A), 12  $\mu\text{M}$  monomers (B), 66vol% FCS depleted medium+33vol% buffer without additives (C) and in the presence 100  $\mu\text{M}$  dopamine (D). In the presence of dopamine (D) we have observed presence of cell debris, pointed with white arrows. The scale bar represents 20  $\mu\text{m}$ . The blue channel depicts Hoechst nuclear labeling and the green channel visualizes tubulin using a primary anti-tubulin antibody, and an Alexa488 labeled secondary antibody (Alexa Fluor® 488 Goat Anti-Mouse IgG (H+L) Antibody).

To be able to determine if the oligomers are toxic to the cells, we therefore tested the viability of the cells using a more sensitive CTB assay after exposure to a concentration series of the different oligomeric species described in this thesis.



Although several groups have reported that  $\alpha$ S oligomers can be toxic to cells [8, 17, 22], our data does not agree with this.

To test the sensitivity of the CTB assay to the metabolic activity of SH-SY5Y neuroblastoma cells, the cells were incubated with the protein kinase C inhibitor staurosporine. Compared to the control, the presence of staurosporine resulted in a more than 20 fold decrease of the metabolic activity (**Figure 5.2A**). This result shows that the CTB assay works in our hands. If oligomers are toxic to cells, we would expect that the metabolic activity assay would show a decrease in viability as oligomer concentration is increased. However A-oligomers in concentrations as high as 5  $\mu$ M did not have any effect on the measured metabolic activity. To test if the oligomer toxicity in the literature reported resulted from the presence of monomers in the oligomer preparation, the cells were also incubated with monomeric protein. As observed for A-oligomers, the presence of  $\alpha$ S monomers did not significantly affect the metabolic activity.

For cells incubated with oligomers prepared in the presence of dopamine, similar results were obtained. DA-oligomers in concentrations as high as 7  $\mu$ M (equivalent monomer concentration) did not significantly impair the cell viability as monitored in the CTB assay. Dopamine has been reported to stabilize  $\alpha$ S oligomers and prevent the formation of fibrils by covalent or non-covalent coupling to  $\alpha$ S. The presence of dopamine in the DA-oligomers or the monomers purified from the DA-oligomer preparation did not affect the metabolic activity of SH-SY5Y cells. Dopamine itself was however toxic. When different concentrations of dopamine were added to the cells in a 96-well plate, a concentration dependent reduction in cell viability was observed (**Figure 5.2B**). In the presence of 20  $\mu$ M dopamine the metabolic activity dropped as much as 40%, while for 7  $\mu$ M dopamine a 20% reduction was observed (**Figure 5.2B**). The literature reports a 1:1 binding ratio of  $\alpha$ S and dopamine [15]. If there were an equilibrium between unbound dopamine and dopamine bound to  $\alpha$ S, 7  $\mu$ M oligomers would be expected to result in some decrease in cell viability. The absence of DA-oligomer toxicity probably means that the exchange of dopamine is very slow or that it is covalently coupled to  $\alpha$ S. The low concentration of dopamine that may persist in a solution is apparently not enough to lead to cell death.

## Are alpha-synuclein oligomers toxic species?

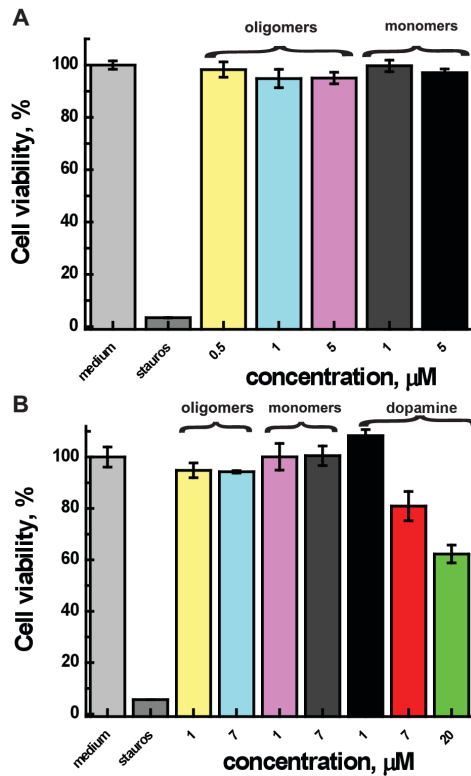


**Figure 5.2:** Here we show that A-oligomers (A) and DA-oligomers (B) are not toxic when incubated with SH-SY5Y cells. Dopamine itself in the same concentration showed reduced cell viability. Stauros = staurosporine. Medium = control (66vol% FCS depleted medium and 33vol% buffer). Error bars represent standard deviation. Cell viability is calculated using cell viability of the control (66vol% FCS depleted medium and 33vol% buffer) as a 100%.

We showed (Figure 5.2A and 5.2B) that, although A- and DA- oligomers can permeabilize negatively charged vesicles and bilayers mimicking the mitochondrial inner membrane [23], both oligomer types are not toxic when added extracellularly to SH-SY5Y cells. For HNE oligomers we did observe toxicity for the oligomer concentrations tested (Figure 5.3A). After exposure to 2.5 μM HNE-oligomers the metabolic activity dropped to 20% of the control and exposure to 5 μM HNE-oligomers resulted in a decrease to only 2% of the control value. We can however not exclusively attribute the observed toxicity to the HNE-oligomers. The addition of monomers purified from the HNE-oligomer preparation in concentrations of 1-5 μM also reduced cell viability considerably. It can therefore not be excluded that the toxicity results from the presence of protein-associated HNE or unbound HNE

in a solution. HNE is highly toxic, and concentrations as low as 0.5  $\mu\text{M}$  HNE result in a 20 times reduced metabolic activity. The presence of unbound HNE in the solution of both monomers and oligomers could thus explain the reduced cell viability. HNE covalently modifies and alters the protein function [17, 24] by binding to lysine, histidine and cysteine residues of the proteins [25]. Binding to  $\alpha\text{S}$  and covalent protein modification occurs via His50 [26]. The toxicity of HNE-oligomers was reported by Näsström et al [17] but in their experiments a much lower oligomer concentration (0.05  $\mu\text{M}$ ) was observed to be toxic. This observed difference in toxicity may be the result of a different assay used for measuring the cell viability. The same authors showed that oligomers that do not incorporate HNE do not result in a reduced cell viability [17]. The reduction in cell viability may therefore be an effect of released or free HNE as suggested by the toxicity of the monomers and of free HNE shown here (**Figure 5.3**).

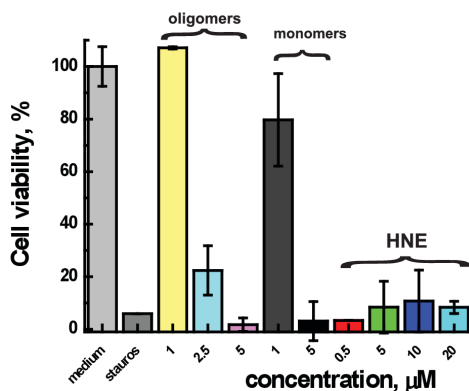


**Figure 5.3: HNE oligomers and monomers in higher concentration show toxicity, while HNE is toxic even in 10X lower concentration (0.5  $\mu\text{M}$ ).** Stauros = staurosporine. Medium = control (66vol% FCS depleted medium and 33vol% buffer). Error bars represent standard deviation. Cell viability is calculated using cell viability of the control (66vol% FCS depleted medium and 33vol% buffer) as a 100%.

Summarizing, here we have tested three different protocols and shown that the toxicity of oligomers depends primarily on the availability and toxicity of additional compounds (DA and HNE) in the oligomers. We are not in a position to unequivocally attribute cell toxicity to the oligomers themselves when added extracellularly.

In the literature there are conflicting reports about the toxicity of oligomers. Many oligomeric species have proven to be cytotoxic to CNS derived cells in culture [4, 8, 27]. Some other authors have reported that HNE oligomers are not taken up by the cell and therefore not cytotoxic [28]. Others have shown that HNE oligomers are taken up and already toxic at concentrations of 50 nM [17]. Treatment of cells with dopamine in concentrations >100  $\mu$ M has been shown to lead to the accumulation of oligomers and cell death [29].  $\alpha$ S oligomers formed by the addition of dopamine are promoted in cultured cells and they have been reported to be alternatively toxic [30] or non-toxic [31, 32]. Although  $\alpha$ S is a cytosolic protein the toxicity assay performed here and many assays reported in the literature refer to extracellularly added oligomers [8, 33]. Uptake of oligomers from the extracellular space [7] can happen across the membranes and cell-to-cell transfer has also been observed [34-36]. Although our data on model systems [23] shows that oligomers cannot permeabilize plasma model membranes, some authors [37] suggest that oligomers can be taken up via receptor-mediated endocytosis. This means that oligomers may not directly permeabilize plasma membranes, but rather cause damage when internalized. The absence of a toxic effect of oligomers in our experiments can possibly be explained by the fact that  $\alpha$ S is an intracellular protein. The intracellular structures that are vulnerable to oligomer-induced damage and accessible when oligomers appear intracellularly may simply not be available to extracellularly added oligomers.

Although oligomers may be excreted by cells or become available in the extracellular fluid when cells die, the extracellular addition of oligomers may not be the best test to determine if oligomers are toxic. We also cannot exclude that if our oligomers would be incubated with the cells differently, e.g. injected intracellularly or expressed by the cells, they could be toxic.

## **5.4 Acknowledgments**

We thank Kirsten van Leijenhorst-Groener, Marloes ten Haaff-Kolkman, Ine Segers-Nolten and Kerensa Broersen for instructive discussions about the experiments performed for this chapter. K.L.G expressed and purified  $\alpha$ -synuclein. K.L.G and A.N.D.S performed the experiments and analyzed the data.

## 5.5 References

1. Pham, C. L., Kirby, N., Wood, K., Ryan, T., Roberts, B., Sokolova, A., Barnham, K. J., Masters, C. L., Knott, R. B., Cappai, R., Curtain, C. C. & Rekas, A. (2014) Guanidine hydrochloride denaturation of dopamine-induced alpha-synuclein oligomers: a small-angle X-ray scattering study, *Proteins*. **82**, 10-21.
2. Conway, K. A., Harper, J. D. & Lansbury, P. T. (1998) Accelerated in vitro fibril formation by a mutant alpha-synuclein linked to early-onset Parkinson disease, *Nat Med*. **4**, 1318-20.
3. Sharon, R., Bar-Joseph, I., Frosch, M., Walsh, D., Hamilton, J. & Selkoe, D. (2003) The formation of highly soluble oligomers of alpha-synuclein is regulated by fatty acids and enhanced in Parkinson's disease, *Neuron*. **37**, 583 - 595.
4. Outeiro, T. F., Putcha, P., Tetzlaff, J. E., Spoelgen, R., Koker, M., Carvalho, F., Hyman, B. T. & McLean, P. J. (2008) Formation of toxic oligomeric alpha-synuclein species in living cells, *PLoS One*. **3**, e1867.
5. Tetzlaff, J. E., Putcha, P., Outeiro, T. F., Ivanov, A., Berezovska, O., Hyman, B. T. & McLean, P. J. (2008) CHIP targets toxic alpha-Synuclein oligomers for degradation, *J Biol Chem*. **283**, 17962-8.
6. Putcha, P., Danzer, K. M., Kranich, L. R., Scott, A., Silinski, M., Mabbett, S., Hicks, C. D., Veal, J. M., Steed, P. M., Hyman, B. T. & McLean, P. J. (2010) Brain-permeable small-molecule inhibitors of Hsp90 prevent alpha-synuclein oligomer formation and rescue alpha-synuclein-induced toxicity, *J Pharmacol Exp Ther*. **332**, 849-57.
7. Danzer, K. M., Ruf, W. P., Putcha, P., Joyner, D., Hashimoto, T., Glabe, C., Hyman, B. T. & McLean, P. J. (2011) Heat-shock protein 70 modulates toxic extracellular alpha-synuclein oligomers and rescues trans-synaptic toxicity, *FASEB J*. **25**, 326-36.
8. Danzer, K., Haasen, D., Karow, A., Moussaud, S., Habeck, M., Giese, A., Kretschmar, H., Hengerer, B. & Kostka, M. (2007) Different species of alpha-synuclein oligomers induce calcium influx and seeding, *J Neurosci*. **27**, 9220 - 9232.
9. Cremades, N., Cohen, S. I., Deas, E., Abramov, A. Y., Chen, A. Y., Orte, A., Sandal, M., Clarke, R. W., Dunne, P., Aprile, F. A., Bertonecini, C. W., Wood, N. W., Knowles, T. P., Dobson, C. M. & Klenerman, D. (2012) Direct observation of the interconversion of normal and toxic forms of alpha-synuclein, *Cell*. **149**, 1048-59.
10. Paleologou, K. E., Kragh, C. L., Mann, D. M., Salem, S. A., Al-Shami, R., Allsop, D., Hassan, A. H., Jensen, P. H. & El-Agnaf, O. M. (2009) Detection of elevated levels of soluble alpha-synuclein oligomers in post-mortem brain extracts from patients with dementia with Lewy bodies, *Brain*. **132**, 1093-101.
11. Colla, E., Coune, P., Liu, Y., Pletnikova, O., Troncoso, J. C., Iwatsubo, T., Schneider, B. L. & Lee, M. K. (2012) Endoplasmic reticulum stress is important for the manifestations of alpha-synucleinopathy in vivo, *J Neurosci*. **32**, 3306-20.
12. Volles, M. J., Lee, S. J., Rochet, J. C., Shtilerman, M. D., Ding, T. T., Kessler, J. C. & Lansbury, P. T., Jr. (2001) Vesicle permeabilization by protofibrillar alpha-synuclein: implications for the pathogenesis and treatment of Parkinson's disease, *Biochemistry*. **40**, 7812-9.
13. Huls, S., Hogen, T., Vassallo, N., Danzer, K. M., Hengerer, B., Giese, A. & Herms, J. (2011) AMPA-receptor-mediated excitatory synaptic transmission is enhanced by iron-induced alpha-synuclein oligomers, *J Neurochem*. **117**, 868-78.
14. van Rooijen, B. D., Claessens, M. M. & Subramaniam, V. (2009) Lipid bilayer disruption by oligomeric alpha-synuclein depends on bilayer charge and accessibility of the hydrophobic core, *Biochim Biophys Acta*. **1788**, 1271-8.
15. Cappai, R., Leck, S. L., Tew, D. J., Williamson, N. A., Smith, D. P., Galatis, D., Sharples, R. A., Curtain, C. C., Ali, F. E., Cherny, R. A., Culvenor, J. G., Bottomley, S. P., Masters, C. L., Barnham, K. J. & Hill, A. F. (2005) Dopamine promotes alpha-synuclein aggregation into SDS-resistant soluble oligomers via a distinct folding pathway, *FASEB J*. **19**, 1377-9.

16. Näsström, T., Wahlberg, T., Karlsson, M., Nikolajeff, F., Lannfelt, L., Ingelsson, M. & Bergström, J. (2009) The lipid peroxidation metabolite 4-oxo-2-nonenal cross-links  $\alpha$ -synuclein causing rapid formation of stable oligomers, *Biochem Biophys Res Commun.* **378**, 872-876.
17. Nasstrom, T., Fagerqvist, T., Barbu, M., Karlsson, M., Nikolajeff, F., Kasrayan, A., Ekberg, M., Lannfelt, L., Ingelsson, M. & Bergstrom, J. (2011) The lipid peroxidation products 4-oxo-2-nonenal and 4-hydroxy-2-nonenal promote the formation of alpha-synuclein oligomers with distinct biochemical, morphological, and functional properties, *Free Radic Biol Med.* **50**, 428-37.
18. Carbone, D. L., Doorn, J. A., Kiebler, Z., Ickes, B. R. & Petersen, D. R. (2005) Modification of heat shock protein 90 by 4-hydroxynonenal in a rat model of chronic alcoholic liver disease, *J Pharmacol Exp Ther.* **315**, 8-15.
19. Jain, S., van Kesteren, R. E. & Heutink, P. (2012) High content screening in neurodegenerative diseases, *J Vis Exp*, e3452.
20. Broersen, K., Jonckheere, W., Rozenski, J., Vandersteen, A., Pauwels, K., Pastore, A., Rousseau, F. & Schymkowitz, J. (2011) A standardized and biocompatible preparation of aggregate-free amyloid beta peptide for biophysical and biological studies of Alzheimer's disease, *Protein Eng Des Sel.* **24**, 743-50.
21. Alvarez-Erviti, L., Seow, Y., Schapira, A. H., Gardiner, C., Sargent, I. L., Wood, M. J. & Cooper, J. M. (2011) Lysosomal dysfunction increases exosome-mediated alpha-synuclein release and transmission, *Neurobiol Dis.* **42**, 360-7.
22. Cappai, R., Leck, S., Tew, D., Williamson, N., Smith, D., Galatis, D., Sharples, R., Curtain, C., Ali, F., Cherny, R., Culvenor, J., Bottomley, S., Masters, C., Barnham, K. & Hill, A. (2005) Dopamine promotes alpha-synuclein aggregation into SDS-resistant soluble oligomers via a distinct folding pathway, *FASEB J.* **19**, 1377 - 1379.
23. Stefanovic, A. N., Stockl, M. T., Claessens, M. M. & Subramaniam, V. (2014) alpha-Synuclein oligomers distinctively permeabilize complex model membranes, *FEBS J.* **281**, 2838-50.
24. Esterbauer, H., Schaur, R. J. & Zollner, H. (1991) Chemistry and biochemistry of 4-hydroxynonenal, malonaldehyde and related aldehydes, *Free Radic Biol Med.* **11**, 81-128.
25. Shamoto-Nagai, M., Maruyama, W., Hashizume, Y., Yoshida, M., Osawa, T., Riederer, P. & Naoi, M. (2007) In parkinsonian substantia nigra, alpha-synuclein is modified by acrolein, a lipid-peroxidation product, and accumulates in the dopamine neurons with inhibition of proteasome activity, *J Neural Transm.* **114**, 1559-67.
26. Trostchansky, A., Lind, S., Hodara, R., Oe, T., Blair, I. A., Ischiropoulos, H., Rubbo, H. & Souza, J. M. (2006) Interaction with phospholipids modulates alpha-synuclein nitration and lipid-protein adduct formation, *Biochem J.* **393**, 343-9.
27. Conway, K., Lee, S., Rochet, J., Ding, T., Williamson, R. & Lansbury, P. (2000) Acceleration of oligomerization, not fibrillization, is a shared property of both alpha-synuclein mutations linked to early-onset Parkinson's disease: implications for pathogenesis and therapy, *Proc Natl Acad Sci U S A.* **97**, 571 - 576.
28. Qin, Z., Hu, D., Han, S., Reaney, S. H., Di Monte, D. A. & Fink, A. L. (2007) Effect of 4-hydroxy-2-nonenal modification on alpha-synuclein aggregation, *J Biol Chem.* **282**, 5862-70.
29. Jiang, P., Gan, M. & Yen, S. H. (2013) Dopamine prevents lipid peroxidation-induced accumulation of toxic alpha-synuclein oligomers by preserving autophagy-lysosomal function, *Front Cell Neurosci.* **7**, 81.
30. Ito, S., Nakaso, K., Imamura, K., Takeshima, T. & Nakashima, K. (2010) Endogenous catecholamine enhances the dysfunction of unfolded protein response and alpha-synuclein oligomerization in PC12 cells overexpressing human alpha-synuclein, *Neurosci Res.* **66**, 124-30.
31. Mazzulli, J. R., Mishizen, A. J., Giasson, B. I., Lynch, D. R., Thomas, S. A., Nakashima, A., Nagatsu, T., Ota, A. & Ischiropoulos, H. (2006) Cytosolic catechols inhibit alpha-synuclein aggregation and facilitate the formation of intracellular soluble oligomeric intermediates, *J Neurosci.* **26**, 10068-78.
32. Yamakawa, K., Izumi, Y., Takeuchi, H., Yamamoto, N., Kume, T., Akaike, A., Takahashi, R., Shimohama, S. & Sawada, H. (2010) Dopamine facilitates  $\alpha$ -synuclein oligomerization in human neuroblastoma SH-SY5Y cells, *Biochem Biophys Res Commun.* **391**, 129-134.

## Chapter 5

33. Kaye, R., Head, E., Thompson, J. L., McIntire, T. M., Milton, S. C., Cotman, C. W. & Glabe, C. G. (2003) Common structure of soluble amyloid oligomers implies common mechanism of pathogenesis, *Science*. **300**, 486-9.
34. Danzer, K., Kranich, L., Ruf, W., Cagsal-Getkin, O., Winslow, A., Zhu, L., Vanderburg, C. & McLean, P. (2012) Exosomal cell-to-cell transmission of alpha synuclein oligomers, *Mol Neurodegener.* **7**, 42.
35. Hansen, C., Angot, E., Bergstrom, A. L., Steiner, J. A., Pieri, L., Paul, G., Outeiro, T. F., Melki, R., Kallunki, P., Fog, K., Li, J. Y. & Brundin, P. (2011) alpha-Synuclein propagates from mouse brain to grafted dopaminergic neurons and seeds aggregation in cultured human cells, *J Clin Invest.* **121**, 715-25.
36. Angot, E., Steiner, J. A., Lema Tome, C. M., Ekstrom, P., Mattsson, B., Bjorklund, A. & Brundin, P. (2012) Alpha-synuclein cell-to-cell transfer and seeding in grafted dopaminergic neurons in vivo, *PLoS One.* **7**, e39465.
37. Lee, H. J., Suk, J. E., Bae, E. J., Lee, J. H., Paik, S. R. & Lee, S. J. (2008) Assembly-dependent endocytosis and clearance of extracellular alpha-synuclein, *Int J Biochem Cell Biol.* **40**, 1835-49.

## Chapter 6

# Alpha-synuclein amyloid multimers act as multivalent nanoparticles to cause hemifusion in negatively charged bilayers

### 6.1 Abstract

Alpha-synuclein ( $\alpha$ S) is a brain specific membrane binding protein whose putative function has been associated with synaptic processes and other membrane trafficking pathways. In Parkinson's disease, aggregation of  $\alpha$ S, and specifically the formation of  $\alpha$ S amyloid oligomers has been associated with cell death. The toxicity mechanism of these oligomeric species is not fully understood but has been suggested to result from membrane interactions causing membrane thinning or permeabilization by pore formation. Here we show that amyloid oligomers are reminiscent of multivalent nanoparticles, and that the multivalent membrane binding sites on the oligomer result in clustering of vesicles and spontaneous hemifusion of negatively charged model membranes. Binding of oligomers to multiple vesicles caused exchange of lipids present in the outer membrane leaflets. However, no full fusion or vesicle content mixing was observed. To get insight into the number of oligomers required for hemifusion, the binding affinity of the oligomers to the membranes was determined. Oligomers were shown to be very efficient in inducing lipid exchange, with only a few (<10) oligomers/vesicle required to complete hemifusion. The observed uncontrolled and efficient hemifusion of vesicles sheds a new light on the possible toxicity of oligomers in Parkinson's disease. Our results suggest that the presence of multivalent oligomers may directly interfere with the well-controlled membrane fusion machinery of the cell.

\*Parts of this chapter represent content of a manuscript submitted for publication: Stefanovic, A. N., Claessens, M. M. A. E., Blum, C., & Subramaniam, V. Alpha-synuclein amyloid oligomers act as multivalent nanoparticles to cause hemifusion in negatively charged vesicles



## 6.2 Introduction

Alpha-synuclein ( $\alpha$ S) is a brain specific protein found in presynaptic terminals where it colocalizes with synaptic vesicles [1]. This colocalization resulted in the hypothesis that  $\alpha$ S interacts with membranes. The affinity of  $\alpha$ S for phospholipid bilayers has been confirmed;  $\alpha$ S directly binds to negatively charged vesicles [2-4]. Upon binding, part of the initially intrinsically disordered protein adopts an amphipathic helical structure that orients parallel to the membrane surface [5]. The membrane-bound protein consists of two helical fragments separated by a non-helical membrane immersed region and a flexible solution-exposed C-terminal fragment [6, 7]. Although the exact function of  $\alpha$ S is still unclear, membrane binding is thought to be critical for its physiological function [8]. Membrane bound  $\alpha$ S has been suggested to play a role in vesicle trafficking [9], synaptic vesicle fusion [10] and in the regulation of the mitochondrial fusion/fission machinery [8]. The mechanism by which  $\alpha$ S affects these membrane remodeling processes is still under debate. Binding of  $\alpha$ S might affect fusion and fission by directly changing the physical properties of membranes. Observed  $\alpha$ S binding-induced changes in membrane properties include the adoption of a fusion prone positive mean curvature and a negative Gaussian curvature in PS/PC membranes [11] and the annealing of raft-like membrane structures involved in membrane fusion [12]. Besides affecting membrane properties, the binding of the two helical domains of  $\alpha$ S to opposing membranes has been suggested to result in the close contact required for membrane fusion [13]. An alternative hypothesis is that  $\alpha$ S does not directly affect fusion and fission but is part of the SNARE complex fusion machinery and promotes SNARE-mediated fusion [14].

Not only the putative function of  $\alpha$ S, but also its role in Parkinson's disease (PD) pathology has been associated with the ability to bind membranes. In PD,  $\alpha$ S aggregates and forms cross- $\beta$ -sheet rich amyloid fibrils. The toxicity of this aggregation process probably does not involve fibrils; instead intermediate oligomeric structures are thought to be responsible [15-17]. These oligomers are small, multivalent, biological nanoparticles, and their toxicity mechanism has been described to be markedly similar to the mechanisms proposed for inorganic nanoparticles [18, 19].

It has been reported that inorganic nanoparticles can induce disruption of supported lipid bilayers by the formation of holes, membrane thinning, and/or membrane erosion [20]. Similar observations have been made for  $\alpha$ S oligomers:  $\alpha$ S oligomer

binding results in permeabilization of highly charged model lipid bilayers [21-23] by a mechanism that has been proposed to either involve membrane thinning [24] or the formation of membrane spanning pores [25]. Whether disruption of membrane integrity is indeed the major damaging process *in vivo* remains to be elucidated. In yeast cells,  $\alpha$ S overexpression, and the tendency of the protein to misfold and oligomerize, were shown to interfere with transport pathways by accumulating vesicles into massive intracellular clusters [26]. In PC12 and chromaffin cells, overexpression of  $\alpha$ S inhibited transmitter release in a late step after docking but before fusion [27]. These results suggest that *in vivo* aggregation into multimers and oligomers directly interferes with the cell's fusion machinery. Here we will address the hypothesis that aggregation of multiple  $\alpha$ S molecules results in the formation of particles with multivalent membrane binding sites. We show that these multivalent binding sites are able to connect opposing membranes and result in the formation of hemifusion contacts. We speculate that the toxicity of oligomers may originate from their vesicle clustering and hemifusion docking activity and that this effect might not be limited to the  $\alpha$ S oligomers studied here, but may be generic for small, membrane-binding nanoparticles.

## **6.3 Material and Methods**

### **6.3.1 Expression and purification of $\alpha$ S**

Expression and purification of human wild-type (WT)  $\alpha$ S and A140C  $\alpha$ S was done as previously described [28]. Concentration of  $\alpha$ S was determined by measuring the absorbance on a Shimadzu spectrophotometer at 276 nm using molar extinction coefficients of  $5600 \text{ M}^{-1}\text{cm}^{-1}$  [29, 30] for WT and  $5745 \text{ M}^{-1}\text{cm}^{-1}$  for A140C and  $\alpha$ S was stored at  $-80^\circ\text{C}$  until further use.

### **6.3.2 Labeling of $\alpha$ S-A140C**

The cysteine mutant  $\alpha$ S-A140C was used for labeling the protein with an Alexa Fluor 488 C5 maleimide dye (A488). Prior to labeling, a six-fold molar excess of dithiothreitol (DTT) was added to  $\alpha$ S-A140C to reduce disulfide bonds. After 30 minutes of incubation, DTT was removed using Zeba Spin desalting columns, and a two-fold excess of A488 was added. After 1 hour incubation, excess of free dye

was removed using two desalting steps. The labeling efficiency was estimated to be between 90-100% from absorption spectra. To determine the protein and A488 concentration the absorbance at 276 nm was measured using a molar extinction coefficient of 5745 M<sup>-1</sup> cm<sup>-1</sup> for the protein and at 495 nm using a molar extinction coefficient of 72000 M<sup>-1</sup> cm<sup>-1</sup> for the dye.

### 6.3.3 Preparation of unlabeled and labeled $\alpha$ S oligomers

Briefly, oligomers were obtained by incubating  $\alpha$ S at high concentrations in the absence of additional factors [22]. Alexa 488-labeled oligomers with 7.5 % labeling density, achieved by mixing appropriate quantities of labeled protein ( $\alpha$ S-A140C) with unlabeled protein (WT), were used for FCS experiments. Oligomers were purified and separated from monomers using size-exclusion chromatography on a Superdex<sup>TM</sup> 200 10/300 GL column (GE Healthcare Bio-Sciences AB, Uppsala, Sweden). Separation of oligomers from monomers is based on size, where larger particles (oligomers) elute first. We have previously demonstrated that oligomers prepared in this manner are composed of ~ 30 monomers, and are stable [30].

### 6.3.4 LUVs preparation

All lipids used in our experiments were purchased from Avanti Polar Lipids (Alabaster, AL). 1,2-dioleoylphosphatidylglycerol (DOPG) DOPG LUVs were prepared by mixing 1mM of lipids in chloroform. 1 mol% of (1-palmitoyl-2-sn-glycero-3-phosphocholine) NBD-PC was added to the lipid mixture. The solvent was removed by drying under nitrogen flow. The resulting lipid films were then hydrated for 1 hour using 10 mM TRIS (Tris(hydroxymethyl)aminomethane), 150 mM NaCl. The sample was then subjected to 5 freeze-thaw cycles using liquid nitrogen and a water bath. The temperature of the water bath was kept above the transition temperature of the lipid mixture. The solution was subsequently extruded 11 times through 100 nm pore size filters (Whatman).

### 6.3.5 GUVs preparation for clustering experiment and imaging of clustered vesicles

DOPG giant unilamellar vesicles (GUVs) were prepared in sucrose solution as previously described by Angelova [31]. The sucrose concentration was equiosmolar to the 10 mM TRIS, 150 mM NaCl solution in which the proteins were dissolved. 1 mol% DOPE-Rhodamine (N-(1-lyssamine Rhodamine B sulfonyl)-1,2-dioleoyl-sn-3-phosphatidylethanolamine) was included in the previously mentioned lipid mixtures to facilitate visualization of the lipid membrane.

DOPG GUVs fluorescently labeled with DOPE-Rhodamine were equilibrated with fluorescently labeled NBD-PC DOPG LUVs for 30 minutes before imaging. DOPE-Rhodamine was excited with a He/Ne laser (543 nm) and Alexa 488 was excited with an Argon laser (488 nm) on a Zeiss CLSM 510 confocal microscope. To observe the effect of oligomers on the membranes we added oligomers and observed that oligomers initiate clustering of DOPG vesicles (**Figure 6.2B**). Our experiments were performed using the same experimental settings (master gain, digital offset and laser power) and at least 15 GUVs were imaged. **Figures 6.2A** and **2B** are representative confocal images of performed clustering experiment.

### 6.3.6 Content mixing

An ANTS/DPX fluorescence quenching assay is widely used to study content mixing in membrane fusion and was done using the method previously described by [32, 33]. Briefly this assay is based on the collisional quenching of ANTS (8-aminonaphthalene-1,3,6-trisulfonic acid disodium salt) by the cationic quencher DPX (p-xylene-bis-pyridinium bromide). ANTS and DPX were both obtained from Sigma Aldrich (St. Louis). Mixing of vesicle contents upon fusion was assayed by mixing equal amounts of ANTS- and DPX-containing DOPG LUVs and monitoring ANTS fluorescence after the addition of  $\alpha$ S oligomers.

The fluorescence was measured using a Varian Cary Eclipse fluorescence spectrophotometer (Mulgrave, Australia), with excitation at 470 nm and emission recorded between 400 and 600 nm.

### 6.3.7 Lipid mixing

$\alpha$ S-induced lipid mixing in DOPG vesicles was measured by a Förster resonance energy transfer (FRET) assay. This assay is based on the decrease in resonance energy transfer between two membrane probes DOPE-Rhodamine and NBD-PC [34, 35]. DOPG LUVs labeled with DOPE-Rhodamine and NBD-PC were premixed with unlabeled DOPG LUVs. The concentration of each of the fluorescent probes within the pre-fusion liposome membrane was 0.8 mol %. LUVs were prepared as described above. Prior to the experiment, labeled and unlabeled vesicles were mixed at 1:4 ratio respectively, at a total final lipid concentration of 40  $\mu$ M. The fluorescence was measured using a Varian Cary Eclipse fluorescence spectrophotometer, with excitation at 470 nm and emission recorded between 500 and 650 nm. Excitation and emission slit widths were 10 nm. Lipid mixing was quantified using the following equation:

$$fraction = \frac{F - F_0}{F_{rx} - F_0} \quad (1)$$

where *fraction* is the fraction of mixed lipids, *F* is the ratio of the intensity of NBD-PC at 530 nm and the intensity of DOPE Rhodamine at 588 nm. The values for *F*<sub>0</sub> were measured in the absence of the  $\alpha$ S monomers and oligomers as a hemifusion trigger. The values for *F*<sub>rx</sub> were measured to obtain the 100% value of lipid mixing by solubilization of the vesicles in 1% (v/v) Triton X-100.

### 6.3.8 Fluorescence Correlation Spectroscopy

FCS was performed on a custom-built inverted confocal microscope, which is described in more detail in [30]. In this study, a 15  $\mu$ m confocal pinhole was used. Excitation powers were  $\sim$  3 kW/cm<sup>2</sup>. For each sample, the autocorrelation of 20 timetraces of each 30 s was calculated using the Symphotime software (Picoquant). Subsequently, the 30 autocorrelations were averaged and fitted with a two species free diffusion model using Matlab R2013a (Mathworks) from which the fraction of bound  $\alpha$ S oligomers was determined as described in [2]. **Figure 6.1** shows autocorrelation curves for 3 different lipid concentrations in the presence of 100 nM oligomers (equivalent monomer concentration). The black curve in **Figure 6.1** represents the autocorrelation curve of oligomers alone; the red curve corresponds to oligomers + 4  $\mu$ M lipids (70 % free oligomers + 30 % oligomers bound to

**Alpha-synuclein amyloid multimers act as multivalent nanoparticles to cause hemifusion in negatively charged bilayers**

vesicles) and the blue curve to oligomers + 10  $\mu\text{M}$  lipids (30 % free oligomers + 70 % oligomers bound to vesicles).

### 6.3.9 Estimation of $\alpha\text{S}$ oligomers-membrane binding equilibrium

From the FCS binding curve we could obtain the binding constant  $K_d$  using the following two-state equilibrium:



where  $O$  is the free oligomer concentration (0.1  $\mu\text{M}$ ),  $L$  is the free lipid concentration in  $\mu\text{M}$ , and  $C$  is the concentration of the formed complex. Substituting the total  $\alpha\text{S}$  concentration  $O_{tot} = O + C$  and total lipid concentration

$L_{tot} = L + C$  into equation 2:

$$K_d = (O_{tot} - C)(L_{tot} - C) / C \quad (3)$$

Rearranging this equation yields the following equation:

$$C^2 + C(-L_{tot} - O_{tot} - K_d) + O_{tot}L_{tot} = 0 \quad (4)$$

Since our data are proportional to  $P_{bound} = C / O_{tot}$  and

$$C = \frac{(L_{tot} + O_{tot} + K_d) \pm \sqrt{((L_{tot} + O_{tot} + K_d)^2 - 4O_{tot}L_{tot})}}{2} \quad (5)$$

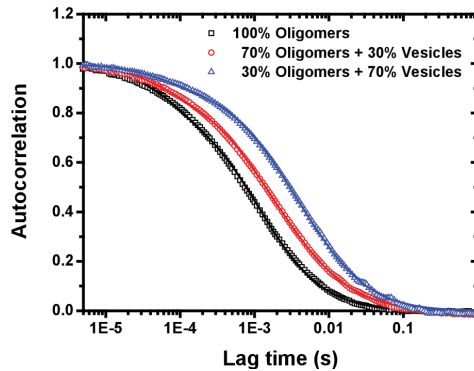


**Figure 6.1:** Normalized autocorrelation curves of 3 different lipid:oligomer ratios: black curve are only oligomers (100 % free oligomers); red curve (70 % free oligomers + 30 % oligomers bound to vesicles) corresponds to 4  $\mu\text{M}$  lipids and blue curve (30% free oligomers + 70% oligomers bound to vesicles) corresponds to 10  $\mu\text{M}$  lipids. Oligomer concentration is 100 nM (7.5% labeling density).

From these equations we could calculate fraction bound protein ( $P_{bound}$ ) for any protein and lipid concentration and this was used to estimate the number of oligomers per DOPG vesicle in our fusion experiment.

## 6.4 Results

### 6.4.1 $\alpha$ S oligomers induce vesicle clustering

To study if the presence of  $\alpha$ S oligomers can induce the formation of membrane contacts, vesicles composed of the negatively charged phospholipid 1,2-dioleoylphosphatidylglycerol (DOPG) were used as a model membrane system. Giant and large unilamellar DOPG vesicles (GUVs and LUVs) were doped with 1% fluorescently labeled lipids to be able to visualize and follow the effect of oligomers on these vesicles. Oligomeric  $\alpha$ S was prepared following an established protocol based on a high protein concentration and purification by size exclusion chromatography [22]. The effect of  $\alpha$ S oligomers on a mixture of DOPE-Rhodamine doped GUVs and NBD-PC doped LUVs was visualized using confocal microscopy (See **Figure 6.2**). Before the addition of  $\alpha$ S oligomers to the vesicle mixture there were no signs of GUV and LUV clustering. In confocal images the GUVs are clearly visible as rings in the red channel of the confocal slice. The size of the LUVs is below the diffraction limit and these structures can therefore not be resolved. The LUVs appear as a diffuse signal in the green channel, and as expected, there is no signal originating from LUVs in the volume excluded by GUVs. The overlay between the red GUV channel and the green LUV channel confirms that there is no interaction or clustering of vesicles in the absence of  $\alpha$ S oligomers. This observation changes upon incubation of the vesicles with  $\alpha$ S oligomers. After the addition of oligomers, the initially diffuse LUV signal transforms into patchy structures in solution and results in what we interpret to be an accumulation of LUVs at the GUV surface. The overlay of the red and green channels confirms that LUVs are enriched at the GUV membrane.

The clustering of vesicles observed by fluorescence microscopy was confirmed by dynamic light scattering (DLS) experiments. Before the addition of  $\alpha$ S oligomers the average diameter of the LUVs was  $112 \pm 6$  nm, while upon addition of  $\alpha$ S oligomers we observed a clear change in the average size of the vesicles to a diameter of  $215 \pm 8$  nm (**Figure 6.3B**). LUV clustering also affected the width of

## Alpha-synuclein amyloid multimers act as multivalent nanoparticles to cause hemifusion in negatively charged bilayers

the size distributions. For DOPG LUVs alone, the width of the size distribution was observed to be  $37 \pm 1$  nm, and increased to  $75 \pm 7$  nm upon the addition of oligomers. The observed clustering of LUVs and GUVs suggests that oligomers are able to form connections between different membranes.

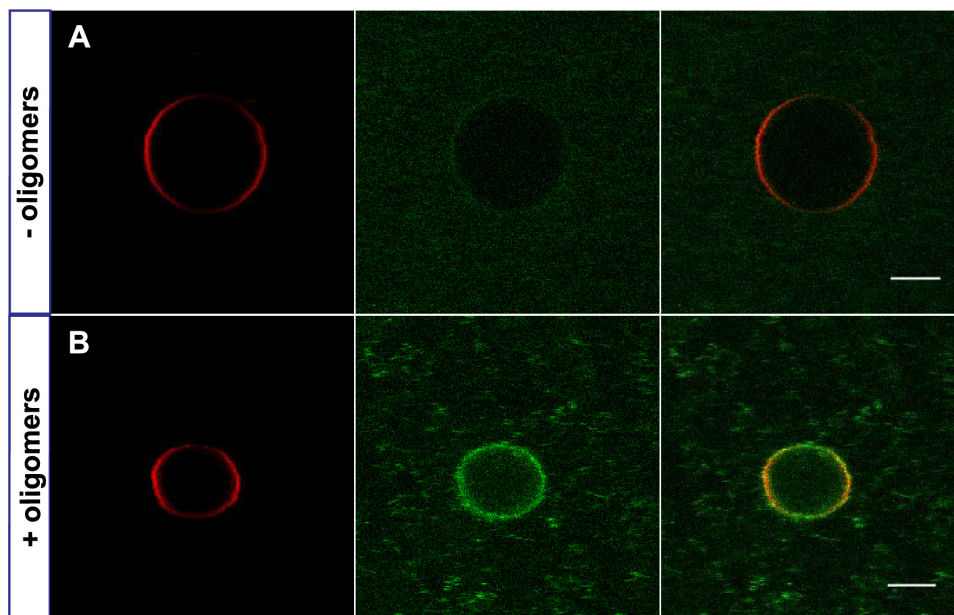


**Figure 6.2:** A) In the absence of  $\alpha$ S oligomers we observe no clustering between DOPE-Rhodamine labeled DOPG GUVs (red channel, first column) and NBD-PC labeled DOPG LUVs (green channel, second column). The overlay between the channels (third column) confirms that there is no interaction between the vesicles. B) After the addition of oligomers we find a clear accumulation of NBD-PC labeled LUVs at the GUV surface and a clustering of LUVs in solution. The scale bars indicate 5  $\mu$ m. The size of the LUVs is below the diffraction limit and these structures can therefore not be resolved.

### 6.4.2 Oligomer-induced vesicle fusion

The idea that  $\alpha$ S oligomers can connect membranes was further investigated. Oligomers may simply connect vesicles, induce hemi-fusion or even full fusion of the vesicles by merging one or both leaflets of the bilayers.

To test if the oligomer binding results in full fusion of vesicles we used a classical content mixing assay based on fluorescence quenching [36]. We prepared two batches of DOPG LUVs, one containing the fluorophore ANTS, and the other



containing the quencher DPX. Full fusion of fluorophore and quencher containing vesicles will result in content mixing and hence a drop in fluorescence due to quenching of ANTS by DPX. Equal amounts of ANTS and DPX containing vesicles were mixed and incubated with  $\alpha$ S oligomers, while the change of fluorescence was monitored (**Figure 6.3A**). The recorded ANTS fluorescence spectra showed no drop in ANTS fluorescence after the addition of  $\alpha$ S oligomers to the vesicle mixture and incubation for three hours. Although our DLS data (**Figure 6.3B**) shows that oligomer binding results in vesicles clustering, oligomers cannot induce full fusion of the vesicles.

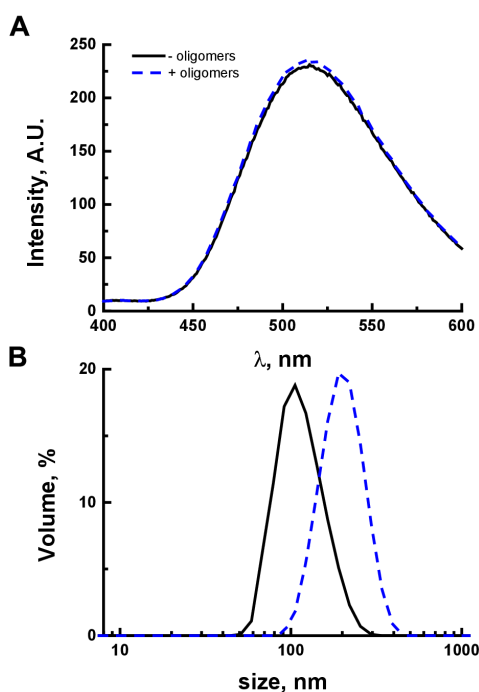


**Figure 6.3:** (A) Fluorophore (ANTS) and quencher (DPX) filled DOPG vesicles were mixed in solution and the ANTS emission spectrum was recorded (black curve).  $\alpha$ S oligomers were added to the vesicle containing solution and 3 hours after addition the spectrum was recorded again (blue dashed line). The absence of a change in the emission intensity shows that the addition of oligomers did not result in content mixing and quenching of DPX by ANTS, and hence that no full fusion of the vesicles occurs. (B) Dynamic light scattering measurements before (black line) and after incubation with  $\alpha$ S oligomers (blue dashed line) demonstrate the increase in diameter of the vesicles due to clustering from  $112 \pm 6$  nm to  $215 \pm 8$  nm (standard error based on 3 different measurements). The width of the size distribution peak also increased from  $37 \pm 1$  nm for DOPG LUVs alone to a width of  $75 \pm 7$  nm for DOPG LUVs in the presence of oligomers.

### 6.4.3 Oligomer-induced hemifusion

To discriminate between the formation of hemifusion contacts and  $\alpha$ S oligomers simply acting as connectors between vesicles, we used a Forster Resonance Energy Transfer (FRET) dilution assay that probes the mixing of membrane lipids originating from different vesicles. The assay is based on the preparation of two populations of vesicles; one population is labelled with a FRET pair, the other population is unlabeled. The membrane of the FRET labeled vesicles contains two fluorophores that are present in a concentration that allows for FRET: upon excitation of the donor fluorophore, energy can be transferred to an acceptor fluorophore. FRET occurs on length scales in the nanometer range and is very sensitive to the distance ( $\sim 1/r^6$ , where  $r$  represents the distance between donor and acceptor) between the fluorophores. Fusion of FRET labeled vesicles with unlabeled vesicles results in a dilution of the FRET system by the unlabeled lipids. The resulting drop in FRET efficiency can easily be detected as a drop in FRET acceptor intensity and increase in FRET donor intensity.

For our assay we prepared DOPG vesicles containing 0.8 mol% of both the donor fluorophore NBD-PC and acceptor fluorophores DOPE-Rhodamine. To study any dilution of the FRET pair that may result from lipid mixing upon addition of  $\alpha$ S oligomers we prepared a 1:4 mixture of vesicles containing the FRET system and vesicles without fluorophores. Upon addition of  $\alpha$ S oligomers we recorded the change of emission spectra over time (**Figure 6.4A**).

Before the addition of  $\alpha$ S oligomers we observe upon excitation of the FRET donor, NBD-PC, a strong emission from the FRET acceptor, DOPE-Rhodamine, and a moderate emission from NBD-PC, which provides strong evidence of effective FRET. Upon addition of  $\alpha$ S oligomers the intensity of the FRET acceptor decreases over time with a commensurate increase of the FRET donor signal (see **Figure 6.4A**). The observed changes in the emission spectra result from a decrease of FRET efficiency caused by the dilution of the FRET-pair forming fluorophores upon fusion of labeled and unlabeled lipid bilayers. The membrane fusion-induced changes in the emission spectra upon the addition of oligomers are completed after approximately 10 minutes (See **Figure 6.4A**). We repeated the experiment for different concentrations of  $\alpha$ S oligomers and determined the fraction of diluted lipids from the ratio between donor and acceptor fluorescence intensity after reaching a constant value for each  $\alpha$ S oligomer concentration (See **Material and Methods**).

## Chapter 6

We observe a strong increase of the fraction of lipids mixed upon increasing the  $\alpha$ S concentration from 0.01 to 0.1  $\mu$ M oligomers (equivalent monomer concentration). The fraction of lipids mixed reaches a plateau at  $\sim$ 50%, and increasing the  $\alpha$ S oligomer concentration does not result in higher values. Our data therefore indicates that only half of the labeled lipids are sensitive to the presence of oligomers.

Since oligomers have a clear effect on membrane fusion, we estimated the number of oligomers bound to each vesicle from the equilibrium dissociation constant  $K_d$ . To determine  $K_d$  for oligomers binding to DOPG vesicles, we determined the fraction of DOPG LUV-bound  $\alpha$ S oligomers at different  $\alpha$ S oligomer concentrations using Fluorescence Correlation Spectroscopy (FCS). Membrane bound and free  $\alpha$ S oligomers were discriminated with FCS on the basis of the difference in diffusion coefficient. The fraction of membrane bound protein,  $P_{bound} = C / O_{tot}$ , where C is the complex concentration and  $O_{tot}$  is the total protein concentration, was obtained as a function of the total DOPG concentration (**Figure 6.3B**). To determine the dissociation constant,  $K_d$ , the following oligomer-membrane binding equilibrium was assumed:  $O + L \longleftrightarrow C$  and  $K_d = \frac{O \cdot L}{C}$  where

O and L are the protein and lipid concentrations respectively (for more details see **Materials and Methods**). Rewriting the expression for  $K_d$  in terms of the known  $L_{tot}$  and  $O_{tot}$  made it possible to determine  $K_d$  (See **Figure 6.4B** and **Material and Methods**). By fitting the binding curve with this expression,  $K_d$  was calculated to be  $\sim$ 1.7  $\mu$ M (**Figure 6.4B**).

In the fusion experiment 40 $\mu$ M DOPG LUVs were mixed with different oligomer concentrations. Previous experiments have shown that 1 oligomer contains  $\sim$  30 monomers [30]. The DOPG vesicles have an average diameter of  $112.5 \pm 6$  nm, (**Figure 6.3B**) and the mean headgroup area was assumed to be  $0.8$  nm<sup>2</sup>. Using this information and the obtained  $K_d$ , the protein concentrations in the fusion experiments could be expressed in number of  $\alpha$ S oligomers per vesicle (see **Figure 6.4C**, bottom axis). This figure shows that a very low average number of  $\alpha$ S oligomers per vesicle is sufficient to induce membrane fusion. At an average of  $<10$   $\alpha$ S oligomers per vesicle we observe a saturation of the fraction of mixed lipids at about 50%.

It has been hypothesized that  $\alpha$ S monomers are also able to cluster and fuse vesicles [37]. To test this idea we used the FRET dilution assay to detect lipid mixing as a function of the concentration of  $\alpha$ S monomers instead of  $\alpha$ S oligomers.

**Alpha-synuclein amyloid multimers act as multivalent nanoparticles to cause hemifusion in negatively charged bilayers**

Indeed we observe the characteristic signs for lipid mixing in the assay. However, compared to oligomers, monomers were less efficient in inducing membrane fusion (See **Figure 6.4D**). According to our data at least 100 fold higher monomer concentrations are necessary to induce membrane fusion compared to oligomers.

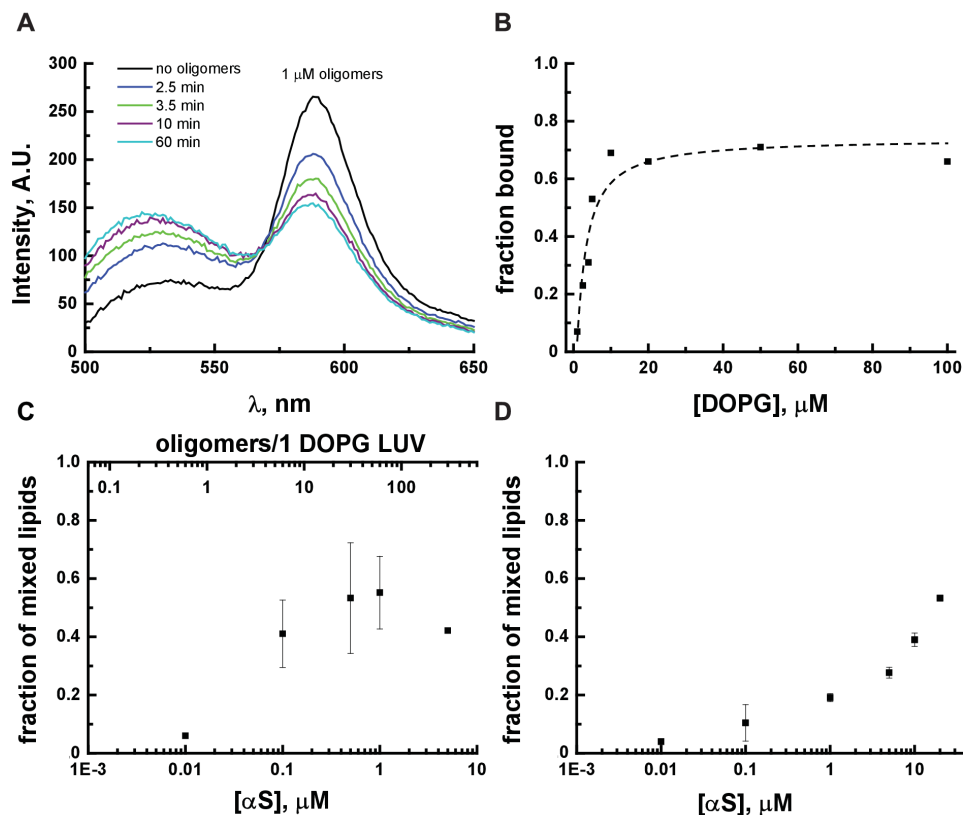


**Figure 6.4: Membrane mixing.** (A) Oligomer-induced time dependent changes in the emission spectra of a NBD-PC and Rhodamine-DOPE mixture in LUVs after excitation of NBD-PC. The changes reflect a decrease in FRET efficiency due to a dilution of the FRET pair with lipids from unlabeled DOPG LUVs. (B) The fraction of membrane-bound oligomers estimated from FCS experiments as a function of the lipid concentration. In the FCS experiments oligomers containing 7.5 % Alexa488 labeled  $\alpha$ S monomers were used. The dotted line shows the fit to the data assuming a  $K_d$  of 1.7  $\mu$ M (C) The maximal fusion efficiency expressed as the fraction of mixed lipids was determined as a function of the oligomer (monomer equivalent) concentration. Using the obtained  $K_d$  values this concentration was expressed as a function of bound oligomers per vesicle. The fusion efficiency was limited to  $\sim$ 50% and this maximum fusion efficiency was reached for values  $<10$  oligomers/LUV. (D) For monomers higher concentrations compared to oligomers are necessary to reach comparable fractions of mixed lipids.

## 6.5 Discussion

Here we have shown that oligomeric  $\alpha$ S has a propensity to cluster DOPG vesicles. In the presence of in vitro produced isolated oligomers, DOPG LUVs cluster and accumulate at the surface of GUVs (**Figure 6.2B and 6.3B**). The multivalent membrane binding sites on the oligomer seem very efficient in clustering negatively charged vesicles. The effect of  $\alpha$ S oligomer binding is not limited to clustering; FRET experiments indicate that it also enhances the exchange of lipids between connected bilayers (**Figure 6.4A and 6.4C**). However, not all lipids in the vesicles are available for the exchange. With increasing  $\alpha$ S oligomer concentrations a plateau is reached in which only 50-60% of the FRET-labeled lipids are diluted by unlabeled lipids (**Figure 6.4C**). This suggests that only the outer leaflets of the vesicles are affected by  $\alpha$ S oligomers. We attribute the slight overshoot over the expected 50% for one leaflet to the previously reported oligomer-enhanced lipid flip-flop [38]. The finding that oligomer binding does not result in content mixing of DOPG LUVs is in agreement with the formation of hemifusion contacts (**Figure 6.3A**).

Several factors may play a role in the oligomer-induced formation of hemifusion contacts between LUVs. The binding of monomeric  $\alpha$ S has been shown to induce a local negative Gaussian membrane curvature [11]. Negative Gaussian curvatures ( $1/R_1R_2 < 0$ ) are associated with saddle surfaces and hence the formation of fusion intermediates [39]. Since the membrane binding properties are largely preserved in the oligomer, oligomers may also favor the formation of saddle surfaces. Moreover the close contact between opposing membranes that is established by binding of oligomers to multiple vesicles may in itself be sufficient to drive the formation of hemifusion contacts. The release of hydration energy when contacts with an inter-membrane distance of  $\leq 1$  nm are formed can be enough to compensate for the elastic energy of hemifusion stalks.[39] A low resolution oligomer structure obtained by small angle X-ray scattering shows that oligomers are elongated structures with a long axis of  $\sim 18$  nm and a diameter of 4.5-9 nm [40]. Considering the required small inter-membrane distance this suggests that to induce hemifusion oligomers will have to partially insert into the bilayer and perhaps deform upon binding.

By obtaining the equilibrium binding constant for the oligomer-membrane binding reaction (**Figure 6.4B**) we were able to estimate the mean number of bound oligomers required for hemifusion (**Figure 6.4C**). The fusion plateau is reached for

less than 10 oligomers per vesicle indicating that the formation of hemifusion contacts is very efficient. This is in good agreement with observations for fusogenic proteins and peptides [41, 42]. The energy landscape of the fusion reaction is relatively flat and fusion itself is therefore not a very specific reaction [43]. The complex fusion machinery employed by cells has been suggested to be involved in controlling docking rather than in carrying out fusion itself [43]. The toxicity of oligomers may thus result from the spontaneous formation of hemifusion contacts between membranes and subsequent interference with the fusion control machinery.

In our experiments with oligomers, fusion did not proceed beyond the hemifusion state. The transformation of a hemifusion contact to an expanding pore is more energy demanding and probably controlled by the buildup of lateral membrane tension [39, 44]. Binding or incorporation of oligomers is however known to result in a (transient) increase in membrane permeability [22, 38]. The buildup of membrane tension by bound proteins necessary for full fusion is therefore probably not possible in this model system. The heterogeneous sizes of aggregated vesicles observed in cells at high  $\alpha$ S concentrations suggests that  $\alpha$ S monomer- or aggregate-binding can result in full fusion *in vivo* [26].

Because of the presence of multiple membrane binding domains  $\alpha$ S oligomers are very efficient in connecting DOPG vesicles, but vesicles also fuse in the presence of monomeric protein albeit at higher concentrations (**Figure 6.4D**). The observation that monomers can induce fusion does not agree with the inhibition of vesicle fusion by  $\alpha$ S observed by Kamp et al. [45]. In this report the observed inhibition probably results from a stabilization by  $\alpha$ S of defects in the gel-phase SUVs used, and thus likely has another origin than the increased vesicle fusion observed here. Interestingly the formation of hemifusion contacts in the presence of  $\alpha$ S monomers becomes very efficient around the critical aggregation concentration [46]. This suggests that also in this experiment performed with monomeric  $\alpha$ S, incipient multimeric  $\alpha$ S is responsible for the formation of hemifusion.

In PD the formation of membrane-binding oligomeric  $\alpha$ S species has been associated with cell death. In previous studies oligomeric  $\alpha$ S has been observed in cells and has been hypothesized to form membrane pores or cause membrane thinning. By thus disrupting the integrity of cellular membranes, oligomers are thought to decrease cell viability. This toxic mechanism is currently under debate; although oligomeric  $\alpha$ S has been shown to disrupt the integrity of anionic

phospholipid vesicles, bilayers with more physiological relevant lipid compositions are hardly affected [23].

Our data suggests that there is an additional mechanism involved in the toxicity of  $\alpha$ S oligomers. The protein  $\alpha$ S binds membranes by adopting an amphipathic  $\alpha$ -helical structure. The ability to adopt a membrane-binding  $\alpha$ -helical conformation is largely preserved in oligomeric  $\alpha$ S [22, 23]. The membrane-bound oligomers may interfere with the physiological function of the  $\alpha$ S protein. Ultrastructural analysis shows that with increasing cellular  $\alpha$ S levels transport vesicles bud normally from their parent membrane, but at the cell periphery these now heterogeneously sized vesicles no longer dock and fuse normally. At the plasma membrane morphologically undocked vesicles appear and with increasing  $\alpha$ S levels massive intercellular vesicular clusters show up [26]. Increased cellular  $\alpha$ S concentrations have been associated with  $\alpha$ S aggregation and the formation of toxic  $\alpha$ S oligomers. The oligomer-induced formation of hemifusion contacts between DOPG vesicles indicates that the vesicle docking and fusion problems observed *in vivo* may directly result from the presence of oligomers.

As proposed for  $\alpha$ S oligomers, the toxicity of nanoparticles has been suggested to involve nanoscale hole formation or membrane thinning. Indeed cationic gold, polystyrene and core-shell nanoparticles are able to bind and disrupt negatively charged vesicles [47] but membrane disruption depends on the number of charges on the surface and probably also on the membrane charge density [48]. Interestingly nanoparticles with a diameter smaller than tens of nm have been reported to be more toxic than larger nanoparticles. These observations suggest that the toxic mechanism we propose here may not be limited to the specific  $\alpha$ S oligomers (aggregation number of  $\sim 30$ ) studied. When small cationic nanoparticles become available in the cell cytoplasm, binding to multiple vesicles or other membrane structures may result in the close membrane contacts required for (hemi)fusion. Therefore the clustering and possible fusion of membrane bound cellular structures may also contribute to the toxicity of small cationic nanoparticles..

## 6.6 Acknowledgments

We thank Kirsten van Leijenhorst-Groener and Nathalie Schilderink for assistance in expression and purification of alpha-synuclein. We also thank Niels Zijlstra for the help with performing the FCS experiments and data analysis.

## 6.7 References

1. Iwai, A., Masliah, E., Yoshimoto, M., Ge, N., Flanagan, L., de Silva, H. A., Kittel, A. & Saitoh, T. (1995) The precursor protein of non-A beta component of Alzheimer's disease amyloid is a presynaptic protein of the central nervous system, *Neuron*. **14**, 467-75.
2. Rhoades, E., Ramlall, T. F., Webb, W. W. & Eliezer, D. (2006) Quantification of alpha-synuclein binding to lipid vesicles using fluorescence correlation spectroscopy, *Biophys J*. **90**, 4692-700.
3. Davidson, W. S., Jonas, A., Clayton, D. F. & George, J. M. (1998) Stabilization of alpha-synuclein secondary structure upon binding to synthetic membranes, *J Biol Chem*. **273**, 9443-9.
4. Stockl, M., Fischer, P., Wanker, E. & Herrmann, A. (2008) Alpha-synuclein selectively binds to anionic phospholipids embedded in liquid-disordered domains, *J Mol Biol*. **375**, 1394-404.
5. Jao, C. C., Hegde, B. G., Chen, J., Haworth, I. S. & Langen, R. (2008) Structure of membrane-bound alpha-synuclein from site-directed spin labeling and computational refinement, *Proc Natl Acad Sci U S A*. **105**, 19666-71.
6. Shvachak, V. V. & Subramaniam, V. (2014) A four-amino acid linker between repeats in the alpha-synuclein sequence is important for fibril formation, *Biochemistry*. **53**, 279-81.
7. Eliezer, D., Kutluay, E., Bussell, R., Jr. & Browne, G. (2001) Conformational properties of alpha-synuclein in its free and lipid-associated states, *J Mol Biol*. **307**, 1061-73.
8. Guardia-Laguarta, C., Area-Gomez, E., Rub, C., Liu, Y., Magrane, J., Becker, D., Voos, W., Schon, E. A. & Przedborski, S. (2014) alpha-Synuclein is localized to mitochondria-associated ER membranes, *J Neurosci*. **34**, 249-59.
9. Chai, Y.-J., Kim, D., Park, J., Zhao, H., Lee, S.-J. & Chang, S. (2013) The secreted oligomeric form of alpha-synuclein affects multiple steps of membrane trafficking, *FEBS Lett*. **587**, 452-459.
10. Bellani, S., Sousa, V. L., Ronzitti, G., Valtorta, F., Meldolesi, J. & Chieregatti, E. (2010) The regulation of synaptic function by alpha-synuclein, *Commun Integr Biol*. **3**, 106-109.
11. Braun, A. R., Sevcsik, E., Chin, P., Rhoades, E., Tristram-Nagle, S. & Sachs, J. N. (2012) alpha-Synuclein induces both positive mean curvature and negative Gaussian curvature in membranes, *J Am Chem Soc*. **134**, 2613-20.
12. Leftin, A., Job, C., Beyer, K. & Brown, M. F. (2013) Solid-State <sup>13</sup>C NMR Reveals Annealing of Raft-Like Membranes Containing Cholesterol by the Intrinsically Disordered Protein alpha-Synuclein, *J Mol Biol*. **425**, 2973-2987.
13. Dikiy, I. & Eliezer, D. (2012) Folding and misfolding of alpha-synuclein on membranes, *Biochim Biophys Acta*. **1818**, 1013-8.
14. Burre, J., Sharma, M., Tsetsenis, T., Buchman, V., Etherton, M. R. & Sudhof, T. C. (2010) Alpha-synuclein promotes SNARE-complex assembly in vivo and in vitro, *Science*. **329**, 1663-7.
15. Kaye, R., Head, E., Thompson, J. L., McIntire, T. M., Milton, S. C., Cotman, C. W. & Glabe, C. G. (2003) Common structure of soluble amyloid oligomers implies common mechanism of pathogenesis, *Science*. **300**, 486-9.
16. Danzer, K. M., Ruf, W. P., Putcha, P., Joyner, D., Hashimoto, T., Glabe, C., Hyman, B. T. & McLean, P. J. (2011) Heat-shock protein 70 modulates toxic extracellular alpha-synuclein oligomers and rescues trans-synaptic toxicity, *FASEB J*. **25**, 326-36.
17. Cappai, R., Leck, S. L., Tew, D. J., Williamson, N. A., Smith, D. P., Galatis, D., Sharples, R. A., Curtain, C. C., Ali, F. E., Cherny, R. A., Culvenor, J. G., Bottomley, S. P., Masters, C. L., Barnham, K. J. & Hill, A. F. (2005) Dopamine promotes alpha-synuclein aggregation into SDS-resistant soluble oligomers via a distinct folding pathway, *FASEB J*. **19**, 1377-9.
18. Schulz, M., Olubummo, A. & Binder, W. H. (2012) Beyond the lipid-bilayer: interaction of polymers and nanoparticles with membranes, *Soft Matter*. **8**, 4849-4864.
19. Verma, A. & Stellacci, F. (2010) Effect of Surface Properties on Nanoparticle-Cell Interactions, *Small*. **6**, 12-21.



## Chapter 6

20. Leroueil, P. R., Berry, S. A., Duthie, K., Han, G., Rotello, V. M., McNerny, D. Q., Baker, J. R., Jr., Orr, B. G. & Holl, M. M. (2008) Wide varieties of cationic nanoparticles induce defects in supported lipid bilayers, *Nano Lett.* **8**, 420-4.
21. Volles, M. & Lansbury, P. (2002) Vesicle permeabilization by protofibrillar alpha-synuclein is sensitive to Parkinson's disease-linked mutations and occurs by a pore-like mechanism, *Biochemistry.* **41**, 4595 - 4602.
22. van Rooijen, B. D., Claessens, M. M. & Subramaniam, V. (2009) Lipid bilayer disruption by oligomeric alpha-synuclein depends on bilayer charge and accessibility of the hydrophobic core, *Biochim Biophys Acta.* **1788**, 1271-8.
23. Stefanovic, A. N., Stockl, M. T., Claessens, M. M. & Subramaniam, V. (2014) alpha-Synuclein oligomers distinctively permeabilize complex model membranes, *FEBS J.* **281**, 2838-50.
24. Sparr, E., Engel, M. F., Sakharov, D. V., Sprong, M., Jacobs, J., de Kruijff, B., Hoppener, J. W. & Killian, J. A. (2004) Islet amyloid polypeptide-induced membrane leakage involves uptake of lipids by forming amyloid fibers, *FEBS Lett.* **577**, 117-20.
25. Lashuel, H. A., Petre, B. M., Wall, J., Simon, M., Nowak, R. J., Walz, T. & Lansbury, P. T. (2002)  $\alpha$ -Synuclein, Especially the Parkinson's Disease-associated Mutants, Forms Pore-like Annular and Tubular Protofibrils, *J Mol Biol.* **322**, 1089-1102.
26. Gitler, A., Bevis, B., Shorter, J., Strathearn, K., Hamamichi, S., Su, L., Caldwell, K., Caldwell, G., Rochet, J., McCaffery, J., Barlowe, C. & Lindquist, S. (2008) The Parkinson's disease protein alpha-synuclein disrupts cellular Rab homeostasis, *Proc Natl Acad Sci USA.* **105**, 145 - 150.
27. Larsen, K. E., Schmitz, Y., Troyer, M. D., Mosharov, E., Dietrich, P., Quazi, A. Z., Savalle, M., Nemani, V., Chaudhry, F. A., Edwards, R. H., Stefanis, L. & Sulzer, D. (2006) Alpha-synuclein overexpression in PC12 and chromaffin cells impairs catecholamine release by interfering with a late step in exocytosis, *J Neurosci.* **26**, 11915-22.
28. van Raaij, M. E., Segers-Nolten, I. M. J. & Subramaniam, V. (2006) Quantitative Morphological Analysis Reveals Ultrastructural Diversity of Amyloid Fibrils from  $\alpha$ -Synuclein Mutants, *Biophys J.* **91**, L96-L98.
29. Pace, C. N., Vajdos, F., Fee, L., Grimsley, G. & Gray, T. (1995) How to measure and predict the molar absorption coefficient of a protein, *Protein Sci.* **4**, 2411-23.
30. Zijlstra, N., Blum, C., Segers-Nolten, I. M., Claessens, M. M. & Subramaniam, V. (2012) Molecular composition of sub-stoichiometrically labeled alpha-synuclein oligomers determined by single-molecule photobleaching, *Angew Chem Int Ed Engl.* **51**, 8821-4.
31. Angelova, M. I. & Dimitrov, D. S. (1986) Liposome Electroformation, *Faraday Disc Chem Soc.* **81**, 303-311.
32. Smolarsky, M., Teitelbaum, D., Sela, M. & Gitler, C. (1977) A simple fluorescent method to determine complement-mediated liposome immune lysis, *Journal of Immunological Methods.* **15**, 255-265.
33. Ellens, H., Bentz, J. & Szoka, F. C. (1984) pH-induced destabilization of phosphatidylethanolamine-containing liposomes: role of bilayer contact, *Biochemistry.* **23**, 1532-8.
34. Bereswill, S., Domingues, M. M., Castanho, M. A. R. B. & Santos, N. C. (2009) rBPI21 Promotes Lipopolysaccharide Aggregation and Exerts Its Antimicrobial Effects by (Hemi)fusion of PG-Containing Membranes, *PLoS ONE.* **4**, e8385.
35. Müller, M., Zschörnig, O., Ohki, S. & Arnold, K. (2003) Fusion, Leakage and Surface Hydrophobicity of Vesicles Containing Phosphoinositides: Influence of Steric and Electrostatic Effects, *Journal of Membrane Biology.* **192**, 33-43.
36. Ellens, H., Bentz, J. & Szoka, F. C. (1985) Proton- and calcium-induced fusion and destabilization of liposomes, *Biochemistry.* **24**, 3099-3106.
37. Diao, J., Burre, J., Vivona, S., Cipriano, D. J., Sharma, M., Kyoung, M., Sudhof, T. C. & Brunger, A. T. (2013) Native alpha-synuclein induces clustering of synaptic-vesicle mimics via binding to phospholipids and synaptobrevin-2/VAMP2, *Elife.* **2**, e00592.
38. Stockl, M., Claessens, M. M. & Subramaniam, V. (2012) Kinetic measurements give new insights into lipid membrane permeabilization by alpha-synuclein oligomers, *Mol Biosyst.* **8**, 338-45.

**Alpha-synuclein amyloid multimers act as multivalent nanoparticles to cause hemifusion in negatively charged bilayers**

39. Chernomordik, L., Kozlov, M. M. & Zimmerberg, J. (1995) Lipids in biological membrane fusion, *J Membr Biol.* **146**, 1-14.
40. Giehm, L., Svergun, D. I., Otzen, D. E. & Vestergaard, B. (2011) Low-resolution structure of a vesicle disrupting  $\alpha$ -synuclein oligomer that accumulates during fibrillation, *Proc Natl Acad Sci U S A.* **108**, 3246-51.
41. van den Bogaart, G., Holt, M. G., Bunt, G., Riedel, D., Wouters, F. S. & Jahn, R. (2010) One SNARE complex is sufficient for membrane fusion, *Nat Struct Mol Biol.* **17**, 358-64.
42. Reuven, E. M., Dadon, Y., Viard, M., Manukovsky, N., Blumenthal, R. & Shai, Y. (2012) HIV-1 gp41 Transmembrane Domain Interacts with the Fusion Peptide: Implication in Lipid Mixing and Inhibition of Virus–Cell Fusion, *Biochemistry.* **51**, 2867-2878.
43. Jahn, R. & Grubmüller, H. (2002) Membrane fusion, *Curr Opin Cell Biol.* **14**, 488-495.
44. Chernomordik, L., Chanturiya, A., Green, J. & Zimmerberg, J. (1995) The hemifusion intermediate and its conversion to complete fusion: regulation by membrane composition, *Biophys J.* **69**, 922-9.
45. Kamp, F., Exner, N., Lutz, A. K., Wender, N., Hegermann, J., Brunner, B., Nuscher, B., Bartels, T., Giese, A., Beyer, K., Eimer, S., Winklhofer, K. F. & Haass, C. (2010) Inhibition of mitochondrial fusion by alpha-synuclein is rescued by PINK1, Parkin and DJ-1, *EMBO J.* **29**, 3571-89.
46. van Raaij, M. E., Segers-Nolten, I. M. & Subramaniam, V. (2006) Quantitative morphological analysis reveals ultrastructural diversity of amyloid fibrils from alpha-synuclein mutants, *Biophys J.* **91**, L96-8.
47. Laurencin, M., Georgelin, T., Malezieux, B., Siaugue, J. M. & Menager, C. (2010) Interactions Between Giant Unilamellar Vesicles and Charged Core-Shell Magnetic Nanoparticles, *Langmuir.* **26**, 16025-16030.
48. Arvizo, R. R., Miranda, O. R., Thompson, M. A., Pabelick, C. M., Bhattacharya, R., Robertson, J. D., Rotello, V. M., Prakash, Y. S. & Mukherjee, P. (2010) Effect of Nanoparticle Surface Charge at the Plasma Membrane and Beyond, *Nano Lett.* **10**, 2543-2548.



## Chapter 7

### Conclusion and future recommendations

Alpha-synuclein ( $\alpha$ S) was first described more than 25 years ago and since then a very large number of studies have been done in order to better determine the physiological function of the protein in the human body and its role in Parkinson's disease (PD). More than 6000 articles (~600 this year) have been published about  $\alpha$ S.

$\alpha$ S oligomers are still thought to be the toxic species involved in PD. One of the proposed molecular mechanisms involved in oligomer toxicity suggests that oligomers can disrupt membrane integrity leading to increased presence of reactive oxygen species in the cell, ultimately causing cell death. Membranes are considered a major site at which  $\alpha$ S oligomers cause damage. The goal of this thesis was to gain insights into the biophysical mechanisms of  $\alpha$ S oligomer-membrane interactions.

To look more closely into the damage of specific membranes we used model membrane mimics and investigated how the membrane binding and permeabilization depends on the lipid composition and overall membrane charge. These studies are described in more detail in **Chapters 2, 3 and 4**. In **Chapters 2 and 3** particular attention is given to oligomer binding to increasingly complex membrane compositions. We observed that membranes that contain at least 25 % DOPG bind oligomers. However, oligomers cannot permeabilize membranes with a more physiologically relevant cholesterol and sphingomyelin content. The increased structural integrity of the membrane resulting from the incorporation of cholesterol into the model membrane mimics likely leads to decreased vulnerability of the membrane to oligomer-induced disruption. Because both the mitochondrial inner membrane and the plasma membrane inner leaflet are proposed sites of  $\alpha$ S oligomer-induced damage, most of the research in this thesis was done using model systems mimicking these two membranes. An intriguing finding in **Chapter 2** showed that in addition to binding vesicle membranes, the oligomers appeared to be present in the vesicle interior, suggesting that they were able to diffuse through or across the vesicle membrane. A possible future experiment to confirm the presence of oligomers *inside* the vesicles could be to add a membrane-impermeable quencher (DPX) to the solution after the addition and incubation of fluorescently-labeled oligomers. The quencher molecule should then effectively quench fluorophores (ANTS or HPTS) in the exterior solution and on the

membrane, but should leave those fluorophores coupled to oligomers inside the vesicles unaffected. These studies could be used to gain more mechanistic insights into oligomer-induced permeabilization of physiologically relevant model membranes.

In **Chapter 3** we showed that model mitochondrial membranes are more vulnerable to permeabilization by oligomers than model plasma membrane mimics composed from brain-derived lipids. We believe that it is not necessarily the specific membrane composition that determines the oligomer-induced membrane permeabilization, but rather the complexity of the membrane composition.

The  $\alpha$ S oligomers isolated using the specific protocol used in this thesis contain approximately 30 monomers for all variants (WT, A30P, E46K, H50Q, G51D and A53T) studied (**Chapter 4**). Among the different disease mutants only G51D oligomers showed differences in permeabilization of negatively charged DOPG membranes and almost no effect was observed for inner mitochondrial membrane mimics (**Chapter 4**). However the difference in permeabilization cannot be attributed to any appreciable differences in the oligomer aggregation number or overall structure. We therefore suggest that G51D oligomers may either not bind membranes very well or that the G51D substitution may make it more difficult to distort the lipid bilayer because fewer amino acid residues are immersed in the bilayer. The exchange of the small neutral amino acid glycine (G) with the polar negatively charged aspartic acid (D) could result in exposure to a lipophilic environment, while the partially folded structure of the G51D oligomer may prevent binding of the complete  $\alpha$ -helix (**Chapter 4**).

Based on our results in **Chapter 5**,  $\alpha$ S oligomers did not show toxicity when they were added externally to neuroblastoma cells. The toxicity of the externally added oligomers tested here seems to depend on the availability and toxicity of additional compounds (dopamine and HNE) rather than on the oligomers themselves. From these experiments we cannot exclude that the oligomers are toxic if they are incubated differently, injected intracellularly, or expressed by the cells. An open question for future research remains whether oligomers produced intracellularly during  $\alpha$ S aggregation are toxic to cells. Therefore,  $\alpha$ S oligomers could be introduced into the cell differently e.g. using microinjection, electroporation or scrape loading. Besides the CTB assay that we used, other approaches using the Cell Counting Kit-8 (Sigma-Aldrich, St Louis, MO, USA) or an MTT assay could be also used as cell viability assays. Nonviable cells could be detected by the CytoTox-ONE assay (Promega, Madison, WI, USA) which would show the release

of lactate dehydrogenase from cells with a damaged membrane. Dynamics of the oligomers in live cells could be studied using e.g. quantitative imaging techniques for measuring the lipid order and oligomer-induced permeabilization similar to the one described by Owen et al. [1], or by non-invasive optical recording of nanoscale membrane domains [2]. The deformation of cell shape and rupture of the cells upon the addition of oligomers could be measured using the method of single cell compression by AFM [3]. Sensitive detection techniques will be necessary to resolve if oligomers are toxic species that can damage mitochondrial and other cellular membranes *in vivo* upon injection of the oligomers inside of the cells.

To get access to more details about toxicity of  $\alpha$ S oligomers in **Chapter 6** we proposed that the oligomer-induced formation of hemifusion contacts between DOPG vesicles indicates that the vesicle docking and fusion problems observed *in vivo* may directly result from the presence of oligomers. Our data suggested that the presence of multivalent oligomers may directly interfere with the well-controlled membrane fusion machinery of the cell. We observed that only a few oligomers are required for complete hemifusion. We therefore hypothesize that the clustering and possible fusion of membrane-bound cellular structures may also contribute to the toxicity of oligomeric  $\alpha$ S. Therefore,  $\alpha$ S oligomers could be considered as biological nanoparticles whose toxicity is involved in nanoscale hole formation or membrane thinning. These observations suggest that the toxic mechanism we propose here may not be limited to the specific  $\alpha$ S oligomers (aggregation number of  $\sim 30$ ) studied. When small cationic nanoparticles become available in the cell cytoplasm, binding to multiple vesicles or other membrane structures may result in the close membrane contacts required for (hemi)fusion. We could also consider that the positively charged N-terminal membrane binding part of  $\alpha$ S contributes similarly as small cationic nanoparticles to membrane binding and permeabilization leading to cellular toxicity [4]. Furthermore, uncontrolled and efficient hemifusion of the vesicles could play a role in the putative toxicity of oligomers in Parkinson's disease.

During the course of this thesis work, we have systematically studied the interaction of oligomeric  $\alpha$ S species with complex model membranes using a range of biophysical approaches. In particular, we have focused on the ability of  $\alpha$ S oligomers to bind and permeabilize membranes. We made a conceptual step to consider  $\alpha$ S oligomers as multivalent biological nanoparticles, that were shown to be capable of inducing hemifusion of vesicles. While these studies have yielded further insights into structural characteristics and membrane interactions of  $\alpha$ S

oligomers, there still remain several compelling open questions for further research, a small subset of which are listed below:

- Could it be that oligomers that were able to permeabilize negatively charged and mitochondrial model membranes and result in hemifusion of negatively charged membranes cause *in vivo* disruption of fusion machinery in mitochondria? Is this enough to cause the leakage of cellular content and further cell death of neurons in *substantia nigra* in the midbrain?
- Is the neurodegeneration caused by the G51D mutation [5] happening with a different mechanism?
- Which membrane is the relevant one for  $\alpha$ S oligomer-induced damage?
- Are the oligomers indeed the relevant toxic species when injected intracellularly?

The answers to these questions will help establish the role of  $\alpha$ S oligomers, and their interactions with membranes, in the molecular mechanisms of the disease.

## 7.1 References

1. Owen, D. M., Rentero, C., Magenau, A., Abu-Siniyeh, A. & Gaus, K. (2012) Quantitative imaging of membrane lipid order in cells and organisms, *Nat. Protocols*. **7**, 24-35.
2. Eggeling, C., Ringemann, C., Medda, R., Schwarzmann, G., Sandhoff, K., Polyakova, S., Belov, V. N., Hein, B., von Middendorff, C., Schonle, A. & Hell, S. W. (2009) Direct observation of the nanoscale dynamics of membrane lipids in a living cell, *Nature*. **457**, 1159-1162.
3. Lulevich, V., Zink, T., Chen, H.-Y., Liu, F.-T. & Liu, G.-y. (2006) Cell Mechanics Using Atomic Force Microscopy-Based Single-Cell Compression, *Langmuir*. **22**, 8151-8155.
4. Laurencin, M., Georgelin, T., Malezieux, B., Siaugue, J. M. & Menager, C. (2010) Interactions Between Giant Unilamellar Vesicles and Charged Core-Shell Magnetic Nanoparticles, *Langmuir*. **26**, 16025-16030.
5. Fares, M. B., Ait-Bouziad, N., Dikiy, I., Mbefo, M. K., Jovicic, A., Kiely, A., Holton, J. L., Lee, S. J., Gitler, A. D., Eliezer, D. & Lashuel, H. A. (2014) The novel Parkinson's disease linked mutation G51D attenuates *in vitro* aggregation and membrane binding of alpha-synuclein, and enhances its secretion and nuclear localization in cells, *Hum Mol Genet*. **23**, 4491-509.

## Summary

This thesis gives insights into the biophysical mechanisms of  $\alpha$ -synuclein ( $\alpha$ S) oligomer-membrane interactions. A number of studies have suggested that  $\alpha$ S oligomers are the toxic species involved in Parkinson's disease (PD). These data confirm that cellular membranes are the major sites of oligomer-induced damage. Disruption of the membrane integrity in the cell by oligomers could, for example, lead to the increased accumulation of reactive oxygen species and consequently cell death.

**Chapter 1** gives a general overview of different types of  $\alpha$ S oligomers prepared using different protocols. For most of the studies in this thesis model membranes of different compositions are used to mimic physiological membranes. We have systematically investigated how  $\alpha$ S oligomers bind and permeabilize model membranes and how these activities are modulated by membrane charge and lipid composition. These studies are described in **Chapters 2, 3** and **4**. Oligomer binding to complex model membranes is addressed in **Chapter 2** and **3**. Our studies show that at least 25% of negatively charged DOPG is necessary for  $\alpha$ S oligomer binding. We have also observed that  $\alpha$ S oligomers are not able to damage membranes that contain physiologically relevant cholesterol and sphingomyelin content. Most of the studies in this thesis focus on mitochondrial inner membrane and plasma membrane inner leaflet mimics because these two membranes are thought to be the primary sites of  $\alpha$ S oligomer-induced damage. From microscopy images in **Chapter 2** we were able to observe that upon the binding to giant unilamellar vesicles (GUVs)  $\alpha$ S oligomers could also be found in the vesicle interior, possibly diffusing through or across the membrane.

In **Chapter 3** we showed that mitochondrial model membranes are more prone to oligomer-induced damage at longer timescales while the more complex plasma membrane model systems do not show a concentration dependent permeabilization on the same time scale. We attribute this result to the complexity of the composition of the model plasma membranes.

In **Chapter 4** we show by SAXS studies that all  $\alpha$ S oligomers studied (WT, and disease mutants A30P, E46K, A53T, H50Q and G51D) contain approximately 30 monomers. We have found that the binding affinity of the monomeric protein and the aggregation number of the oligomers formed under our specific protocol are comparable for WT, H50Q and G51D. However, G51D oligomers were not able to disrupt negatively-charged and physiologically-relevant model membranes.



Replacement of the membrane-immersed small amino acid glycine by a negatively charged aspartic acid at position 51 prevents membrane destabilization whereas a mutation in the solvent-exposed part of the membrane-bound alpha helix, such as in the H50Q mutant, has little effect on the bilayer disrupting properties of  $\alpha$ S oligomers.

Our data in **Chapter 5** suggest the toxicity of the externally added oligomers tested here depend on the availability and toxicity of additional compounds rather than on the oligomers themselves. Although externally added  $\alpha$ S oligomers tested here were not toxic, we cannot draw any conclusions about the toxicity of oligomers produced intracellularly during aggregation of  $\alpha$ S or if the oligomers were somehow injected into the cell.

In **Chapter 6** we wanted to gain more details about toxicity of  $\alpha$ S oligomers and we suggested that oligomer-induced hemifusion could be connected to the vesicle docking and fusion problems observed *in vivo*. Multivalent oligomers may be directly involved in disturbing the well-controlled membrane fusion machinery of the cell. Our data have shown that only a few oligomers are necessary to cause hemifusion. Therefore clustering and fusion could be associated with the toxicity of the oligomers in the cells. We make the conceptual step of considering  $\alpha$ S oligomers as small multivalent biological nanoparticles that cause formation of holes in the membrane or membrane thinning. The observed uncontrolled and efficient hemifusion of vesicles sheds a new light on the possible toxicity of oligomers in Parkinson's disease.

## Samenvatting

Dit proefschrift geeft inzicht in de biofysische mechanismen van  $\alpha$ -synucleïne ( $\alpha$ S) oligomeer-membraan interacties. Een aantal studies suggereert dat het oligomeer de  $\alpha$ S aggregatie toestand is die toxisch is bij de ziekte van Parkinson (PD). De schade die oligomeren aanrichten wordt toegeschreven aan de interactie van  $\alpha$ S oligomeren met cellulaire membranen. In de cel kan verstoring van de membraan integriteit door oligomeren bijvoorbeeld leiden tot accumulatie van reactieve oxygen species en vervolgens celdood.

**Hoofdstuk 1** geeft een algemeen overzicht van de verschillende types van  $\alpha$ S oligomeren die verkregen kunnen worden met verschillende protocollen. Voor de meeste studies in dit proefschrift worden modelmembranen met verschillende samenstellingen gebruikt om fysiologische membranen na te bootsen. We hebben systematisch onderzocht hoe  $\alpha$ S oligomeren binden en modelmembranen lek maken en hoe binding en lekkage worden gemoduleerd door membraan lading en lipide samenstelling. Deze studies worden beschreven in **Hoofdstukken 2, 3 en 4**. De interactie van oligomeren met complexe modelmembranen komt aan de orde in **Hoofdstuk 2 en 3**. Onze studies tonen aan dat ten minste 25% van negatief geladen lipide zoals DOPG noodzakelijk is voor  $\alpha$ S oligomeer binding. We hebben waargenomen dat  $\alpha$ S oligomeren desondanks membranen met een fysiologisch relevant percentage cholesterol en sfgomyeline beschadigen. De meeste studies in dit proefschrift zijn gericht op lipide mengsels die het mitochondriale binnenmembraan of het plasmamembraan binnenblad nabootsen omdat van deze twee membranen wordt gedacht dat de ze lijden onder  $\alpha$ S-oligomeer geïnduceerde schade. Microscopie beelden in **Hoofdstuk 2** laten zien dat  $\alpha$ S oligomeren niet alleen binden aan reus unilamellaire vesicles (GUVs), oligomeren worden ook gevonden in de binnenkant van het vesicle. Oligomeren diffunderen mogelijk door of over het (beschadigde) membraan.

In **Hoofdstuk 3** hebben we aangetoond dat mitochondriële model membranen gevoeliger zijn voor oligomeer-geïnduceerde schade op langere tijdschalen terwijl voor de meer complexe plasmamembraan modelsystemen geen concentratieafhankelijke permeabilisatie op dezelfde tijdschaal wordt gezien. We wijten dit resultaat aan de complexiteit van de samenstelling van het model plasmamembraan.

In Hoofdstuk 4 laten we met behulp van SAXS studies zien dat alle  $\alpha$ S oligomeren die hier zijn onderzocht (WT, en de ziekte van mutanten A30P, E46K, A53T,

H50Q en G51D) ongeveer 30 monomeren bevatten. Daarnaast hebben wij gevonden dat de membraanbindingsaffiniteit van het monomere eiwit vergelijkbaar is voor WT, H50Q en G51D. Echter, ondanks deze overeenkomsten, waren G51D oligomeren niet in staat de integriteit van negatief geladen en fysiologisch relevante modelmembranen verstoren. In de ziekte gerelateerde G51D mutatie voorkomt vervanging van het membraan ondergedompeld kleine aminozuur glycine door een negatief geladen asparaginezuur op positie 51 membraan destabilisatie terwijl een mutatie in het oplosmiddel blootgestelde deel van de membraangebonden alpha helix, zoals de H50Q mutatie, resulteert in oligomeren die weinig effect hebben op de membraan integriteit.

Onze gegevens in **Hoofdstuk 5** suggereren dat de toxiciteit van de geteste extern toegevoegde oligomeren afhangt van de beschikbaarheid en de toxiciteit van additionele verbindingen die gebruikt zijn voor de productie van de oligomeren en niet van de oligomeren zelf. Hoewel de hier geteste extern toegevoegde  $\alpha$ S oligomeren niet toxisch waren, kunnen we hieruit geen conclusies trekken over de toxiciteit van oligomeren die intracellulair worden geproduceerd tijdens de aggregatie van  $\alpha$ S.

In **Hoofdstuk 6** bestuderen we een alternatief toxiciteitsmechanisme van  $\alpha$ S oligomeren en we suggereren dat- de door ons waargenomen oligomeer geïnduceerde hemifusion verband heeft met de vesicle docking en fusie problemen waargenomen in neuronen. Multivalente oligomeren kunnen rechtstreeks betrokken zijn bij het verstoren van de goed gecontroleerde membraanfusie machinerie van de cel. Uit onze gegevens blijkt dat slechts enkele oligomeren noodzakelijk hemifusion veroorzaken. De waargenomen ongecontroleerde en efficiënte hemifusie van vesicles werpt een nieuw licht op de mogelijke toxiciteit van oligomeren in de ziekte van Parkinson.

## List of abbreviations

A488	Alexa Fluor 488 C5 maleimide dye
AFM	atomic force microscope
$\alpha$ S	alpha-synuclein
CD	circular dichroism
ch	cholesterol
CL	18:1 cardiolipin
CTB	The Cell Titer-Blue assay
cys	cysteine
DA	dopamine
DOPA	1,2-Dioleoyl phosphatidic acid
DOPC	1,2-Dioleoyl phosphatidylcholine
DOPG	1,2-dioleoylphosphatidylglycerol
DPPG	1,2-dipalmitoylphosphatidylglycerol
DOPS	1,2-dioleoyl phosphatidylserine
DTT	dithiothreitol
EPR	electron paramagnetic resonance spectroscopy
ER	endoplasmic reticulum
FCS	fluorescence correlation spectroscopy
FRAP	fluorescence recovery after photobleaching
GUV	giant unilamellar vesicle
HEPES	4-(2-Hydroxyethyl)piperazine-1-ethanesulfonic acid
His	histidine
HNE	4-hydroxy-2-nonenal
Ig	immunoglobulin
LB	Lewy bodies
LN	Lewy neuritis
LUV	large unilamellar vesicle
MRE	mean residue ellipticities
NMR	Nuclear magnetic resonance
ONE	4-oxo-2-nonenal
PA	phosphatidic acid
PAGE	polyacrylamide gel electrophoresis
PD	Parkinson's disease

PE	phosphatidylethanolamine
PI	phosphatidylinositol
POPA	1-palmitoyl, 2-oleoyl phosphatidic acid
POPC	1-Palmitoyl, 2-oleoyl phosphatidylcholine
POPG	1-palmitoyl, 2-oleoyl phosphatidylglycerol
POPE	1-palmitoyl, 2-oleoyl phosphatidylethanolamine
POPS	1-palmitoyl, 2-oleoyl phosphatidylserine
PS	phosphatidylserine
ROS	reactive oxygen species
SAXS	small angle X-ray scattering
SNCA	synuclein, alpha (non A4 component of amyloid precursor)
sm	sphingomyelin
SUV	small unilamellar vesicle
WT	wild type

## Acknowledgement/Dankwoord/Zahvalnica

Yes, finally, I have succeeded! Today is that day!

This is in the same time the end and the beginning of one journey, that has started exactly 4 years, 7 months and 4 days ago. I can say that it was worth it. During these past years I have met really nice people, my colleagues and friends. Together we have shared everything from small lab talks to real science and real life events (a couple of us got married and started a family). Today is my turn to defend what I have begun on that 1<sup>st</sup> April 2010 and to thank all the people that were there with me all these years sharing the laughs, silence, happiness and sadness, long hours in the lab and office, movies, dinners, drinks and events.

Mireille, my PhD journey started when I first knocked on your door. Beste Mireille, hartelijke bedankt voor alles dat je voor mij hebt gedaan, voor alle correcties, suggesties, praatjes over mijn manuscript, presentatie en andere belangrijke dingen. In mijn PhD heb ik van jou heel veel geleerd. Ik ben echt blij dat jij mijn supervisor bent en dat jij altijd aan mijn zijde staan. Volgens mij alleen een grote bedankt is niet genoeg. Ik wens jou heel veel succes als de vakgroep leider en professor van NBP!

Vinod, as my promotor and direct supervisor; thank you for giving me the opportunity to do the PhD in Nanobiophysics group and to develop my ideas on so called "Bart's oligomers" which we had then renamed to A oligomers just before my first talk in EBSA conference in Budapest. Thank you for supporting me in the last steps and for reading all my e-mails in the middle of the night. From you I have learned to be always available and to constantly search for the new scientific ideas. Thank you for correcting my English (especially adding the articles; for me that was the most difficult part ☺).

Syl, bedankt voor de praatjes, de hulp met de administratie en het plannen van de vergaderingen met Vinod en Mireille.

Martin Stöckl, for being my colleague and helper, my Wikipedia for lipids and AKTA. I remember how many times we had to fix the AKTA, when oligomers went to waste. Thanks for all the inputs for my first manuscript, which we had finally published after many difficulties on the way.

Burçu and Slav, thanks for being my paranymphs and friends. Himanshu, if I could choose the third paranymph that would be definitely you. We all have also started at approximately the same time and I remember that every time when I needed a

good laugh I had come to your office and you made my day. Burçu, for the long time we were the only two foreign female PhD students in NBP. Slav, you always wanted to be cool and funny and believe me you have succeeded. Your office definitively could be called "shoes office" (you know what I mean ☺). Himanshu, you have learned to be "punctual" and we all enjoyed in your punctuality. ZH165 thanks for being my friends!

Mijn kamergenoten (Liesbeth, Peter, Martijn, Carla, Kristian), bedankt voor alles: dag tot dag praatjes en kletsen. Ik ben blij dat jullie mijn kamergenoten waren. En ook bedankt voor jullie hulp om mijn Nederlands beter te leren!

Saskia, bedankt voor het lezen van mijn hoofdstuk en suggesties over SAXS. Dank je wel voor de ESRF bezoek en mooi reis naar Grenoble.

Niels, bedankt voor de eerste input over oligomeren en dag tot dag praatjes over de gewone dingen!

Kirsten, je hebt zo veel eiwitten voor mij gemaakt en je hebt mij met de experimenten van mijn hoofdstuk 5 geholpen. Bedankt!

Natalie, Yvonne en Irene ook heel erg bedankt voor de eiwitten en lab organisatie!

Ine en Kerensa, bedankt voor de input over de cel toxiciteit.

Christian Blum, thanks for the help with my manuscript and some nice ideas.

Here I would like to thank all the other members from alpha-synuclein subgroup: Arshdeep, Dirk Roelof, Christian Raiss, Aditya, Vova and all the other people from NBP group that I have met during my PhD: Robert (met de hulp van confocale microscopy en mijn computerproblemen), Ron (for inputs and constant questions, I really like your sentence: "I have a question."), Hans, Jord, Amin, Harmen, Maurice, Ellen, Annelies, Kim, Shashank...

Special thanks to all the people from Nanomi BV: Gert (for giving me the opportunity to work in Nanomi), Okke (for all scientific inputs and advices), Erwin (for daily talks and advices), Lucie (for introducing me with the first steps in a formulation lab), Rob (for technical inputs about the process), Resi (for the help with administration), Miriam, Merline, Aline, Christina, Alena, Remco, Gabriel, Emillie, Augustine, Maarten, Kate, Maryline, Gerard and Florian. I am glad that I am a part of Nanomi team.

In this part I would like to thank my friends from UT and Enschede, our moving crew that has moved us in one day from Enschede to Hengelo: special thanks to Jozef (for organizing KFC, de Vluchte and movie events), Matteo and Andrea L. for the nice Italian dinners, Žarko (for football events, good dinners and even better parties)... All Serbian friends: Stanko and Tamara (from Duisburg/Belgrade, for

the nice trips that we took across Nordrhein-Westfalen region), Luka and Marija, Miloš and Ivana, Nikola and Jelena (for the trip to Portugal), Okica, Miladin and Mina, Sanja and Maxa.

My long lasting friends from Belgrade: Marija, hvala ti što si mi najbolje drugarica i kuma! Vanja, hvala ti za divna druženja i kafenisanja. I Tamara, želim ti puno uspeha u završetku doktorata. Girls you are the best! Miloše, takođe hvala na svemu!

Last but not least I would like to thank my family for all the support that they have given me:

Dragi tata, mama i Darko hvala vam za nesebičnu podršku za sve ove godine ljubavi i sve druge stvari koje se ne mogu opisati rečima, hvala vam puno svima;

tata, tebi posebno hvala što si verovao u mene

i pružio mi mogućnost da potražim svoj put 1800 km daleko od kuće;

mama, hvala ti što si uvek bila uz mene

kada je to bilo potrebno, što si me slušala i verovala da ću istrajati

i za najlepše posete i za sve mudre savete i dane.

Dare, šta reći,

a da već rečeno nije,

uživaj u životu i sreći

i istraj u svemu što ti život nudi

jer sreća se sama stvara

sve je u principu deo životne volje i dara.

Dragi Snežana i Miroslave, hvala vam što ste danas uz mene i za svu podršku tokom svih ovih godina koju ste mi nesebično pružili. Srećna sam što ste danas ovde.

And at the end I owe my special thanks, gratitude and love to you my loving husband, Bojan. We are together almost 10 years and I feel that I love you more each day. Thanks for being always with me and helping me to be persistent and to succeed in finishing my PhD thesis.

*Anja*





## List of publications

1. Stefanovic, A. N. D., Stockl, M. T., Claessens, M. M. A. E., Subramaniam, V., Alpha-synuclein oligomers distinctively permeabilize complex model membranes. *FEBS J.* 2014, 281 (12), 2838-50.
2. Stefanovic, A. N. D., Claessens, M. M. A. E., Blum, C., Subramaniam, V. Alpha-synuclein amyloid oligomers act as multivalent nanoparticles to cause hemifusion in negatively charged vesicle, *manuscript submitted*
3. Stefanovic, A. N. D., Lindhoud S., Semerdzhiev S.A., Claessens, M. M. A. E., Subramaniam, V. Characterization of oligomers formed from disease-related alpha-synuclein amino acid mutations, *manuscript in preparation*
4. Chaudhary, H., Stefanovic, A. N. D., Claessens, M. M. A. E., Subramaniam, V., Membrane interactions and fibrillization of  $\alpha$ -synuclein play an essential role in membrane disruption, *manuscript submitted*

## Conference contributions

### Talks

1. Stefanovic, A. N. D., Stockl, M. T., Claessens, M. M. A. E., Subramaniam, V., Mechanistic insights into oligomeric alpha-synuclein/membrane interactions, 8th European Biophysics congress, August 23-27, 2011, Budapest, Hungary
2. Stefanovic, A. N. D., Stockl, M. T., Claessens, M. M. A. E., Subramaniam, V., Amyloids on the nanoscale: the mechanism of membrane-protein interactions, 4th IRUN symposium on Nanotechnology, October 27-28 2011, Radboud University Nijmegen, Nijmegen, the Netherlands
3. Stefanovic, A. N. D., Claessens, M. M. A. E., Subramaniam, V., From phospholipid bilayers to natural membranes-the role of alpha-synuclein in membrane permeabilization, SRO meeting, November 22 2012, University of Twente, Enschede, the Netherlands
4. Stefanovic, A. N. D., Stockl, M.T., Zijlstra, N., Claessens, M.M.A.E., Subramaniam, V., Alpha-synuclein oligomers distinctively permeabilize model plasma and mitochondrial membranes, *Molecules: Synthesis and Properties*, November 4-5 2013, Lunteren, the Netherlands

## Posters

1. Stefanovic, A. N. D., Stockl, M. T., Claessens, M. M. A. E., Subramaniam, V., The amyloid pore hypothesis-The mechanism of membrane disruption, Annual Dutch meeting on Molecular and Cellular Biophysics, October 4-5 2010, Veldhoven, the Netherlands
2. Stefanovic, A. N. D., Stockl, M. T., Claessens, M. M. A. E., Subramaniam, V., The amyloid pore hypothesis-The mechanism of membrane disruption. Scientific meeting on the area of Organic Chemistry, October 25-27 2010, Lunteren, the Netherlands
3. Stefanovic, A. N. D., Stockl, M. T., Claessens, M. M. A. E., Subramaniam, V., Oligomer-phospholipid bilayer interactions-the mechanism of membrane disruption, Scientific Meeting NWO - study groups Protein Research, Nucleic Acids and Lipids & Biomembranes, December 6-7 2010, Veldhoven, the Netherlands
4. Stefanovic, A. N. D., Stockl, M. T., Claessens, M. M. A. E., Subramaniam, V., Disruption of cellular and mitochondrial membrane morphology is associated with permeabilization of oligomeric alpha-synuclein, Dutch meeting on Molecular and Cellular Biophysics, October 3-4 2011, Veldhoven, The Netherlands
5. Stefanovic, A. N. D., Stockl, M. T., Claessens, M. M. A. E., Subramaniam, V., Mechanistic insights into oligomeric alpha-synuclein/membrane interactions, Chains 2011, November 28-30 November 2011, De Fabrique, Maarssen, the Netherlands
6. Stefanovic, A. N. D., Stockl, M. T., Claessens, M. M. A. E., Subramaniam, V., Alpha-synuclein oligomers elicit permeability of model systems mimicking mitochondrial membranes, MESA+ Meeting 2012, September 18-2012, Enschede, the Netherlands
7. Stefanovic, A. N. D., Stockl, M. T., Claessens, M. M. A. E., Subramaniam, V., Oligomeric alpha-synuclein elicits permeability of model systems mimicking synaptic vesicles, neuronal and mitochondrial membranes, Annual Dutch meeting on Molecular and Cellular Biophysics, October 1-2 2012, Veldhoven, the Netherlands
8. Stefanovic, A. N. D., Stockl, M. T., Zijlstra, N., Claessens, M. M. A. E., Subramaniam, V., Alpha-synuclein oligomers distinctively permeabilize

model plasma and mitochondrial membranes, 9th European Biophysics Congress, July 13-17 2013, Lisbon, Portugal

9. Stefanovic, A. N. D., Claessens, M. M. A. E., Subramaniam, V. (2013), Alpha-synuclein oligomers distinctively permeabilize model plasma and mitochondrial membranes, Dutch Meeting on Molecular and Cellular Biophysics 2013, 30-September-1-October-2013, Veldhoven, the Netherlands



## Curriculum vitae

Anja Stefanović was born on August 14<sup>th</sup>, 1984 in Belgrade, Serbia. After finishing a high school in 2003, she started her studies at the Faculty of Pharmacy, University of Belgrade, Serbia. In January 2009 she obtained her MSc and began her internship in Clinical-biochemistry laboratory, Clinical Center of Serbia, Belgrade.

In October 2009 she started working in BIOS group, at the University of Twente as a researcher on the project about single cell analysis in glass-PDMS microchip. In April 2010 she joined Nanobiophysics group as a PhD candidate under supervision of Prof. dr. Vinod Subramaniam and Prof. dr. ir. Mireille Claessens. The aim of the project was to gain insights into the biophysical mechanisms of  $\alpha$ S oligomer-membrane interactions. The results of this multidisciplinary research resulted in this thesis. Currently Anja Stefanović is working as Scientist in Nanomi BV.